



12-2006

## **Design and Optimization of a Wind Deflector for Round-Nose MD-500 Series Helicopters**

James Joseph Wright  
*University of Tennessee - Knoxville*

Follow this and additional works at: [https://trace.tennessee.edu/utk\\_gradthes](https://trace.tennessee.edu/utk_gradthes)



Part of the [Aerospace Engineering Commons](#)

---

### **Recommended Citation**

Wright, James Joseph, "Design and Optimization of a Wind Deflector for Round-Nose MD-500 Series Helicopters. " Master's Thesis, University of Tennessee, 2006.  
[https://trace.tennessee.edu/utk\\_gradthes/1842](https://trace.tennessee.edu/utk_gradthes/1842)

This Thesis is brought to you for free and open access by the Graduate School at TRACE: Tennessee Research and Creative Exchange. It has been accepted for inclusion in Masters Theses by an authorized administrator of TRACE: Tennessee Research and Creative Exchange. For more information, please contact [trace@utk.edu](mailto:trace@utk.edu).

To the Graduate Council:

I am submitting herewith a thesis written by James Joseph Wright entitled "Design and Optimization of a Wind Deflector for Round-Nose MD-500 Series Helicopters." I have examined the final electronic copy of this thesis for form and content and recommend that it be accepted in partial fulfillment of the requirements for the degree of Master of Science, with a major in Aviation Systems.

Rodney C. Allison, Major Professor

We have read this thesis and recommend its acceptance:

Stephen Corda, U. Peter Solies

Accepted for the Council:

Carolyn R. Hodges

Vice Provost and Dean of the Graduate School

(Original signatures are on file with official student records.)

To the Graduate Council:

I am submitting herewith a thesis written by James Joseph Wright entitled "Design and Optimization of a Wind Deflector for Round-Nose MD-500 Series Helicopters." I have examined the final electronic copy of this thesis for form and content and recommend that it be accepted in partial fulfillment of the requirements for the degree of Master of Science, with a major in Aviation Systems.

Rodney C. Allison

Major Professor

We have read this thesis  
and recommend its acceptance:

Stephen Corda

U. Peter Solies

Accepted for the Council:

Linda Painter

Interim Dean of Graduate Studies

(Original signatures are on file with official student records.)

**DESIGN AND OPTIMIZATION OF A  
WIND DEFLECTOR FOR  
ROUND-NOSE MD-500 SERIES HELICOPTERS**

A Thesis Presented for  
the Master of Science  
Degree  
The University of Tennessee, Knoxville

James Joseph Wright  
December 2006

Copyright © 2006 by James J. Wright  
All rights reserved.

## **DEDICATION**

This thesis is dedicated to my best friends and partners through life; my wife Barbara and my children, Meghan and Christopher. They give me the love, understanding and encouragement that have enabled me to achieve my dreams.

## **ACKNOWLEDGEMENTS**

I wish to express my sincerest appreciation to the faculty of the Aviation Systems Department, Professor Rodney Allison, Dr. U. Peter Solies, Dr. Stephen Corda and Dr. George Masters who have shared their incredible knowledge and experience with me. I would like offer additional thanks to Rodney Allison, a friend and role model, for his assistance, advice, and guidance on this thesis and the road ahead. I would also like to thank Greg Heatherly and Mark Blanks for excellent professionalism and skill in maintaining the fleet, and my fellow students, Kim Elsholz and Adam Cowan, whose assistance on this project was as constant as it was invaluable. Last, but not least, many thanks to Betsy Harbin, the one who once ran the show.

## **ABSTRACT**

This thesis examines the problem experienced by the numerous rotary wing operators whose operations require flight with personnel seated outside the fuselage or with doors off. This investigation is specific to the round nose configured MD-500 series aircraft due to test aircraft availability and the wide range of missions it conducts worldwide. During cruise flight, personnel exposed to the aircraft slipstream are subjected to high wind loads and extreme wind chill effects, compromising their ability to perform required tasks. External passengers also add to the overall helicopter parasite drag, decreasing its performance as well as interfering with the crew through increased noise, wind and turbulence in the cockpit. Prior research indicates that attachment of wind deflectors to the helicopter forward fuselage diverts the wind away from the fuselage, reducing overall parasite drag and slipstream effects on external passengers. The purpose of this investigation is threefold, identification of the structural requirements for airframe integration, design and fabrication of airworthy test deflectors, and evaluation of effects of the devices on external passengers, helicopter performance and pilot interface. Seven full-scale wind deflector configurations were flight tested at airspeeds of 0 to 80 knots. The deflector configured with a sweep angle of 50° and width of 8 inches with Gurney flap provided for reductions of 52% in external passenger load, 2 psi main rotor torque in 80 knot cruise and significantly less wind, noise and turbulence in the cockpit.



# TABLE OF CONTENTS

Chapter	Page
CHAPTER I .....	1
INTRODUCTION .....	1
Background .....	1
General.....	1
Requirement.....	2
Literature Search .....	2
Previous Research .....	2
Computational Methods .....	5
Research Conclusions.....	6
Objectives .....	7
MD-500 Test Aircraft Description .....	7
MD-500 Test Aircraft Description .....	8
CHAPTER II .....	10
SYSTEMS ENGINEERING .....	10
Introduction .....	10
Functional Decomposition.....	10
Interfaces .....	11
Constraints.....	14
Alternatives .....	15
CHAPTER III .....	17
WIND DEFLECTOR DESIGN, FABRICATION AND ANALYSIS.....	17
Design Requirements .....	17
Air Load Reduction.....	17
Temperature Effects.....	21
Deflector Design .....	22
Deflector Sweep Angle.....	23
Deflector Width.....	24
Deflector Length .....	25
Airframe Integration.....	25
Material Selection.....	28
Deflector System Fabrication .....	31
Leading Edge Fixture .....	31
Deflector.....	32
Hinge Brace.....	37
Leading Edge Fairing .....	38
Gurney Flap.....	40
Structural Analysis .....	45
Static Structural Considerations .....	45
Dynamic Structural Considerations .....	49
CHAPTER IV .....	55
DATA ACQUISITION AND RECORDING .....	55

Data Acquisition Systems .....	55
External Passenger Manikin System .....	55
Flight Data .....	59
Data Reduction .....	60
External Passenger/Manikin Force .....	61
CHAPTER V .....	65
RESULTS AND DISCUSSION .....	65
Design and Fabrication .....	65
Safety Considerations .....	65
Data Acquisition .....	67
External Passenger Air Load .....	69
Helicopter Performance .....	74
Helicopter Handling Qualities .....	76
Pitot Static System .....	78
CHAPTER VI .....	80
CONCLUSIONS AND RECOMMENDATIONS .....	80
Conclusions .....	80
Design Process .....	80
Deflector Mounting System .....	80
Deflector Material Selection .....	80
Optimum Deflector Configuration .....	81
Recommendations .....	84
LIST OF REFERENCES .....	85
APPENDICES .....	88
APPENDIX A .....	89
Data Tables .....	89
APPENDIX B .....	104
Figures .....	104
APPENDIX C .....	124
Flight Permit and Safety/Hazard Review .....	124
APPENDIX D .....	131
Test Plan .....	131
VITA .....	166

## LIST OF TABLES

Table	Page
Table 1: Wind Deflector System Interfaces .....	14
Table 2: Deflector Material Selection Matrix .....	16
Table 3: Drag Force, $D_{EP}$ , on the External Passenger (lbf).....	19
Table 4: Effect of Recording Method of Load Cell Data Dispersion.....	63
Table 5: Deflector Summary 80 Knots [KCAS] .....	82
Table 6: Detailed Deflector Summary 80 Knots [KCAS] .....	90
Table 7: Detailed Deflector Summary 70 Knots [KCAS] .....	91
Table 8: Detailed Deflector Summary 60 Knots [KCAS] .....	92
Table 9: Detailed Deflector Summary 50 Knots [KCAS] .....	93
Table 10: Detailed Deflector Summary 40 Knots [KCAS] .....	94
Table 11: Flight Test Data Card No Deflectors 2 Manikins per Side (Baseline).	95
Table 12: Flight Test Data Card 40 Degree 12 Inch Deflector .....	96
Table 13: Flight Test Data Card 40 Degree 10 Inch Deflector (Flight 1).....	97
Table 14: Flight Test Data Card 40 Degree 10 Inch Deflector (Flight 2).....	98
Table 15: Flight Test Data Card 40 Degree 8 Inch Deflector (Flight 1).....	99
Table 16: Flight Test Data Card 40 Degree 8 Inch Deflector (Flight 2).....	100
Table 17: Flight Test Data Card 50 Degree 12 Inch Deflector .....	101
Table 18: Flight Test Data Card 50 Degree 10 Inch Deflector .....	102
Table 19: Flight Test Data Card 50 Degree 8 Inch Deflector .....	103
Table 20: Test Plan Matrix – Ground Tests. <sup>(1)(2)(3)</sup> .....	160
Table 21: Test Plan Matrix – Performance Tests. <sup>(1)(2)(3)</sup> .....	161
Table 22: Test Plan Matrix – Stability and Control Tests. <sup>(1)(2)(3)</sup> .....	163

## LIST OF FIGURES

Figure	Page
Figure 1. Examples of helicopter External Passenger (EP) applications. ....	1
Figure 2. Water Tunnel Experiment for Flow Diverter, Hicks 1997. ....	3
Figure 3. OH-58A+ Wind Diverter Experiment, Mulnik and McDougall, 2000. ....	4
Figure 4. MD-500D External Passenger Wind Deflector Experiment, Lewis 2005. .....	5
Figure 5. Test Aircraft: MD-500D Helicopter, N500VS. ....	8
Figure 6. Comparison of round- and pointed-nose MD-500 variants. ....	9
Figure 7. Functional Decomposition .....	11
Figure 8. The SHEL Model .....	12
Figure 9. Wind Deflector System Interfaces. ....	13
Figure 10. NOAA/National Weather Service Windchill Chart. ....	22
Figure 11. Wind Deflector Principle Dimensions and Location. ....	23
Figure 12. Determination of Attachment Point and Deflector Sweep Angle. ....	26
Figure 13. Deflector Airframe Integration Diagram .....	29
Figure 14. 40 Degree Leading Edge Fixture. ....	32
Figure 15. Deflector Shaping and Approximate Dimensions .....	33
Figure 16. Prototype Deflector Mounted on MD-500 with Simulated EP. ....	36
Figure 17. Left Lower Hinge Brace Installation. ....	38
Figure 18. Deflector Fairing and Entire Deflector Assembly Installed. ....	39
Figure 19. Gurney Flap on an Airfoil Trailing Edge. ....	40
Figure 20. Gurney Flap Deflector Installation and Potential Performance Enhancement. ....	41
Figure 21. Measurement of Deflector Characteristic Length. ....	42
Figure 22. Deflectors with Gurney Flap Installed. ....	44
Figure 23. Results of Destructive Test of Deflector Sample Sections. ....	46
Figure 24. Deflector Frontal Surface Area Estimation (Front and Oblique). ....	48
Figure 25. Reynolds Number versus Strouhal Number Relationship. ....	52
Figure 26. External Passenger Bench with Manikin Instrumentation .....	55
Figure 27. External Passenger Manikins on Bench .....	56
Figure 28. Rectilinear Field-of-View Diagram: 50 Degree 12 Inch Deflector. ....	66
Figure 29. Rectilinear Field-of-View Diagram: 50 Degree 8 Inch Deflector. ....	66
Figure 30. Time Domain Plot of Time vs. Manikin Load Cell Value .....	68
Figure 31. Calibrated Airspeed vs. Total Mean Perceived Manikin Longitudinal Force - All Deflector Configurations. ....	71
Figure 32. Calibrated Airspeed versus Total Mean Perceived Manikin Longitudinal Force - 40° Deflectors versus No Deflector. ....	72
Figure 33. Calibrated Airspeed versus Total Mean Perceived Manikin Longitudinal Force - 50° Deflectors versus No Deflector. ....	73
Figure 34. Tuft Flight Visualization of 50° 8-inch deflector with Gurney flap. ....	75
Figure 35. Calibrated Airspeed (CAS) versus Main Rotor Torque (Q) - All Deflector Configurations. ....	77

Figure 36. Airflow Visualization on Right Aft Fuselage. ....	79
Figure 37. Airflow Visualization on Left Aft Fuselage.....	79
Figure 38. Deflector Optimization (Non-Weighted Objective). ....	81
Figure 39. Test Aircraft in Flight with 50° 8-inch deflector with Gurney Flap. ....	83
Figure 41. Right Manikin Load Force Calibration.....	105
Figure 42. Left Manikin Load Cell Calibration.....	105
Figure 43. Fuselage Sweep Angle Measurement Protractor (Installed). ....	106
Figure 44. Left Upper and Lower Hinge Brace Assembly (Not installed).....	106
Figure 45. Lower Hinge Brace (Installation). ....	107
Figure 46. Lower Hinge Brace (Installed). ....	107
Figure 47. Upper Hinge Brace (Installed). ....	108
Figure 48. Leading Edge Metal Fixture with Hinge Braces (Installed, Complete). .....	108
Figure 49. Deflector Edge Filling. ....	109
Figure 50. Deflector Attached to Full Leading Edge Fixture .....	109
Figure 51. External Passenger Bench System. ....	110
Figure 52. Deflector Installed on Right Side... ..	110
Figure 53. Pilot Field-of-View with 40 Degree 12 Inch Deflector Installed (Left) .....	111
Figure 54. Pilot Field-of-View with 40 Degree 12 Inch Deflector Installed (Right). .....	111
Figure 55. Deflector Material Test Section (Bending). ....	112
Figure 56. Deflector Test Section Bending Test. ....	112
Figure 57. Deflector Material Test Section (Tear Out). ....	113
Figure 58. Deflector Test Section Tear Out Test. ....	113
Figure 59. Static Load Testing of Installed Deflector (1). ....	114
Figure 60. Static Load Testing of Installed Deflector (2). ....	114
Figure 61. Manikin Longitudinal Force Load Cell.....	115
Figure 62. Manikin Roller Seat Assembly with Load Cell Location.....	115
Figure 63. Manikin Roller Seat Assembly (Front, Installed).....	116
Figure 64. Manikin Roller Seat Assembly (Oblique, Installed). ....	116
Figure 65. External Passenger Bench with Manikins Installed. ....	117
Figure 66. MD-500 Aircraft Configured for Deflector Flight.....	117
Figure 67. 40 Degree 12 Inch Deflector (Installed). ....	118
Figure 68. 40 Degree 10 Inch Deflector (Installed). ....	118
Figure 69. 40 Degree 8 Inch Deflector (Installed). ....	119
Figure 70. 50 Degree 10 Inch Deflector (Installed). ....	119
Figure 71. 50 Degree 8 Inch Deflector (Installed). ....	120
Figure 72. 50 Degree 8 Inch Deflector with Flow Visualization Tufts. ....	120
Figure 73. 50 Degree 8 Inch In-flight Flow Visualization (Right Front View)....	121
Figure 74. 50 Degree 8 Inch In-flight Flow Visualization (Right Close-Up). ....	121
Figure 75. 50 Degree 8 Inch In-flight Flow Visualization (Left Front).....	122
Figure 76. 50 Degree 8 Inch Deflector Flow Visualization Flight (Left Upper). 122	
Figure 77. 50 Degree 8 Inch in-flight Flow Visualization (Left Close-Up).....	123
Figure 78. 50 Degree 8 Inch In-flight Flow Visualization (Front). ....	123

Figure 79. Wind Deflector Test Program Flight Permit. ....	125
Figure 80. Safety/Hazard Review Sheet 1 of 5.....	126
Figure 81. Safety/Hazard Review Sheet 2 of 5.....	127
Figure 82. Safety/Hazard Review Sheet 3 of 5.....	128
Figure 83. Safety/Hazard Review Sheet 4 of 5.....	129
Figure 84. Safety/Hazard Review Sheet 5 of 5.....	130
Figure 85. MD-500D Principle Dimensions.....	157
Figure 86. MD-500D (369D) N500VS.....	158
Figure 87. Bedford Workload Rating Scale. ....	159
Figure 88. Modified Cooper-Harper Rating Scale.....	159

## ABBREVIATIONS AND SYMBOLS

$A_D$	Drag Area
$a_{ssl}$	Standard Sea Level Speed of Sound
AC	Advisory Circular
AEDC	Arnold Engineering Development Center
$C_D$	Coefficient of Drag
CG	Center of Gravity
CFR	Code of Federal Regulation
D	Drag
DOD	Department of Defense
EP	External Personnel
FAA	Federal Aviation Administration
fps	Feet per Second
FTM	Flight Test Manual
GPS	Global Positioning System
HDG	Heading
$H_{PO}$	Pressure Altitude (Observed)
IAW	In Accordance With
KCAS	Knots Calibrated Airspeed
KIAS	Knots Indicated Airspeed
KTAS	Knots True Airspeed
M	Mach Number
OAT	Outside Air Temperature
psi	Pounds per Square Inch
$P_s$	Static Pressure
$P_{ssl}$	Standard Sea Level Static Pressure
$P_t$	Total Pressure
q	Dynamic Pressure
S	Surface Area

SHP	Shaft Horsepower
THA	Tullahoma Regional Airport
USNTPS	United States Naval Test Pilot School
$V_C$	Calibrated Airspeed
$V_H$	Maximum Level Flight Speed
$V_I$	Corrected Indicated Airspeed
$V_{ref}$	Reference Airspeed
$V_T$	True Airspeed
$W$	Weight
$X$	Longitudinal Force
$\bar{X}$	Mean Longitudinal Force
$X_L$	Longitudinal Force (Left Load Cell)
$X_R$	Longitudinal Force (Right Load Cell)
$\bar{X}_L$	Mean Longitudinal Force (Left Load Cell)
$\bar{X}_R$	Mean Longitudinal Force (Right Load Cell)
$X_T$	Total Longitudinal Force (Left and Right Load Cells)
$\bar{X}_T$	Total Mean Longitudinal Force (Left and Right)
$^{\circ}F$	Degree Fahrenheit
$\rho$	Air Density
$\beta$	Sideslip Angle
$\delta$	Pressure Ratio
$\gamma$	Specific Heat Ratio
$\sigma$	Standard Deviation
$\theta$	Pitch Attitude



# CHAPTER I INTRODUCTION

## Background

### *General*

A wide range of organizations have need to conduct helicopter operations in such a manner that exposes both passengers and crew to harsh environmental conditions. Law enforcement, search and rescue, military and long distance electrical power line maintainers often share, for specialized missions, a requirement to fly with aircraft doors removed. In extreme cases, personnel may be situated entirely outside the fuselage (Figure 1). There is a demonstrated need to operate in both doors off and external personnel (EP) configurations. The conduct of these operations, however, causes three significant, related problems.



Figure 1. Examples of helicopter External Passenger (EP) applications.

### ***Requirement***

During cruise flight, the air loading on EP results in significant physical fatigue and a corresponding task performance decrement. The high relative wind also creates a health risk due to wind chill effect, a condition further exacerbated when flight in precipitation is required.

Helicopter performance is significantly decreased by the parasite drag added to the system by the EP. Decreased performance results in increased cost to the operator as a function of increased fuel consumption, and in time lost during enroute legs when maximum speed is reduced by engine or powertrain limitations.

Turbulence created by the EP also causes greater than normal airflow and noise in the cockpit and cabin. Wind in the cockpit typically increases crew workload, particularly when dealing with items such as flight publications and navigation charts. The increased noise levels result in communications difficulties and increase fatigue for the aircrews.

A detailed discussion of these problems is located in Chapter 3 of this document.

## **Literature Search**

### ***Previous Research***

A search of the University of Tennessee Space Institute (UTSI) and the U.S. Air Force's Arnold Engineering Development Center (AEDC) Libraries, both

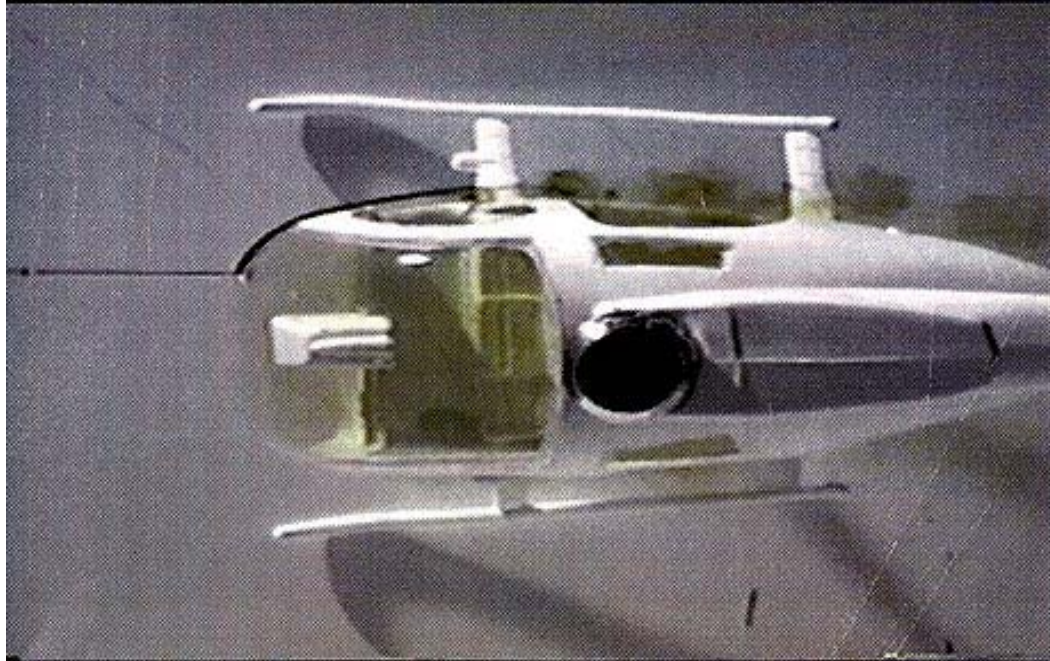


Figure 2. Water Tunnel Experiment for Flow Diverter, Hicks 1997.

located in Tullahoma, Tennessee, found four Master's degree theses that applied directly to this project, and one Doctoral dissertation that had the potential to assist indirectly on the integration of vortex generators.

A possible solution to the problems caused by doors off or the addition of external personnel has previously been researched by Hicks [9] using wind deflectors (also called "flow diverters") attached to a helicopter's forward fuselage. This research began in 1997, at UTSI, using dye injection for flow visualization around a 1/24-scale round-nose MD-500 model in a water tunnel environment (Figure 2). The objective of this study was minimizing the airflow entering the cabin during doors off flight and did not consider the external personnel condition.

In 2000, full-scale flight testing was conducted at UTSI by Mulnik [11] and



Figure 3. OH-58A+ Wind Diverter Experiment, Mulnik and McDougall, 2000.

McDougall [10] using an OH-58A+ Kiowa helicopter equipped with aluminum wind deflectors of various designs (Figure 3). These flight tests provided valuable insight as to the feasibility of such devices. Although there is a distinct difference in the fuselage forms of the OH-58A+ and the MD-500 helicopters, the difference was not expected to be so great as to render those results entirely invalid for the present test. Therefore, the recommendations for in-flight evaluation of a wind deflector solution specifically for the MD-500 were incorporated into the test planning.

Lewis [12] completed a wind tunnel investigation specific to the design of wind deflectors for the round-nose fuselage MD-500 helicopter carrying EP in late 2005 (Figure 4). Thirty-two configurations were tested for total drag increment on the system, both with and without EP, using a 1/8 scale half

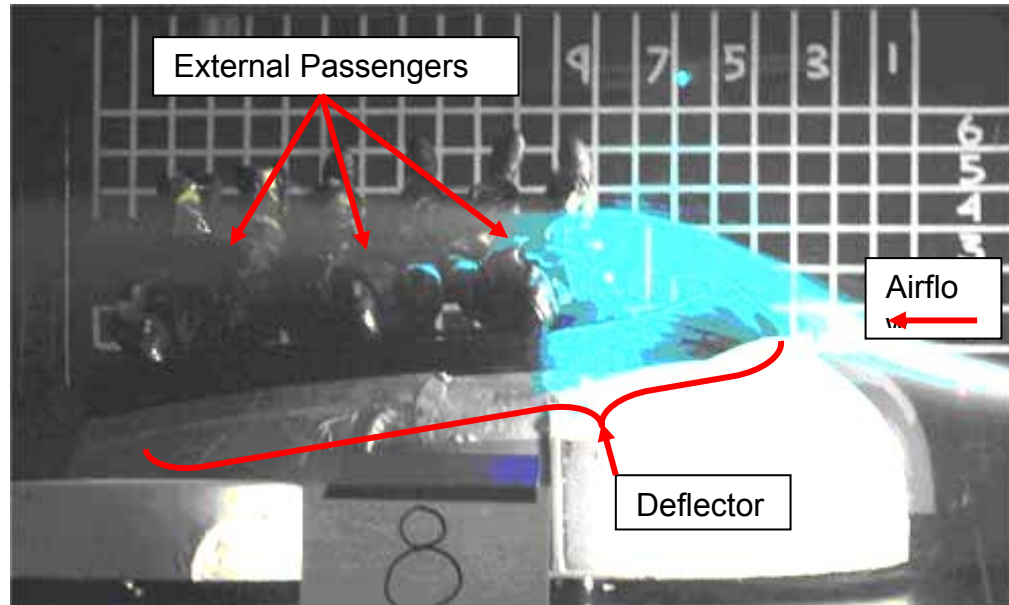


Figure 4. MD-500D External Passenger Wind Deflector Experiment, Lewis 2005.

model of the MD-500 helicopter. The recommendations of this aircraft specific work were followed, and augmented for the limited number of deflector configurations used in this investigation.

The dissertation addressing the flow effects of various vortex generator (VG) arrays by Liver [13] was instrumental in the VG designs and configurations used in this test.

### ***Computational Methods***

The configuration selection process was not limited to the previously cited references. Consultations with Dr. Edward Kraft, Chief Scientist at AEDC, were conducted on the feasibility of using a computational fluid dynamics (CFD) method for estimation of configuration performance. This method was

dismissed due to the inadequacies of conventional CFD involving the separation effects along sharp-edged discontinuities, such as the trailing edge of the proposed deflector. A promising alternative to the CFD problem was investigated through discourse with UTSI's Dr. John Steinhoff of the Mechanical and Aerospace Engineering Department. Dr. Steinhoff has developed computational modeling software for vorticity confinement [3] that is capable of predicting the type of turbulent, separated flow expected with the wind deflectors. Unfortunately, due to cost, personnel and schedule constraints, this technology could not be leveraged for the investigation.

### ***Research Conclusions***

Considering the number of possible design variables and the limited amount of prior research in this area, it was determined that as many deflector designs as possible needed to be studied. Fabricating and flight-testing a large number of prototype deflectors, however, was both time and cost prohibitive. The conclusions and recommendations of the previous studies were subjectively weighted to arrive at the configurations that would be produced for full-scale flight test. This process resulted in selection of a set of seven related configurations for fabrication and test, with provision for up to ten, if data suggested that necessity. Details of the configuration selection process are discussed in Chapter III of this document.

## **Objectives**

The primary design goal of the wind deflectors is to divert the greatest amount of wind force away from the external personnel and opened doors. Of subordinate concern was that this primary goal be met without excessive degradation of the field-of-view, performance, or handling qualities of the MD-500 helicopter.

The purpose of this thesis was to recommend an optimum design for a production wind deflector by evaluating various wind deflector configurations installed on a MD-500D helicopter in full-scale flight test. The evaluation was primarily a comparative analysis of the effects of varying the major design parameters (width, length, and deflection angle). The analyses consider the following (in order of priority):

1. The success of a wind deflector in diverting the airflow away from external personnel.
2. The effect of a wind deflector on aircraft performance.
3. Upon selection of the optimum deflector configuration based upon criteria 1 and 2, the effects on pilot field of view and aircraft handling qualities.

## **MD-500 Test Aircraft Description**

The test aircraft MD-500D (Model 369D, Registration Number N500VS) (Figure 5) was production representative, with the exception of an air data



Figure 5. Test Aircraft: MD-500D Helicopter, N500VS.

### **MD-500 Test Aircraft Description**

boom, external seats, simulated personnel (manikins) and test instrumentation package for the recording of aircraft flight parameters.

MD Helicopter, Inc. has manufactured the 500-series helicopters in both a round-nose (Figure 6) and a pointed-nose configuration. This test is solely concerned with the round-nose variant; any application to the pointed-nose variant is inconclusive.

The MD-500 is a 5 place, turbine powered, rotary wing aircraft. The main rotor is a fully articulated five-bladed system, with anti-torque provided by a





Figure 6. Comparison of round- and pointed-nose MD-500 variants.

2-bladed semi-rigid type tail rotor. The flight control system is a direct mechanical linkage without hydraulic boost. Power from the turboshaft engine is transmitted through the main drive shaft to the main rotor transmission and from the main rotor transmission through a drive shaft to the tail rotor. An overrunning (one way) clutch, placed between the engine and the main rotor transmission permits free-wheeling of the rotor system during autorotation. A more detailed description, including weight class and principle dimensions, is located in the MD-500 Rotorcraft Flight Manual (RFM) [1] and the UTSI Project Test Plan, located in Appendix D.

## **CHAPTER II**

# **SYSTEMS ENGINEERING**

### **Introduction**

A systems engineering approach was selected to better analyze the problem and requirements for material selection of a wind deflector. The systems approach is one in which a large, complex problem is broken down into smaller, more manageable segments through functional decomposition. Application of the systems approach to this problem was in the end highly subjective in nature yet had no negative effect on the outcome. It is crucial that need and the final product are kept in the forefront during the entire process. Each element of the project life cycle, from problem recognition to solution concepts to production and retirement, was considered. The deflector requirements were analyzed and translated into specifications, allowing a trade study to determine the most effective method of meeting the stated objectives.

### **Functional Decomposition**

For a project of this magnitude may be brought into perspective, a functional decomposition process was used (Figure 7). The desired effects of the deflector concept were analyzed and project objectives were defined. The objectives in turn suggested certain specifications, or system characteristics,

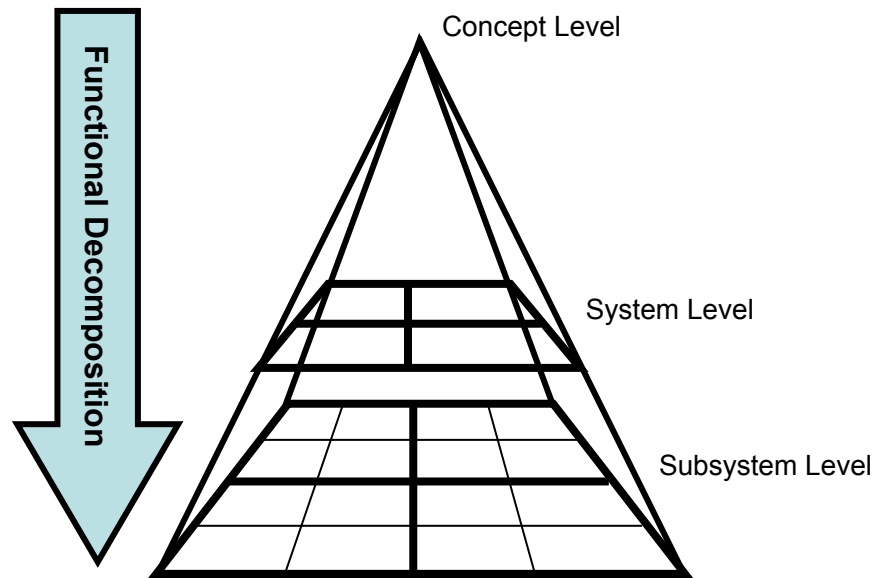


Figure 7. Functional Decomposition

which were then further broken down into subsystems. To satisfy the prioritized requirements stated in the purpose of this investigation, multiple subsystems were delineated to support the engineering solutions. Each subsystem relates to its parent system and adjacent other elements through a series of interfaces. Identification of each subsystem and tracking of its interfaces ensures interoperability of individually developed parts and their subsequent contribution to the whole. Continuity of the overall design is critical, and requires close monitoring.

## **Interfaces**

Each element of the overall project must properly work together to accomplish the end purpose. Once systems and subsystems are identified, the next crucial task is evaluation and identification of how they interface with one

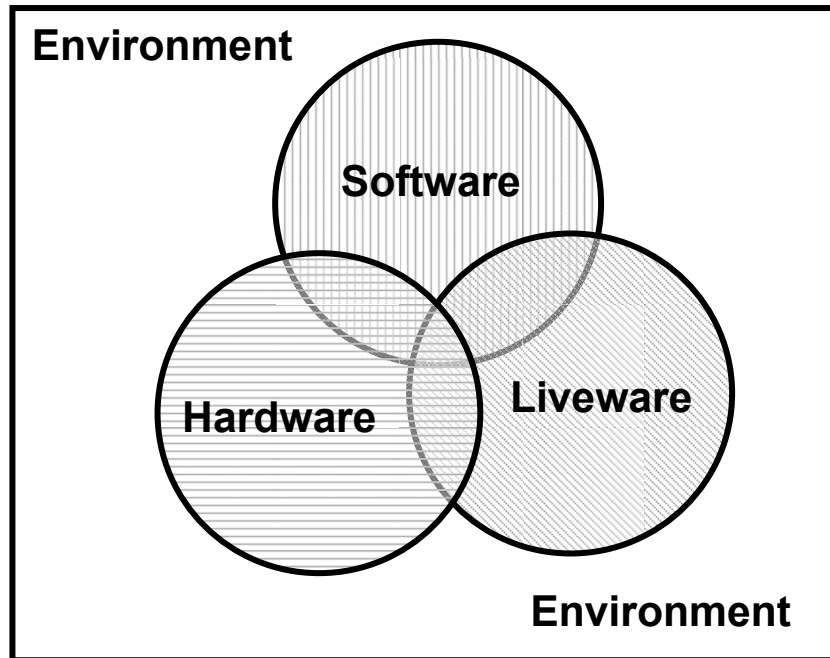


Figure 8. The SHEL Model

another. One of the many accepted methods for accomplishing this is through use of the SHEL model [2] (Figure 8). The SHEL model supports a systemic view defining any productive process as performed by a combination of hardware, (e.g., any material or tool used in the process execution), software, (e.g., computer, procedure, rule, etc.) liveware resources (e.g., crew, passengers, etc.) embedded in a given environment (e.g., physical, socio-cultural, work, etc.). The subsystems required to perform a specific process may be considered as being distributed among these four groups and may or may not interface with each other. Therefore, any productive process may be regarded as an instant of the SHEL model for process execution. The systemic view of the SHEL model encourages the definition of requirements not just for the system to be designed (hardware

and software), but also for those aspects (e.g., procedures, practices, human roles, interaction, etc.) related to Liveware resources. Therefore, SHEL oriented requirements represent a trade-off among hardware, software and liveware resources in a given operating environment. The functional breakdown and application of the SHEL model allows for more accurate subsystem interface identification and tracking.

Six major systems were identified as influencing the wind deflector design and function. They are the deflector itself (H), the helicopter airframe (H), the external passengers (L), the aircrew (L), the data acquisition instrumentation (H, S) and the air flow (E) through which it must operate. The interfaces between these elements are best depicted graphically (Figure 9).

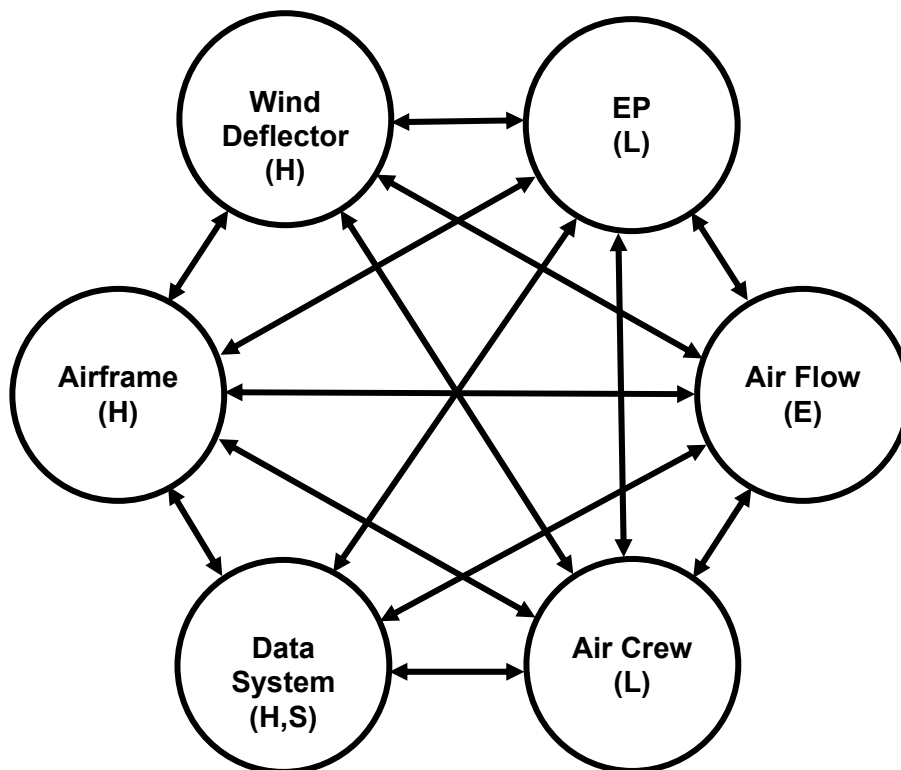


Figure 9. Wind Deflector System Interfaces.

**Table 1: Wind Deflector System Interfaces**

<b>System</b>	<b>Interface Consideration</b>
Air Flow (E)	Air load produced by air speed and direction
Aircrew (L)	Crew field of view (FOV) and ingress/egress
EP (L)	Requirement to divert air flow
Airframe (H)	Airworthy integration to existing structure

All systems except for the data acquisition system and the deflectors had direct interaction. As the wind deflector was the system around which the entire experiment was formed, a further breakdown as to the nature of its interfaces was conducted (Table 1). Evaluation of each of these considerations resulted in a trade study to determine how each must be addressed in turn. For example, the air loads produced by speed and direction became a constraint for which there were not alternatives. However, the airframe integration problem, while bounded by numerous constraints, was surmountable by multiple alternatives.

### **Constraints**

Those portions of a project for which few alternatives exist become constraints on the overall system. They are typically variables that are specified by a customer or outside agency, such the Federal Aviation Administration (FAA) for regulatory requirements. The primary constraint of this design project was scheduling. The test aircraft was acquired on a six-month lease for which the end date was not negotiable. Additional scheduling

pressure came in the form of academic scheduling, periodic maintenance of other fleet aircraft and other research projects. This required a concerted effort of the entire Aviation Systems team to ensure timely completion of the project.

## **Alternatives**

With the systems engineering process having identified the foreseeable requirements and the primary project systems defined, alternatives must be evaluated to determine a best course of action. There must be an organized method of decision making used to ensure that the best alternatives are selected and implemented.

The decision was made to use the following list as a guideline for problem solving during the deflector design process.

- Define the need
- Identify the objectives
- Generate alternatives
- Analyze alternatives
- Select best course of action
- Implement and integrate

Specific to the design of the wind deflector, a weighted analysis was conducted in a tabular form. The weights were assigned both objectively and subjectively, based upon available information and experience. The deflector

material selection matrix is depicted in Table 2, as an example. This same process was used to determine materials and processes for all other subsystems of the deflector system (i.e., leading edge fixture, hinge brace).

While this method was not entirely objective, it provided an organized means to evaluate possible alternatives. The evaluation traits of each material were determined and then assigned a weight value commensurate with their potential contribution to overall success.

Each alternative was then evaluated with either a (+) or (-) indicating the relative degree to which it possessed each of the required traits. Only positive values were tabulated into the final weighted scores and the material with the highest overall score was selected for fabrication. As seen in Table 2, the material with the most favorable characteristics for the deflector was determined to be a composite sandwich of fiberglass and polystyrene foam.

**Table 2: Deflector Material Selection Matrix**

Evaluation Metric	Wt	Material					
		Aluminum	Plastic	Fiberglass		Carbon Fiber	
				Solid	Sandwich	Solid	Sandwich
Strength	3	+	+	+	+	+	+
Stiffness	4	-	-	+	+	+	+
Tooling	3	+	-	-	+	+	+
Experience	2	+	-	+	+	-	-
Availability	2	+	+	+	+	+	+
Cost	1	+	+	-	+	-	-
<b>Total Score</b>		<b>11</b>	<b>6</b>	<b>11</b>	<b>15</b>	<b>12</b>	<b>12</b>



## **CHAPTER III**

### **WIND DEFLECTOR DESIGN, FABRICATION AND ANALYSIS**

#### **Design Requirements**

The primary goal in the design of the wind deflector was reduction of slipstream effects on external personnel. These effects may be broken down into two areas; air loads perceived as a drag force directly proportional to the square of the helicopter airspeed and perceived temperature wind chill effect. Of additional concern is the parasite drag form factor of externally mounted personnel. An aerodynamic fairing forward of the EP location had the greatest potential to reduce the overall drag of the helicopter, resulting in increased performance.

#### ***Air Load Reduction***

The average American male today is 5 foot, 10 inches tall and weighs 175 pounds, according to various sources. Accepting this approximation, a human body of average build, when viewed from the side, presents approximately 4.5 square feet (ft<sup>2</sup>) of surface area. This number is closer to 6.0 ft<sup>2</sup> when viewed from the front. Required clothing, equipment and retention harness add to the drag producing surface area of a person participating in EP helicopter operations. This may result in an additional 1.0 to 1.5 ft<sup>2</sup> of surface area presented to the slipstream. Based upon these assumptions, a median value of 5.5 ft<sup>2</sup> of lateral surface area was selected for

further calculations. A representative value of 1.1 for the parasite drag coefficient of a human body was used to calculate a drag area for the EP (Hoerner, [14]).

$$A_D = C_D S \quad (\text{Equation 1})$$

where

$A_D$  = drag area of the external passenger

$C_D$  = coefficient of parasite drag

$S$  = surface area

This calculation resulted in an estimated drag area of 6.1 ft<sup>2</sup>, which was used for further calculation of the air loads on an individual EP.

$$D_{EP} = A_D \frac{\rho_{ssl}}{2} V_C^2 \quad (\text{Equation 2})$$

where

$D_{EP}$  = drag force exerted on the external passenger

$A_D$  = drag area of the external passenger

$\rho_{ssl}$  = standard sea level air density

$V_C$  = calibrated airspeed

The wind force experienced by a person sitting outside the fuselage will be directly proportional to the square of the calibrated airspeed. Table 3 lists the

**Table 3: Drag Force,  $D_{EP}$ , on the External Passenger (lbf)**

	Calibrated Airspeed (knots)						
	40	50	60	70	80	90	100
<b><math>D_{EP}</math> One Side</b>	33.0	51.6	74.3	101.2	132.2	167.3	206.5
<b><math>D_{EP}</math> Two Sides</b>	66.1	103.3	148.7	202.4	264.3	334.6	413.0

estimated values of wind force in pounds-force (lbf) exerted on a human body in the freestream over an airspeed range typical for helicopter operations.

Due to the EPs being afforded some reduction in drag due to their proximity to the helicopter fuselage and not fully in the freestream, the force experienced is most likely less, but by an as yet unknown quantity. Regardless of the actual amount, the side force experienced by EP does constitute a fatigue factor so high as to render them incapable of optimum performance after even a relatively short duration of high speed flight.

This value also represents an increment of parasite drag to the helicopter itself, an increase that may only be overcome by additional power to maintain the given airspeed. To achieve perspective on the magnitude of performance degradation when operating with EP, an understanding of the MD-500 helicopter's normal drag area is required. Prouty [5] calculates the equivalent flat plate drag of the Vietnam War vintage U.S. Army OH-6A, the militarized variant of the present day MD-500. Taking into account all aircraft components, stationary and rotating, this helicopter presents 5.0 ft<sup>2</sup> of flat

plate equivalent drag area in a cruise attitude. The addition of an estimated 6.1 ft<sup>2</sup> of EP drag area increases the total by more than 120% per side.

The MD-500 RFM performance charts address the addition of drag while conducting sling load operations. These charts for Drag versus Torque, however, only accounted for drag additions up to +10 ft<sup>2</sup> of equivalent flat plate, therefore the following discussion will only consider power requirements for adding EP to one side of the aircraft.

The primary power indication for normal, sea level operations of the MD-500 is a drive train torque system that operates via an oil-filled “wet” line to a cockpit instrument, which measures that pressure in pounds per square inch (psi). The maximum power limit on the MD-500 engine and drive train is 87 psi at an engine output of 270 shaft horsepower (shp).

The addition of 6.1 ft<sup>2</sup> of drag area during cruise flight at 80 knots indicated airspeed (KIAS) creates an added power requirement of +6 psi of torque. This equates to an 18 shp increase, or 6.7% of total horsepower available. This additional power requirement is doubled with EP on both sides, resulting in a 13% reduction in performance. Flight at 100 knots results in performance penalties of up 15% or 30%, for one- or two-sided EP flight, respectively.

Although only a byproduct of the human factor concerns driving this project, the potential for a reduction of total parasite drag as the air flow was diverted away from the high  $C_D$  external passengers by the relatively low  $C_D$  deflector of nearly equal surface area was of great interest in this investigation.

### ***Temperature Effects***

The deleterious effects of personnel exposure to the combination of high wind speeds and low temperatures are potentially more damaging than the air load effects discussed previously. While the drag forces experienced due to air loading resulted in a marked reduction in task performance, exposure to the slipstream may also cause either hypothermia or frostbite.

The normal core body temperature is typically 37.5°C. A person whose body core temperature falls by as little as 2.5°C is in the early stages of hypothermia. Hypothermia is a condition in which the body loses the ability to self-regulate core temperature. In addition to the mental confusion and physical fatigue associated with the early stages, hypothermia is a life threatening condition if it persists. Frostbite is another physical danger to EP operations. While typically not life threatening, it does result in reduced task capability.

Both hypothermia and frostbite onset are aggravated by wind effects, at any temperature. The National Oceanographic and Atmospheric Agency (NOAA)/National Weather Service (NWS) state that the “wind chill” effect is caused, in part, by the forced evaporation of moisture due to high mass flow of air. As portrayed in the NOAA/NWS Wind Chill Chart (Figure 10), the perceived temperature in otherwise moderate conditions are capable of provoking onset of either hypothermia or frostbite. Using the equation



# NWS Windchill Chart

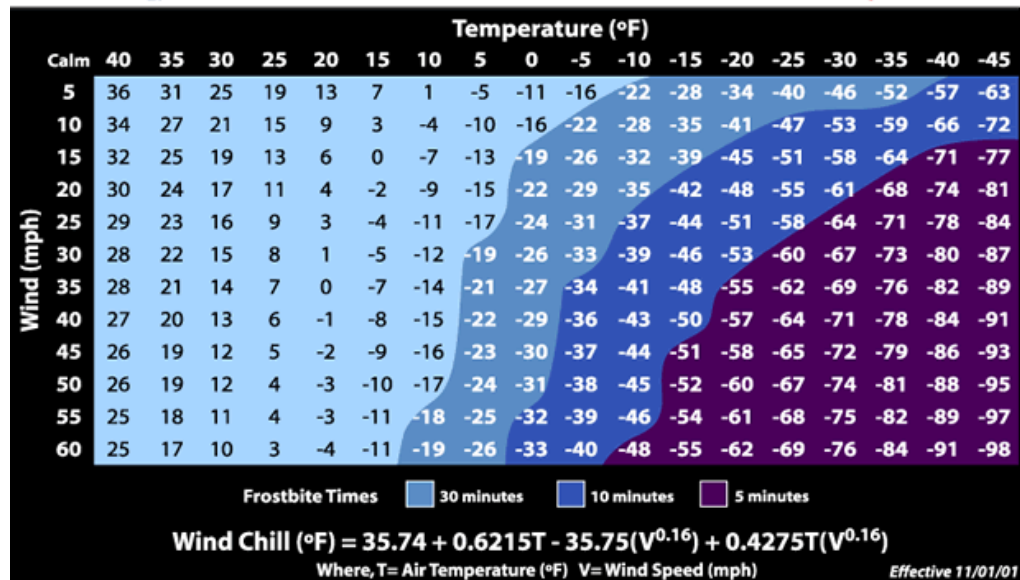


Figure 10. NOAA/National Weather Service Windchill Chart

depicted on the NOAA/NWS chart to calculate the wind chill effect at sea level standard temperature of (59°F), at an airspeed of 115 mph (100 knots), results in a perceived temperature, or wind chill factor, of 48°F in dry conditions. If the flight exposes the EP to liquid precipitation, both the effect and the danger are heightened.

## Deflector Design

The configuration selection process began with a review of the recommendations of McDougall [10] and Lewis [12]. Primary consideration was given to the appropriate deflector angle (referenced to aircraft centerline), width (from leading to trailing edge of the actual deflector) and overall length (from forward lower to upper aft edges) (Figure 11).

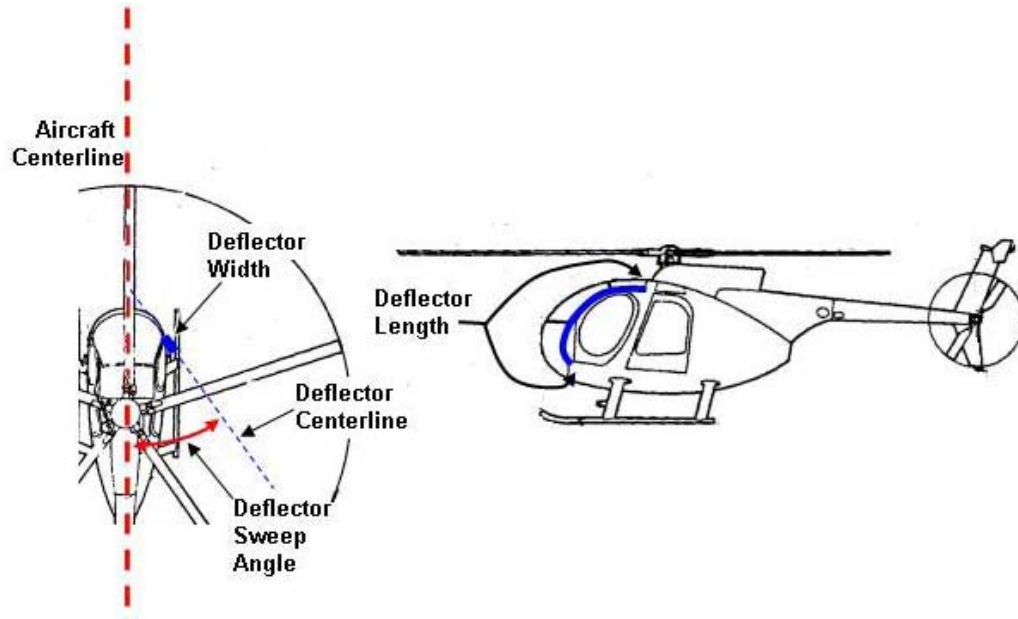


Figure 11. Wind Deflector Principle Dimensions and Location.

### ***Deflector Sweep Angle***

McDougall indicated that the optimum angle derived from his flight test was between  $40^\circ$  and  $50^\circ$ . Lewis' wind tunnel recommendation from wind tunnel tests was for deflector angles between  $49^\circ$  and  $55^\circ$ .

In the OH-58A+ study, one variable sweep deflector was built with a piano-type hinge at the leading edge that allowed for adjustment of the overall deflector sweep angle. This option was used as the leading edge of the OH-58 crew door frame describes a nearly straight line. The MD-500 crew door frame is described by a three dimensional compound curve of varying radius that precluded any type of hinged variable sweep device. Fabrication complexity due to forward fuselage curvature and time constraints dictated that building only two fixed-angle configurations was feasible.

Close review of Lewis' data indicated that lateral deflection of airflow approached maximum near the lower end of the recommended range, but drag continued to increase as the angle increased. This observation, together with McDougall's recommendations, guided the decision to fabricate deflectors with sweep angles of 40° and 50° with respect to the aircraft centerline.

### ***Deflector Width***

The flight tests on the OH-58A+ were conducted with a maximum deflector width of 8 inches. The wind tunnel MD-500 deflectors were built at 1/8 scale in widths ranging from 1 inch to 4 inches. Aerodynamic scaling issues precluded a simple increase in these widths by a factor of eight; however, this did suggest that widths greater than the 8 inches used in the OH-58A+ test may be desired.

Inspection of the cockpit crew doors indicated that at the selected deflector angles, any width greater than 12 inches, would constitute an unacceptable field-of-view (FOV) and emergency egress hazard. Twelve (12) inches was selected as the widest deflector size. In order that a suitable range of data was generated from which valid conclusions might be drawn, additional widths were required to supplement the two selected angles. The deflectors would started at 12 inches and then were down in 2 inch width increments after each data flight to 10 inches, and then 8 inches. This process resulted in six deflector configuration combinations for test flight.



### ***Deflector Length***

The deflector length was defined as the overall measurement from the forward lower edge to the trailing upper edge. The forward lower point was established by available mounting points near the forward lower corner of the crew door frames. Overall deflector length was adjusted by varying the location of the trailing edge only. Drag data from Lewis indicated that deflectors with longer characteristic lengths experienced less parasite drag for any given configuration.

This observation led to the decision that the deflectors fabricated for this project should be as long as practicable. There was a provisional fuselage hard point on the MD-500 fuselage at the approximate mid-point of a line extending between the apexes of the crew and passenger doors on each side. This hard point is typically used for attachment of the rescue hoist or rappelling hardware used in many EP applications. The trailing edge of all deflectors was fixed to a point approximately three inches forward of this hard point.

### ***Airframe Integration***

The MD-500 fuselage is rounded from all aspects. This complex shape limited the airframe integration options. The deflectors were required to be mounted as far forward as is possible, and the factory design provided a ready solution for attachment. The aircraft windscreen and chin bubbles are

affixed to the fuselage along their trailing edges on each side with 36 aircraft grade (AN526) 6-32 steel machine screws with elastic lock nuts (Figure 12). An inspection of this fuselage element revealed that it is a reinforced, multi-layer structural member. The RFM states it is an integral part of a crew compartment “roll cage” designed into the fuselage. This structure was deemed capable of sustaining the deflector’s anticipated loads, particularly when distributed along the entire attachment length.

Determination of the centerline reference for deflector sweep angle required accurate measurement of the local fuselage sweep angle at the point of attachment. The frame of the aircraft battery compartment located in the floor deck of the cockpit left side was used as a true reference for aircraft centerline.

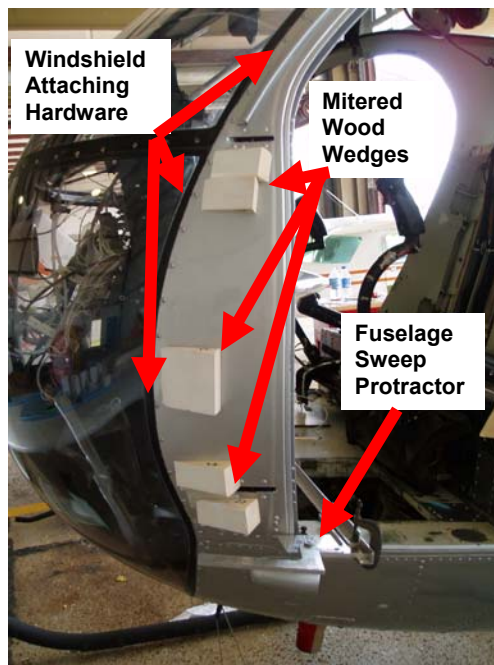


Figure 12. Determination of Attachment Point and Deflector Sweep Angle

A protractor device was fabricated and mounted across this frame (Figure 8). The fuselage local sweep angle at the line of the windshield attaching screws was measured as variable from 17° to 19° from the bottom of the crew door frame to the upper door hinge socket. This region was considered critical for deflection angle because, when viewed from the front, all of the EP torso and head in a seated position falls between these two points.

The decision was made that the deflector sweep angle would be washed out beginning immediately above the upper crew door hinge pocket to minimize crew FOV and egress obstructions. The wash out was at a rate such that the characteristic deflection angle at the upper hinge pocket is smoothly and progressively increased until it becomes parallel to the cockpit floor deck at the apex of the crew door frame. The cockpit floor was chosen as the washout reference because it is approximate parallel to the flight path in cruise. Setting the upper, washed out portion of the deflector parallel to the cockpit floor aligned it with the cruise relative wind and minimized both air loads and drag. Beyond this point of full washout, the angle remains constant with the deflector parallel to the floor deck for the remainder of its length. With the local sweep angle known for the critical deflection area, the additional angle offset required to achieve the desired 40° and 50° was easily calculated. Wooden wedges were cut using a compound miter saw and affixed with two-sided tape to the fuselage skin immediately aft of the windshield attaching hardware (Figure 12).

The original concept of an entirely composite deflector, including an integral attachment flange, was altered at this point due to the complexity of the task of building a mold to accomplish this task. An alternate method of fabricating a leading edge fixture from aluminum sheet metal was selected as the most practicable. This selection obviated the requirement to produce molds for the composite deflector structure but required that the composite sandwiches be layed up in place, on the aircraft, in order that they would conform to the leading fixture geometry.

The opportunity to increase the overall stiffness of the deflector assemblies was used by building additional support structures that made use of the two crew door hinge sockets located immediately aft of the windshield attaching hardware. Figure 13 shows the full componentry of the airframe integration.

### ***Material Selection***

The primary concerns in the design and fabrication of the deflector were airworthiness, strength and stiffness. For these reasons, all hardware to be used for attachment were restricted to aircraft grade (AN) steel machine screws, washers and locking elastic nuts.

All metal parts were fabricated from Alcoa, Incorporated aerospace aluminum alloy Alclad 2024-T3 [17] for its superior combination of strength and light weight. Various thicknesses of the 2024 products were used for the deflector mounting and attachment, with the rationale to always use the greatest thickness from which the individual part could be reasonably fabricated.

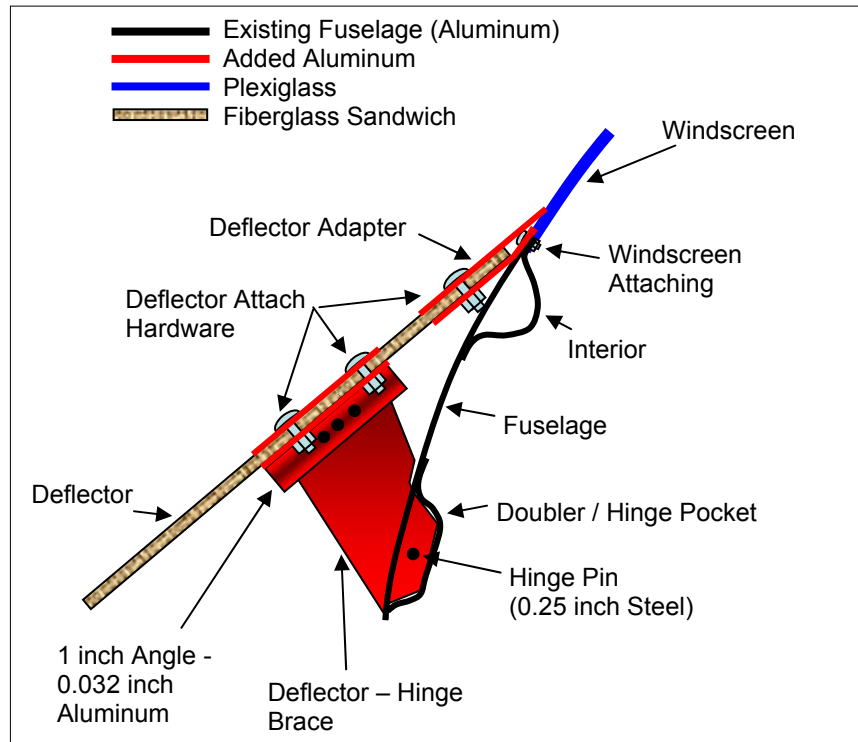


Figure 13. Deflector Airframe Integration Diagram

The optimum wind deflector composition was determined to be a foam core, fiberglass sandwich construction. Many options were investigated for the foam core material. A primary concern in foam selection was the flexibility required to conform to the compound curve of the aluminum leading edge fixture. Of equal importance was the necessity to ensure that the foam core material would provide a strong bond to the epoxy resins. Dow Chemical Company's BlueCor® extruded polystyrene foam sheet of 0.375-inch thickness. Performance specifications stated on the Dow webpage [15] indicate that this product, in addition to being inexpensive and readily

available, met or exceeded all of the deflector strength, flexibility and bonding requirements.

Multiple products were available which met the requirements for the fiberglass to be used for the composite sandwich. Bidirectional glass fabrics are known for high stiffness, once cured, and are often used for aerospace applications. A fabric manufactured by Hexcel, Incorporated, Model 7725 [16] was investigated for use in this project. This product is constructed as a twill-type weave with alternating fiber bundles lying perpendicular to each other. The twill weaves typically result in high strength and stiffness when alternate layers of fabric are layed up at a 45° bias to each other during construction. The Model 7725 fabric is widely used by aviation homebuilders for fuselage components, lift producing surfaces and control surfaces. This product was initially developed for use as a whole aircraft solution for the Rutan Vari-Eze aircraft. Deemed a suitable selection that met all requirements, the Hexcel Model 7725 fabric was chosen for deflector development.

The resin/hardener combination to set the fabric layers selected is the EZ-Poxy 10 epoxy adhesive. This material provides an acceptable level of strength and stiffness [18] and has a usable pot life of two hours at average temperatures. This epoxy is widely used and endorsed by virtually all of the major homebuilt aircraft manufacturing companies in the United States.

The final material requirement was for a deflector edge filler. A mixture of flocked cotton fiber and epoxy was used to fill the edge gaps, provide a strong bond between the two surfaces of the deflector and enhance overall stiffness.

## **Deflector System Fabrication**

### ***Leading Edge Fixture***

The leading edge fixture was fabricated by hand, in place on the aircraft, using 0.025 inch Alclad 2024 T-3 aluminum sheet. This thickness was chosen primarily for its relative ease of hand working.

Strips of approximately 4 inch width were sheared and bent to the required fuselage offset angles of 22° for the 40° deflectors and 32° for the 50° deflectors. The compound curve and variable radius of curvature resulted in significant buckling of the aluminum strip as it was forced to follow the row of windshield screws. These forces were relieved by cutting slits as necessary along the leading and trailing edges that allowed the strip to curve and preserve the approximate desired angle. Once the entire strip was affixed and trimmed to relieve all of the buckling forces, all cuts were stop-drilled to prevent cracking. The wooden wedges were then replaced between the fuselage skin and underside of the aluminum strips. The miter cut wedges were used to set the exact angle for each of the strip sections, which were then clamped into place and riveted together into a single unit (Figure 14). Number 3, flush-mounted aluminum alloy rivets were used to ensure that the composite fibers of the deflector would not be damaged by protruding rivet heads or sharp edges.



Figure 14. 40 Degree Leading Edge Fixture.

### ***Deflector***

The fabrication of the deflector began after completion of the aluminum leading edge fixture, which served as a jig for size and shape of the foam core. The foam sheeting was light weight and easily cut with a standard razor blade. Initially, a sheet section was cut by eye that approximated the shape of the deflector. The approximate form was affixed to the leading fixture using two-sided adhesive tape and trimmed to the shape desired (Figure 15).

As the widest deflector dimension was set at 12 inches, the leading edge was cut to an exact match of the leading edge first, and then the trailing edge was trimmed to roughly 14 inches of total width from end to end. The final length of the foam blank was 6.5 feet. This caused the pattern shape to cross two of



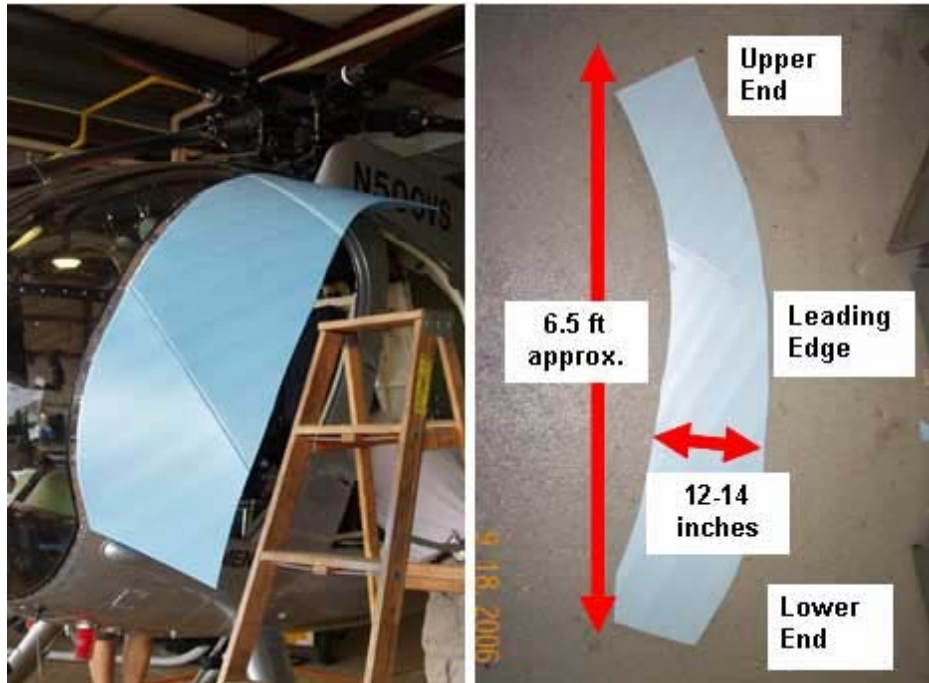


Figure 15. Deflector Shaping and Approximate Dimensions.

the deeply creased folds in the material. In producing the test section, the problem of covering the creases was investigated. The unprepared creases resulted in large, unacceptable voids under the surface of the fabric due the liquid epoxy flowing prior to curing. A paste of epoxy and glass bubbles was prepared and used to prepare other creases, and then it was covered prior to the paste curing. The result was that the epoxy paste and that used to wet the fabric bonded together in a single unit that remained viscous enough to preclude the formation of air bubbles under the surface. A single sided test section was produced using the paste filler and covered with three layers of fiberglass fabric. The fabric bond to the foam surface appeared acceptably strong. The single sided unit retained a great deal of flexibility and could

bend up to 45° on a one-foot radius with no indications of debonding or cracking.

The first full deflector sheet was prepared with the glass bubble paste along all creases and other surface imperfections and then covered with three layers of fiberglass. Each layer of fabric was set at a 45° bias to the previous underlying layer. A top layer of high thread count polyester fabric or “peel ply” was applied to the top layer of glass fabric. The epoxy cannot bond to the polyester fabric, but the fabric does serve as a wick to extract excess epoxy. Another benefit to the “peel ply” was that, after curing, it may be peeled off the article leaving a smoother finish than the glass fabric alone. The entire sheet was then squeegeed to remove as much excess epoxy as possible, and allowed to cure flat on a table for 24 hours. A sample of the epoxy used for this sheet was retained and checked that it had cured to full hardness the next day.

The single sided deflector sheet was trimmed of all excess fabric around the edges and mounted to the airframe leading edge fixture. Because the other side of the sheet would have to be allowed to cure while mounted to the helicopter, the side already fiberglassed was mounted to the inside. This provided for a “gravity assist” for maintaining the fabric on the outside in place while it cured. Fifteen matching holes were drilled through the single sided deflector and the leading fixture for mounting. The fuselage and windscreens were covered with self-adhesive plastic sheeting (commercially available shelf liner) to minimize epoxy exposure.

The reverse side of the deflector sheet was then prepared as previously discussed, and covered with three fabric layers on alternating 45 degree bias to each other. Two additional layers were added to this surface to increase overall stiffness and reinforce the attachment bolt holes. Both of these layers began at the leading edge, encompassing the bolt holes. The first extended from the leading edge to 50% width, the second to 33% width. A layer of peel ply was added to this and the excess epoxy was cleared with a squeegee. A razor blade was used to cut the peel ply and an awl was used to clear the glass fabric fibers from the pre-drilled holes to allow passage of the attaching bolts.

The deflector sheet was then mounted to the leading edge fixture. Large flat washers were used on all bolts, and extreme care was exercised to minimize crushing of the foam core under the bolt heads by over-tightening.

The following day, the deflector was removed from the aircraft and stripped of peel ply. It was noted that a significant number of bubbles had formed under creases in the peel ply that would require sanding prior to painting. Excess glass cloth was trimmed from around the edges with a band saw and the exposed foam at the edges were trimmed out with a routing tool to an approximate depth of 0.375 inches. The edges were then filled a paste made from epoxy and flocked cotton fiber. After curing for an additional 24 hours, the filled edges were sanded smooth and the deflector was remounted. Crush tests were performed on test sections to determine the maximum



Figure 16. Prototype Deflector Mounted on MD-500 with Simulated EP.

permissible torque for the attaching hardware. Torque on the mounting bolts was limited to 10 foot-pounds to preclude crushing of the core material. The result of the composite sandwich deflector and the metal fuselage attachment fixture proved to be very light and strong (Figure 16).

Four sets of deflectors were produced: two at 40° and two at 50° sweep angles. Two sets of each were produced in support of the plan to cut the width down in 2 inch increments after each test. Deflector width was measured from the most forward point of curvature of the deflector attachment along a line parallel to the manikin seat bench to the trailing edge (Figure 16). A plumb laser line parallel to the vertical plane bisecting the helicopter fuselage was then drawn through the desired trailing edge width at the reference point. The trailing edge was cut as defined by this line.

### ***Hinge Brace***

A necessary element of the test plan for the wind deflectors was the conduct of a handling qualities rating (HQR) tests. Adverse handling qualities resulting from installation of the deflectors could render the devices unusable, regardless of their other benefits. A full HQR evaluation requires a critical azimuth test in which the helicopter is flown at airspeeds up to 35 knots along each 45 degree increment of azimuth relative to the nose. One half of these directions consequently have a rearward velocity component, and cause the deflectors to act more as flow “scoops” rather than diverters. The concern in this scenario was that the forces applied to the inner surface of the deflector might be sufficient to peel the entire device off the mounts.

Again, available fuselage attachment points provided a solution. The crew doors were easily removable by a crew accessible hinge pin in the cockpit. With the doors off, the pocket in the exterior fuselage skin and its supporting structure and pin were unused. The concept was to take further advantage of this structure to provide additional bracing for that section of the deflector that presents the largest drag area to the slipstream. While the original impetus for incorporation of the hinge braces was a rearward flight concern, there were added benefits for forward flight and deflector stiffness.

The existing hinge pockets were large enough to accommodate 0.25 inch aluminum flat stock so Alclad 2024 T-3 of that thickness was used to fashion the main brace. This aluminum piece was cut to fit each individual hinge pocket and drilled to accommodate the existing steel hinge pin. A one-inch



Figure 17. Left Lower Hinge Brace Installation.

angle made of the same alloy in 0.032 inch thickness was riveted to the outboard end of the brace to provide a larger surface area for attachment to the deflector (Figure 17).

Upper and lower hinge braces were produced for each side and deflector sweep angle. When inserted, the hinge braces fit under the aluminum leading edge fixture to which the deflector was attached. This configuration allowed for the one-inch angle of the hinge brace to be riveted to the leading edge fixture, further reinforcing the entire structure (Figure 17).

### ***Leading Edge Fairing***

The composite sandwich of the deflector was approximately one-half inch thick and was mounted to the outer surface of the leading edge fixture. A

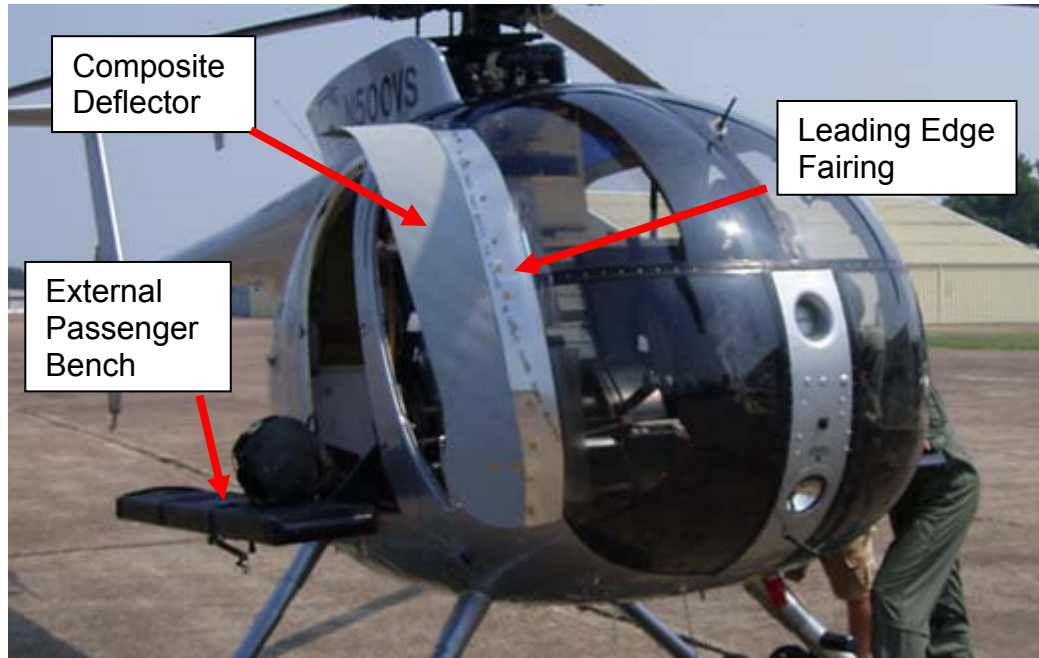


Figure 18. Deflector Fairing and Entire Deflector Assembly Installed.

solution to the added drag from this exposed leading edge was designed once the requirement was identified.

A single strip of 0.025 inch Alcad 2024 T-3 aluminum approximately 5 inches wide was cut to provide an aerodynamic fairing to cover this mounting area (Figure 18).

The fairing is retained by the same hardware as the deflector; with the bolts passed through the fairing, the deflector and then the leading edge fixture before being secured with locking elastic nuts. The fairings were for drag reduction only and provided no structural support to the deflector system. During the incorporation of the fairings, the decision was made to transition from hexagonal-headed bolts for deflector attachment to flat headed,

countersunk machine screws with finishing washers to further reduce drag from the mounting system.

### ***Gurney Flap***

A Gurney flap was planned for addition to the final, optimum deflector configuration after the initial round of flight tests. Gurney flaps are small plates placed perpendicular to the flow at the trailing edge of an airfoil. These flaps generate additional flow turning due to an increase in the effective camber of the airfoil. In the case of an airfoil, a pair of counter-rotating vortices are created in the area of separated flow immediately behind the flap (Figure 19). Because of the flow turning upstream by the flap itself, the vortex on the flap side typically extends above the upper edge of the flap which further turns the flow. In the case of the non-lift producing deflector, it was

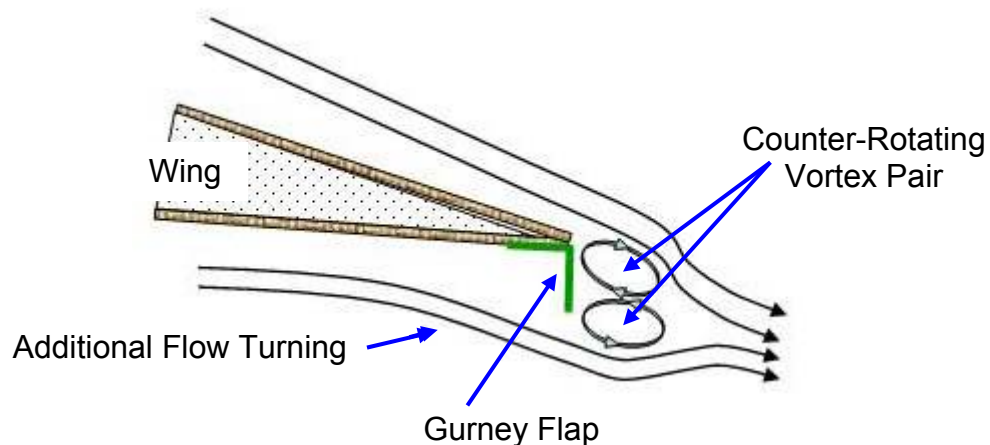


Figure 19. Gurney Flap on an Airfoil Trailing Edge.



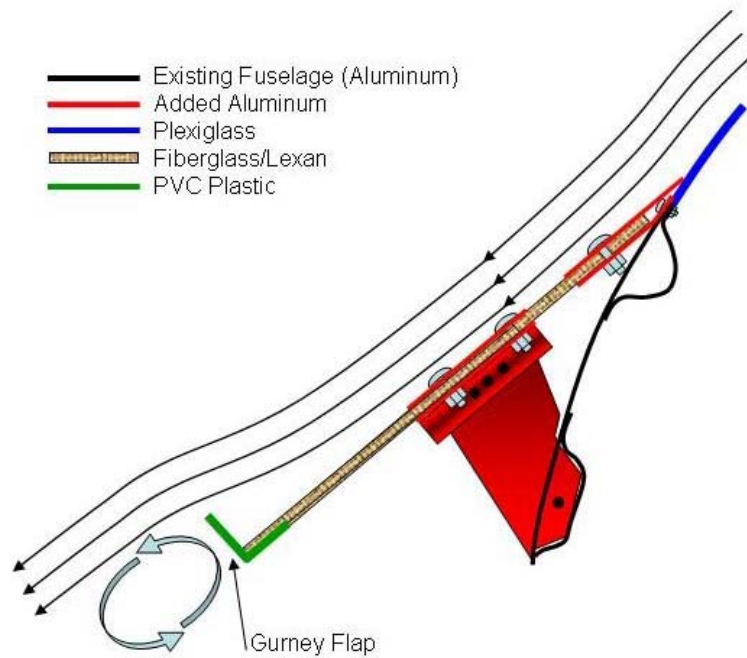


Figure 20. Gurney Flap Deflector Installation and Potential Performance Enhancement.

predicted that the flow would lift off of the flat deflector surface and create an additional lateral displacement of the flow away from the EP with little or no drag penalty (Figure 20). It was anticipated that only a single, larger vortex would form behind the flap as the deflector only has flow along one surface.

Two factors affect the overall performance of an airfoil with a Gurney flap: the height of the flap and its location. As the flap size is increased, increases in both lift and drag occur. Drag increases are negligible as long as the upper edge of the flap does not extend beyond the local boundary layer thickness. Also, as the location of the flap is moved closer to the leading edge of the



Figure 21. Measurement of Deflector Characteristic Length.

airfoil, the Gurney flap becomes less effective. Gurney flap installation at the trailing edge allows for maximum height without drag penalty due to the increased boundary layer thickness and maximum effectiveness in flow turning. as a result of the greater height. Determination of the height of the Gurney flap required calculation of boundary layer thickness at the deflector trailing edge.

Boundary layer thickness is a function of Reynolds number ( $Re$ ).  $Re$  is a function of characteristic length. Because the deflector was designed as near as possible to a seamless extension of the existing forward fuselage, the combined distance was deemed as the most appropriate measure for characteristic length (Figure 21).

For ease of fabrication, the Gurney flap was made from a white one-inch plastic 90°-angle corner molding strip. Further aiding fabrication, the

determination was made that the entire length of the Gurney flap strip would be of the same height. This decision required that the shortest of characteristic lengths (Length A in Figure 21) was used to calculate the **Re** for a cruise airspeed of 80 knots to ensure that the Gurney flap did not extend upwards out of the boundary layer at any point along its length:

$$\mathbf{Re} = \frac{\mathbf{Inertia\ Force}}{\mathbf{Viscous\ Force}} = \frac{\rho V l}{\mu} \quad (\text{Equation 3})$$

where

- $\rho$  = Density of air
- $V$  = Velocity of air
- $l$  = Characteristic length
- $\mu$  = Viscosity of air

The resultant **Re** of  $3.5 \times 10^6$  was then used to calculate the boundary layer thickness using White's [23] **Re**<sup>-1/7</sup> equations for turbulent boundary layers:

$$\delta_{0.99} = 0.14(\mathbf{Re}^{-\frac{1}{7}}) \quad (\text{Equation 4})$$

where

- $\delta_{0.99}$  = Boundary layer thickness
- Re** = Reynolds number

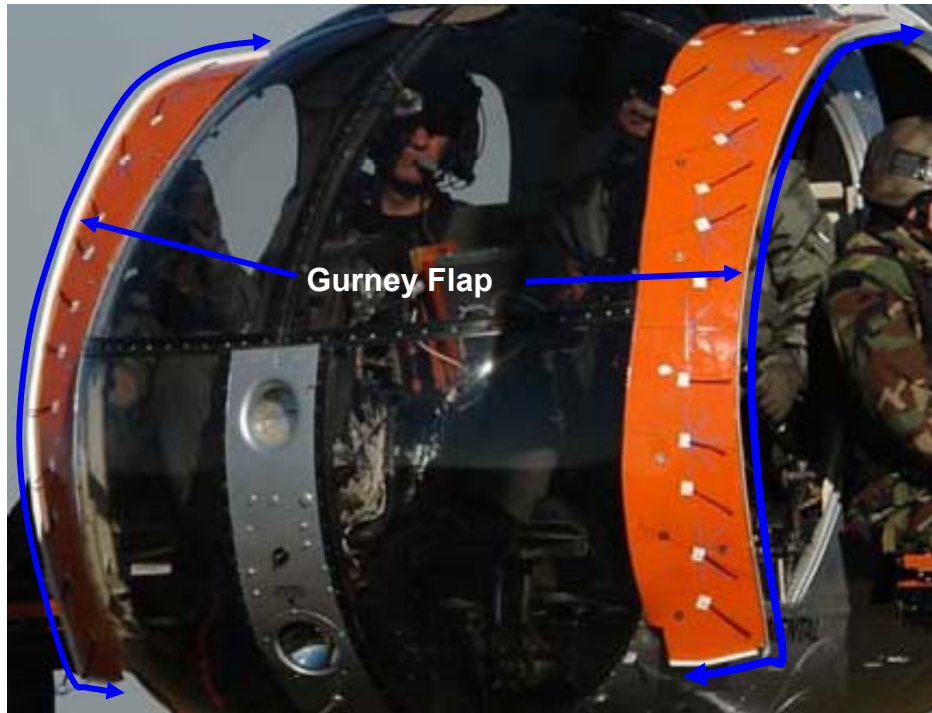


Figure 22. Deflectors with Gurney Flap Installed.

The  $Re^{-1/7}$  equation series was selected as it resulted in a slightly thinner boundary layer estimate of 0.81 inches, as opposed to the 0.89 inches obtained with the  $Re^{-1/5}$  series. This most conservative estimate was used because of the requirement that the Gurney flap not create a drag penalty by contacting the freestream above the local boundary layer.

The white one-inch plastic angle material used was mounted using commercially available fabric reinforced adhesive tape to the inner surface of the deflector along the length of the trailing edge of the candidate deflector (Figure 22). Allowing for the 0.4 inch thickness of the deflector composite sandwich, this provided for a measured Gurney flap height of 0.55 inches above the outer surface of the deflector.

## **Structural Analysis**

The completed deflector assemblies were subjected to a basic structural analysis in accordance with Advisory Circular (AC) 43.13-2A [21] as part of the safety review. The schedule and resource constraints imposed upon the project precluded a more detailed review, but sufficient analysis was conducted to ensure a minimum acceptable level of safety.

### ***Static Structural Considerations***

During the fabrication process, three deflector test sections were produced in the same manner and to the same specifications as the full deflectors. Two of these sections were flat and measured one foot square; one was curved and measured two feet long by one foot wide.

The first flat section was subjected to a destructive tear out test of the bolt holes similar to those for mounting the full deflector to the leading edge fixture. Three separate holes were drilled through the section approximately one inch from the leading edge and fitted with the same AN526 10-32 hardware as used on the full deflectors. A double lasso of 0.041-inch stainless steel safety wire was then wrapped around the bolt head and lock nut. The other end of the lasso was attached to a calibrated spring scale capable of measuring up to 100 pounds of force. Full scale deflection of 100 pounds force was applied for 60 seconds to each set of hardware in succession. No tear out occurred and subsequent inspection of the holes revealed no measurable elongation.

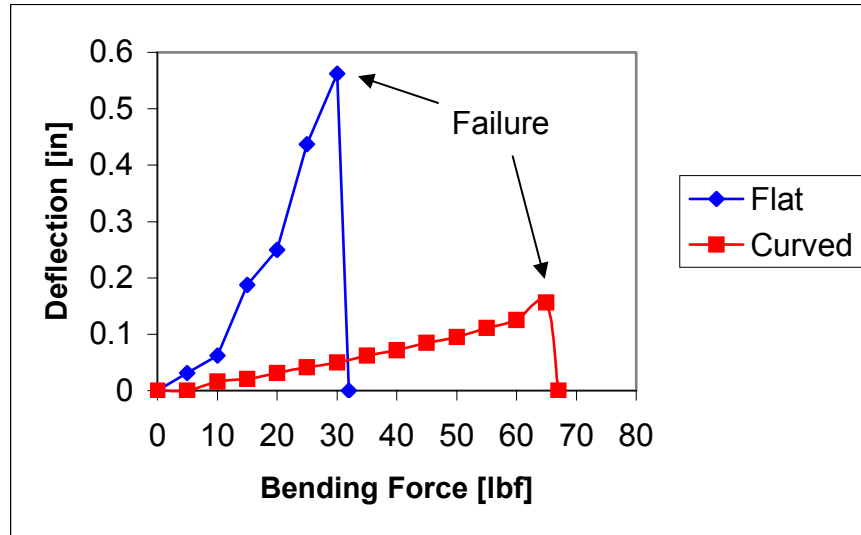


Figure 23. Results of Destructive Test of Deflector Sample Sections

The second flat section was subjected to a destructive bending test. The same 100 pound spring scale was used to apply a force at the edge of the test section while the opposite edge was fixed in a vise. The bending force was plotted versus deflection at the edge furthest from the vise for comparison of the two construction techniques (Figure 23).

The curved section, created by using a full 40° deflector as a mold, was subjected to the same bending test, with significantly different results. Force was applied to the convex side of the section to simulate load application in forward flight. The curved section had a much shallower yield curve, indicating much greater stiffness than the flat section. The stiffness imparted by the curvature also increased the overall strength of the construction. The curved section failed at 67 lbf, more than twice the 32 lbf required to break the flat section. Due to the nature of these destructive tests, the force was

applied as a point load and not widely distributed over the entire surface area, as would the in-flight air load.

A calculation of air loads on the deflectors was difficult, as it is a structure with complex curvature in a separated flow and with very few established precedents. The closest approximation found was Raymer's [19] approximation for the drag on the windscreen of an open cockpit airplane. Raymer states that the drag to dynamic pressure ratio,  $(D/q)$ , is approximately 0.5 per unit of frontal surface area for the open cockpit windscreen. Using this approximation, the drag area may be calculated once the frontal surface area of the deflector may be determined. The estimate of frontal surface area was made using photographs of the 40 degree 12 inch wide deflector mounted on the aircraft from straight ahead and 45 degrees to the side (Figure 24). A ruler was held in the field of view for scale, and an 8 by 8 grid representing one square foot was superimposed over the pictures. The results were 3.28 ft<sup>2</sup> for the full frontal view and 2.56 ft<sup>2</sup> for the oblique view, per side. Application of the Raymer  $D/q$  estimate resulted in a worst case drag area for the deflector of 1.64 ft<sup>2</sup>. The air load exerted upon this one deflector in forward flight at 80 knots was calculated to be approximately 35 pounds force distributed over the frontal surface.

Comparison of this estimate to the forces required to fail the curved test section suggests that in-flight static failure of the deflectors is extremely improbable. One final test was conducted to validate that the full installed

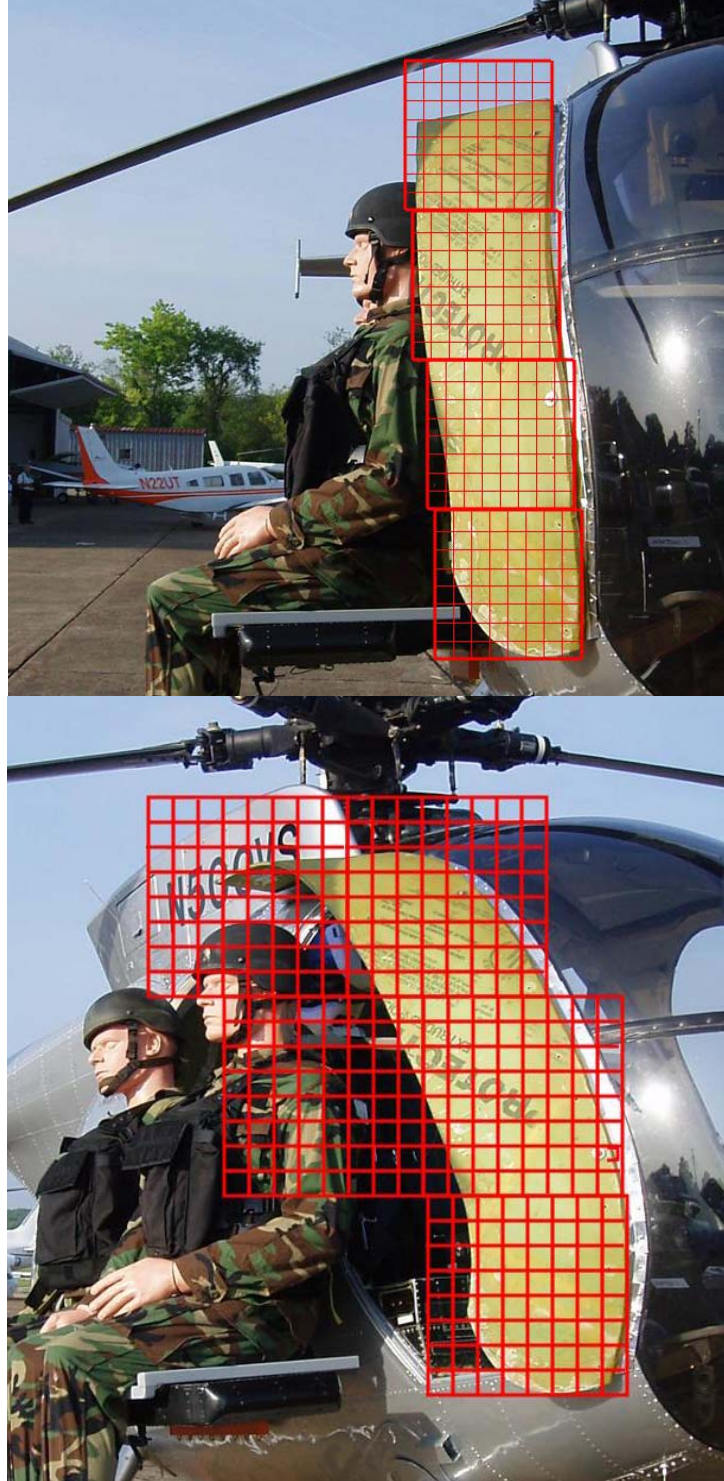


Figure 24. Deflector Frontal Surface Area Estimation (Front and Oblique).



deflector systems on the aircraft possessed the same strength exhibited by the test sections. Using the same calibrated spring scale, point loads of 50 lbf were applied at five separate locations on the outside edge of the deflector and three along the inside. Except for the upper outboard corner of each deflector, the displacement observed never exceeded 0.125 inch. At that corner location, the deflection was approximately 0.25 inch under a 50 pound perpendicular force application. This amount of deflection in test was deemed acceptable as this section of the deflector is approximately parallel to the slipstream. Because of this orientation, this area would never experience even a small fraction of 50 pounds pressure in any foreseeable flight condition.

### ***Dynamic Structural Considerations***

Dynamic response of the deflectors to the helicopter and air flow environment was difficult to predict. As stated previously, the deflector construction techniques were focused upon the need to create a form of great stiffness, as well as strength. High stiffness results in lesser response to oscillatory energy sources.

Due to the nature of rotary wing aircraft, there was a concern that the vibration of various aircraft rotating parts may have excited a natural mode of the deflectors. The possibilities range from mild separation flutter to the excitation of a natural frequency, where the worst-case scenario is an in-flight structural dynamic failure of the deflector. Any occurrence of structural failure

was categorized as unacceptable risk for flight test, as indicated in the detailed hazard analysis and risk mitigation log located in Appendix C.

Although neither the time nor the facility for a detailed vibration analysis of the deflectors was available, multiple approaches to determining vibration related failure potential were investigated. A qualitative natural frequency check was made by “hammer testing” various areas on the mounted deflectors. The amplitude and estimated frequency were noted for comparison to known system frequency generators. All areas on the deflector exhibited strong positive damping due to the rigidity of the materials and mounts. Any observed frequency responses damped out fully in less than one second. The upper, outboard corner of the deflectors exhibited the lowest frequency, the greatest response amplitude and the lowest damping. The frequency of this area was estimated as 250 Hz; the initial amplitude was 0.125 inch and took 1.5-2.0 seconds to damp to half amplitude. In the absence of further available methods to pursue this phenomenon, the deflector was cleared for flight and the in-flight response at the corner closely observed. Any vibration or flutter greater than 0.25 inch would be cause to discontinue flight.

Rotating aircraft parts ranging from rotor systems to powerplant to accessories were cataloged for their normal operating frequencies. Lower frequency subsystems deemed capable of achieving large amplitude displacements were considered with the main and tail rotor systems providing the greatest concern. Main rotor revolutions per minute (rpm) were published at 463 in the RFM, resulting in a frequency of 7.37 Hertz (Hz). The tail rotor

operated at 2923 rpm and a frequency of 48.7 Hz. The ratio of main to tail rotor frequencies was 6.6 Hz. These frequencies, and their first and second harmonics, are low enough relative to the observed frequencies of the deflector that possible coupling was considered unlikely. The deflectors were to be observed closely during all test flights for any type of adverse response. All other rotating parts were both low mass and very high frequency; therefore, their effects were deemed much less significant.

Another source of vibration energy was the possibility of vortex shedding by the deflectors. The shedding frequencies would be of concern if they occurred near any of the observed natural frequencies of the deflector. Possible coupling of shedding frequencies with helicopter rotating part frequencies was also appraised.

This estimation required an order of magnitude estimate of the deflector's natural vortex shedding frequency. While there was a large body of research in this field, the majority dealt with the behavior of various solid shapes exposed to a fluid flow. The sharp-edged discontinuity at the deflector trailing edge and the open fuselage may render any correlation to accepted principles difficult to establish. The nondimensional Strouhal number; a value that relates the vortex shedding frequency of an object to its characteristic length and velocity needed to be estimated for the deflector assembly. As numerous references cite a relationship between the Strouhal number and the Reynolds number of a given object, this method was used to arrive at a best approximation for the Strouhal number.

With the operating speed range of the helicopter known and the helicopter with deflectors available for direct measurement, the Reynolds number range could be established. Varying lengths from 4.5 to 7.25 feet and test point airspeeds between 40 and 80 knots, together with the properties of the standard atmosphere at Tullahoma Airport (field elevation 1083 feet) were used to calculate the range of possible Reynolds numbers ( $Re$ ).

The resulting Reynolds numbers were  $1.9 \times 10^6 < Re < 6.1 \times 10^6$  for all configurations and speeds called for in the test plan. In 1981, Achenbach and Heinecke [20] conducted an extensive investigation of the relationship of Reynolds number to Strouhal number for many common shapes (Figure 25). Although not an exact solution for the derivation of a true Strouhal number for

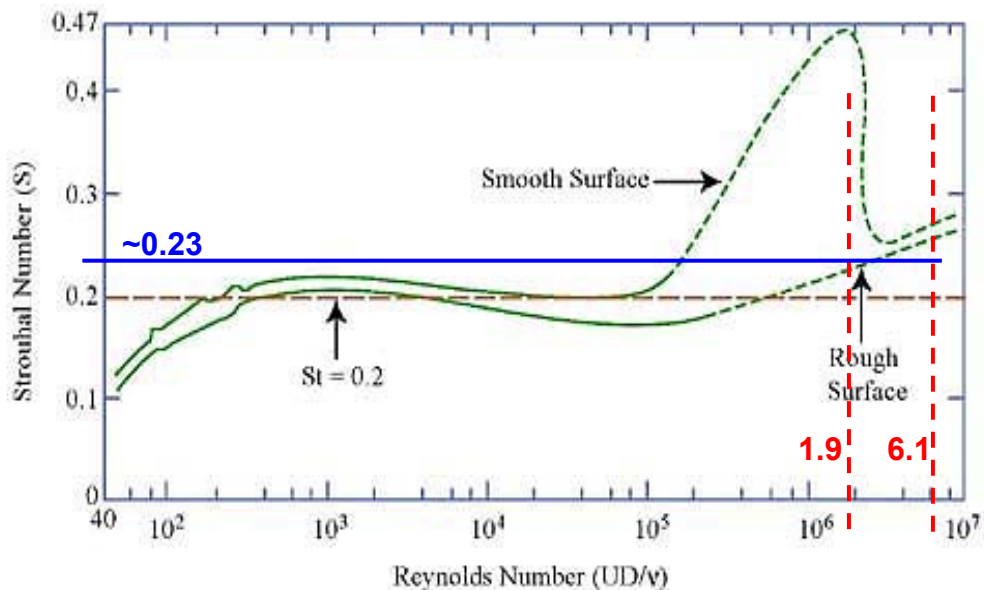


Figure 25. Reynolds Number versus Strouhal Number Relationship (Achenbach and Heinecke 1981).

the helicopter wind deflector geometry, the relationship depicted in Figure 25 allowed for reasonable estimate.

The overall surface area of the MD-500 forward fuselage and deflector are must be characterized as rough due the large number of exposed edges, open holes, attached equipment and screw heads. Entering the chart at the calculated Reynolds number values for the deflectors, an intercept of the “Rough Surface” curve yields an average Strouhal number of 0.22. This value was used for all further estimates of the deflector vortex shedding frequencies using Equation 4.

$$\omega = \frac{St V}{l} \quad (\text{Equation 5})$$

where

$\omega$  = Vortex shedding frequency

$St$  = Strouhal number

$V$  = Velocity of air

$l$  = Characteristic length

The calculated shedding frequency range was 2.0 Hz <  $St$  < 6.6 Hz. Recalling the main and tail rotor operating frequencies, and particularly the ratio of these two (6.6 Hz), some form of coupling was deemed probable.

As this analysis was performed after the production of the deflectors, little could be done to prevent this occurrence other than control measures already put in place. Three discrete design elements had been incorporated

specifically for their contributions to stiffness. These consisted of the hinge brace reinforcements, the additional layers of fabric beyond that which strength dictated, and the epoxy/fiber edge filling.

The dynamic analysis was considered complete with review of these concerns. The project test plan was laid out in a deliberate build-up process to reflect the unknown nature of the deflector devices and to maximize safety during conduct of all flights. The Final Flight Permit & Hazard Report detailing the evaluation of these concerns by both the design team and outside subject matter experts is located in Appendix C.

## CHAPTER IV DATA ACQUISITION AND RECORDING

### Data Acquisition Systems

#### *External Passenger Manikin System*

As the primary objective was to reduce the air load on the EP, the design and installation of an external seating system with instrumented manikins was chosen as the best solution. An aluminum bench seating system was acquired and mounted into the aft cabin of the aircraft. The rear doors were removed, allowing the benches to extend out through door openings, providing a location outside the fuselage for the EP simulator manikins (Figure 26). Although there was sufficient space for three full-scale human manikins on each side bench, due to helicopter weight limitations, only two were acquired for each side. The Rescue Randy Combat Challenge training



Figure 26. External Passenger Bench with Manikin Instrumentation.



Figure 27. External Passenger Manikins on Bench.

devices manufactured by Simulaids, Incorporated of Saugerties, New York were selected for the EP simulators. These manikins were constructed with an internal steel frame and steel cables covered with an approximately 0.25 inch thick rubber skin, and were primarily designed for fire fighting and rescue training where great strength and unit integrity were necessary. Due to concerns about flight hazard caused by flailing or other failures of the simulated EP, the Rescue Randy manikins were selected. The manikins were then dressed in bulky clothing and protective helmets on loan from a local military surplus establishment to simulate the additional drag area from equipment (Figure 27).

Since the forward manikin on each side would be exposed to the greatest air loads in forward flight, only those manikins were instrumented for force measurement. The aft manikin on each side was secured to the bench



without instrumentation. The forward manikins were secured to a force balance that consisted of low friction rollers and a tension load cell. The roller assemblies constrained the manikin displacement to the aircraft longitudinal axis, providing for a measurement of the drag force component created by forward flight.

As helicopter pitch attitude varies as a function of airspeed in forward flight, measurement of this parameter required a precision sensor system. An Attitude Heading Reference System (AHRS) was installed to provide an accurate pitch source. The pitch attitude measurement allowed for load cell reading to be corrected for that component of the manikin's weight along the longitudinal ( $x$ ) axis when the aircraft was in either nose up or nose down attitudes.

The manikin drag force was the parameter that generated the greatest concern. The primary objective of the deflector project was to relieve the longitudinal force perceived by an external passenger in forward flight. The force on the EP is predominantly aligned along the aircraft  $x$ -axis. Due to helicopter flight characteristics, the  $x$ -axis force is not the sole component of EP drag.

Helicopters experience pitch attitude changes as a function of airspeed in straight and level, trimmed flight. A vertical, or  $z$ -axis, component is introduced at any pitch attitude other than that at which the EP bench is aligned with the velocity vector. This component breakdown does not effect

the total drag on the EP, but it does effect the value measured by a sensor constrained to the  $x$ -axis.

Single rotor helicopters exhibit an inherent sideslip relative the aircraft centerline in forward flight. This angle occurs because of the orientation of tail rotor thrust. In helicopters manufactured in the United States (U.S.), the main rotor turns counter-clockwise as viewed from the top. The torque of the main rotor results in a yawing moment to the right, which is countered by the tail rotor thrust. In addition to producing the anti-torque moment required for directional control, the tail rotor thrust also imparts a force aligned with the helicopter lateral, or  $y$ -axis. In the case of U.S. helicopters like the MD-500D, this force will cause the aircraft to translate to the right, unless checked by a counterforce. The tail rotor side force is compensated for by a left lateral force generated by the main rotor, through flight control rigging, pilot flight control input, or a combination of the two. The resultant of these two lateral forces is the helicopter inherent sideslip. The inherent sideslip, therefore, provides for a contaminant in the single axis manikin force measure by introducing a lateral force. The inherent sideslip also had the potential to create asymmetrical manikin load cell readings.

The introduction of these additional forces, plus moments in all three axes generated by flight instability, has the potential to create coupling effects on the single axis force measurement system. The other unknown, but foreseeable, contaminant in the manikin longitudinal force measurement would actually be caused by the deflectors. The two potential deflector based

causes for data dispersion were the cyclical vortex shedding or random effects of a turbulent wake. A full investigation of these effects was beyond the scope of this project.

The ability to instrument the manikin for 2- or 3-axis force measure was investigated, and a 2-axis ( $x-z$ ) system was determined to be feasible, although of considerably greater difficulty to implement. Therefore, the decision was made to install the single axis roller system initially. Calibration data for these systems is located in Appendix B (Figure 35-36). A 2-axis ( $x-z$ ) system was planned to validate the conclusions drawn from the single axis system data. Data related in this thesis is limited to that generated by the single axis system, as that from the two-axis system never became available.

### ***Flight Data***

The second objective of the test was to determine if there was a performance enhancement in use of the deflectors. An indication of the increase in performance could be inferred by a reduction in drag force on the forward manikins. A portion of the force relieved from the manikin, however, would be transferred to the helicopter airframe by the added drag area presented by the deflector.

To capture any performance changes, the following list represents the minimum parameters that were instrumented for this purpose.

- Pitot – Static Values (Ambient and Dynamic Pressure)
- Ambient Temperature (OAT)

- Main Rotor RPM (NR)
- Gas Producer RPM (N1)
- Turbine Outlet Temperature (TOT)
- Main Rotor Torque (Q)
- Fuel Flow

Sensors for these parameters were connected to a data acquisition system mounted in the aft cabin of the aircraft. This system could be triggered multiple times in a given flight to record all attached sensor parameters. Each recording was 5 seconds in duration and collected at a sampling rate of 100 Hz. Data was also hand recorded from ship instrumentation as a backup to the recorded data.

## **Data Reduction**

Data reduction was performed in accordance with procedures specified in the United States Naval Test Pilot School (USNTPS) Flight Test Manual (FTM) 106 [6]. Data reduced and presented for the purposes of satisfying the objectives of deflector design and optimization were limited to the following comparative relationships.

- Calibrated Airspeed versus Manikin Drag Force
- Calibrated Airspeed versus Main Rotor Torque
- Manikin Drag Force versus Main Rotor Torque

### **External Passenger/Manikin Force**

The total drag on the EP is of interest, but the perceived, human factor, effects are of greater importance.

Total drag is that discrete measure of the force provided by the forward flight air load applied to the manikin surface area as presented to the freestream. Cross-axis coupling effects caused by the total airspeed velocity vector orientation were considered; however, the design of the roller seat load cell assembly was selected specifically because of its limited susceptibility to cross-axis coupling effects. The three forces acting along the x-axis are drag, manikin weight component and the restraining force applied to the manikin mount by the load cell. The load cell restraining force in this test configuration served the same function as seat friction does for actual EP. In this simplified system, the sum of forces along the longitudinal axis may be calculated as:

$$\Sigma F_x = F_{LC} - D \cos \theta - W \sin \theta_{EP} \quad (\text{Equation 6})$$

where

$\Sigma F_x$  = Sum of forces along the **x**-axis

$F_{LC}$  = Force applied by load cell

$D$  = Drag force

$W$  = Weight of manikin

$\theta_{EP}$  = Pitch attitude of external passenger seat bench

Restating the primary objective provides a justification for a perspective on force evaluation. The primary objective may reasonably be restated such that the deflector must have a positive impact on external passenger task performance and exposure effects. The sum of forces perceived by the EP induces a physical workload requirement. This workload results in fatigue and a consequent degradation in performance of physically demanding tasks. This allows for a definition of Perceived Force as the sum of all forces experienced by the EP along the longitudinal axis ( $X$ ).

As already identified, these forces are the longitudinal air load force measured by the roller/load cell assembly, the manikin weight component due to gravity and seat friction effects. Because the load cell value being measured is, in fact, a summation of these forces, the use of the Perceived Force metric eliminates the requirement to correct the load cell value using Equation 5. The data presented in this report to select the optimum deflector configuration was uncorrected load cell, or Perceived Force ( $X$ ), as that was deemed most representative of the EP in-flight experience .

For purposes of capturing the manikin load cell measurements, the automatic data recording system was set to a sampling rate of 10 Hz during the instrumentation check out flight, with a data point recording duration of 10 seconds. A plot of the checkout flight data revealed significant scatter with the dispersion increasing as a function of increasing airspeed. The test pilot found it difficult to hold the exact data point flight parameters (altitude, airspeed, power, etc) for the entire 10-second recording time. In several

instances, the point was held for 6-7 seconds, but then drifted off point and induced data dispersion not representative of the deflector/manikin system.

Statistical methods were used to derive usable information from the scatter. Using the 10 second/10 Hz sampling schedule resulted in a sample of 100 points. One standard deviation ( $\sigma$ ) was found to contain points up to  $\pm 50\%$  of the mean value ( $\bar{X} \pm 0.5 \bar{X}$ ). While this did not preclude the formulation of subjective trend-type conclusions as to the efficacy of a given deflector, this wide dispersion would render the data scientifically unusable.

Data point recording time was reduced to 5 seconds to provide the test pilot with a more attainable standard for the flight data points. The sampling rate was increased to 100 Hz to provide a reasonably large sample of recorded values for analysis. This change to the data sampling resulted in more usable data. The  $1\sigma$  limits were reduced to approximately  $\pm 10\%$  of  $\bar{X}$ . Table 4 shows the effects of the data recording changes on the left load cell data dispersion for the baseline

**Table 4: Effect of Recording Method of Load Cell Data Dispersion**

Airspeed [KCAS]	10 second / 10 Hz		5 second / 100 Hz	
	Mean [lbf]	$\sigma$ [lbf]	Mean [lbf]	$\sigma$ [lbf]
40	18.12	2.68	16.78	1.58
50	20.95	2.89	21.59	2.45
60	32.13	4.05	30.90	3.40
70	41.43	5.58	42.99	4.25
80	56.89	8.15	57.13	4.90

configuration (no deflectors, two EP manikins per side). The different recording methods yielded similar median values across the range of evaluated airspeeds, but there was a significant in confidence that allowed the data to be used for quantitative, rather than qualitative, evaluation.



## **CHAPTER V**

### **RESULTS AND DISCUSSION**

#### **Design and Fabrication**

The wind deflector was successfully designed, fabricated, integrated and flight tested. The material choices were satisfactory in terms of ease of fabrication and absence of any material failure from flight. The first set of deflectors required approximately 310 man-hours to complete; the last was completed in less than 70 man-hours. In addition to the time and material savings of on each subsequent set, there was a marked increase in surface smoothness and contour quality.

#### **Safety Considerations**

Rectilinear Field of View (FOV) diagrams were produced for the deflector configurations which created the greatest and the least FOV restriction (Figures 28-29). The rectilinear FOV diagrams represent field of view from the pilot station design eye point  $\pm 90^\circ$  in azimuth and  $\pm 60^\circ$  in elevation. The black areas represent airframe obstructions, white areas are unobstructed fields of view, and the gray shaded areas represent the areas obstructed by the opaque deflectors. The opaque deflectors created a significant safety hazard due to reduction in pilot at the 10 and 12 inch widths. The 8-inch deflectors created some FOV restriction but not sufficient to constitute a safety hazard.

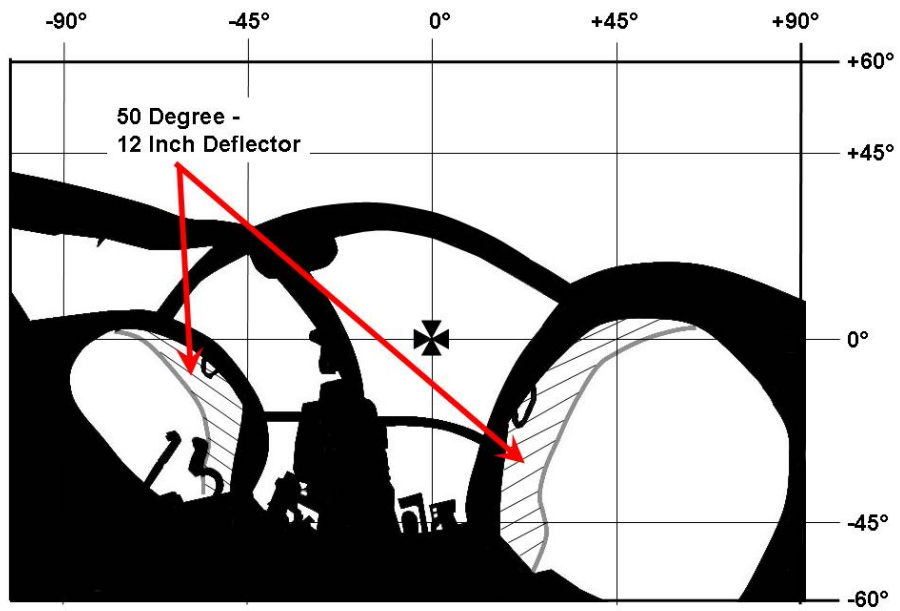


Figure 28. Rectilinear Field-of-View Diagram: 50 Degree 12 Inch Deflector.

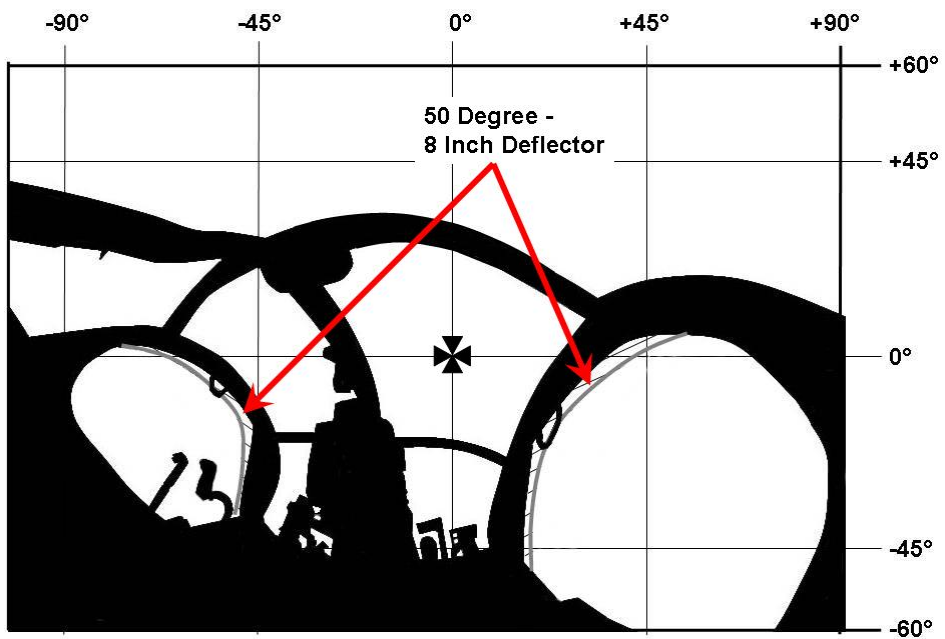


Figure 29. Rectilinear Field-of-View Diagram: 50 Degree 8 Inch Deflector.

An emergency egress hazard was created in all tested deflector configurations. This hazard was an artifact of the test configuration only and will not be as significant in actual EP operations. The egress blockage was created by a combination of the deflector and the rigidly mounted EP manikins. In the event of an emergency egress requirement with actual EP, the evacuation of the external passengers will clear the egress line for the aircrew and any passengers in the aft cabin. A generalization was made relating deflector configuration to egress; crew egress restriction was minimized with shorter deflector width and greater sweep angles. This was applicable to both the test configuration and actual EP operations.

### **Data Acquisition**

The load cell measurement of manikin longitudinal force contained a significant level of dispersion. The minimum and maximum of recorded values for any given data point was approximately  $\pm 30\%$  with respect to the sample mean ( $\bar{X}$ ). Statistical analysis showed that recorded values falling within one standard deviation ( $\sigma$ ) of  $\bar{X}$  for any given data sample was approximately  $0.12 \bar{X}$ . The 95% degree of confidence interval estimate for any data point population mean, however, was only  $\bar{X} \pm 0.5$  lbf. This indicated a fairly well defined central tendency of load cell readings that allowed for a statistically significant evaluation of individual deflectors. Further analysis in the time domain revealed the dispersion of the load cell as an organized, complex frequency response (Figure 30). The frequency

## Time vs. Left and Right Load Cell Values

Configuration: 2 Manikins per side  
Crew: Allison/Wright  
Gross Weight: 2994 lb  
Center of Gravity: 99.0 in

Pressure Alt: 850-1070 ft  
OAT: 8-21 °C  
Aircraft ID: N500VS  
Aircraft Model: MD-500D

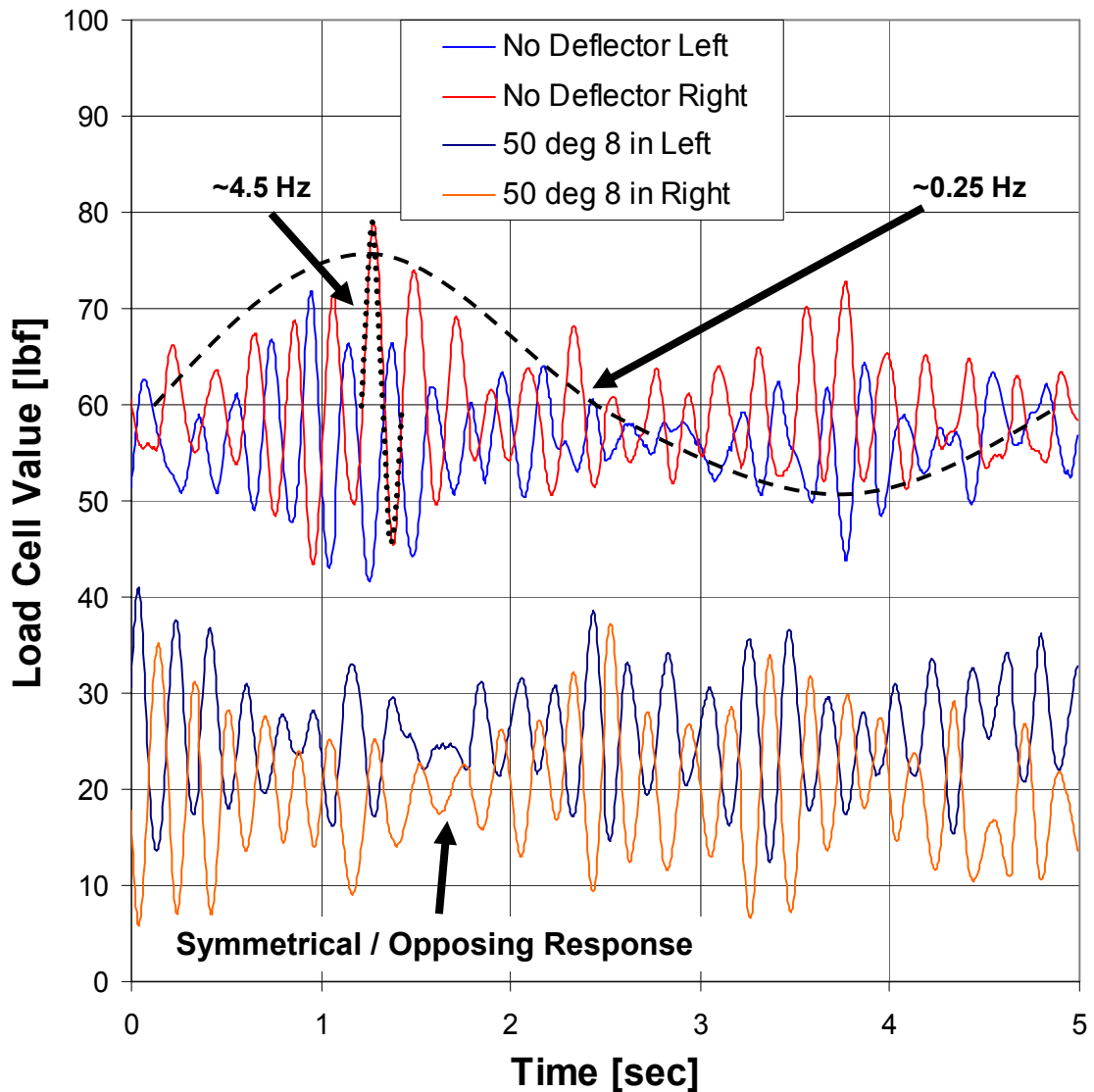


Figure 30. Time Domain Plot of Time vs. Manikin Load Cell Value.

behavior depicted is representative of all data points recorded. Prouty [5] states that all MD-500-series helicopters exhibit a non-suppressed lateral-directional oscillation (LDO) between 0.2 Hz and 0.4 Hz in forward flight. One component of the reciprocal magnitude force reading may be attributable to the yawing moment of this LDO. Additional sources of reciprocal, symmetrical effects may have been sole or coupled effects of any of the following: alternate vortex shedding by the deflectors, main and tail rotor frequencies or natural frequency response of the load cell strain gauge spring. The discovery that the load cell reading dispersion was in response to these unknown forcing functions afforded greater confidence in using the sample means ( $\bar{X}$ ) as an accurate measure of the deflector performance. The full nature and origination of these effects was, however, beyond the scope of this investigation. All other data parameters were hand recorded from ship instrumentation due to delays in integration of the data acquisition system.

### **External Passenger Air Load**

The deflectors were successful in meeting the primary objective of reducing perceived longitudinal forces on the EP manikins. The force reduction was not entirely symmetrical; the right side reduction was typically 3-5 lbf less than the left side. To represent the system as a whole, the sum of the sample means of the left and right forces measured were added into a single quantity and referred to as Total Mean Perceived Manikin Longitudinal Force ( $\bar{X}_T$ ). A

plot of Calibrated Airspeed (CAS) versus  $\bar{X}_T$  showed all deflectors produced force reductions on the manikins (Figure 31). Plots of CAS versus  $\bar{X}_T$  and  $\bar{X}_T$  plus and minus one standard deviation ( $\bar{X}_T \pm \sigma$ ) indicated that the difference between deflectors and no deflector was statistically significant (Figures 32-33). The ability to differentiate between the individual deflector configurations was, however, very difficult due to the similarity of results. In addition to manikin force reduction, the deflectors virtually eliminated the turbulent airflow in the cockpit caused by slipstream deflecting from the forward manikin as noted in the no deflector configuration.

The 50° 12-inch deflector provided the greatest longitudinal force reduction on the EP of 59% at 80 KCAS (Appendix A, Table 5), reducing it from a mean value of 62 lbf per side without deflectors to 24 lbf per side. This was a dramatic result, far beyond expectation, and will have significant favorable impact on EPs.

The differences in the performance of the remaining deflectors approached statistical insignificance. This fact indicated that, all other things being equal, an 8-inch deflector was the most logical choice when the minimum impact on FOV and egress were considered.

At 80 KCAS, the 40° 8-inch deflector provided a reduction of 39% over the no deflector baseline values for total perceived longitudinal manikin force (Appendix A, Table 5). The 50° 8-inch deflectors create reduction of 44% for that same parameter (Appendix A, Table 5). The quantitative values being nearly equal, but slightly favored the 50° 8-inch variant. The fact that the 50°

## Airspeed vs. Total Manikin Force All Deflectors

Configuration: 2 Manikins per side  
 Crew: Allison/Wright  
 Gross Weight: 2994 lb  
 Center of Gravity: 99.0 in

Pressure Alt: 850-1070 ft  
 OAT: 8-21 °C  
 Aircraft ID: N500VS  
 Aircraft Model: MD-500D

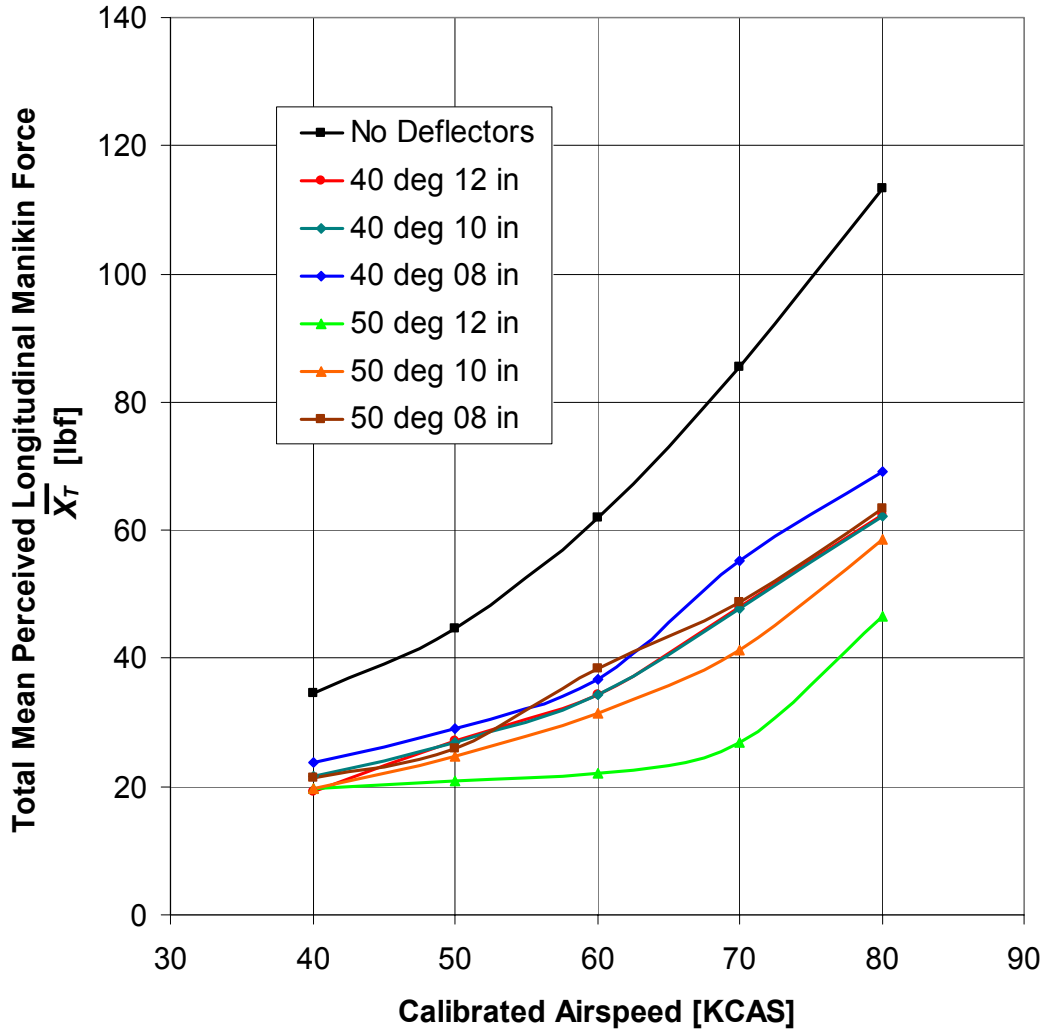


Figure 31. Calibrated Airspeed vs. Total Mean Perceived Manikin Longitudinal Force - All Deflector Configurations.

## Airspeed vs. Total Manikin Force\* 40 Degree Deflectors

Configuration: 2 Manikins per side  
 Crew: Allison/Wright  
 Gross Weight: 2994 lb  
 Center of Gravity: 99.0 in

Pressure Alt: 850-1070 ft  
 OAT: 8-21 °C  
 Aircraft ID: N500VS  
 Aircraft Model: MD-500D

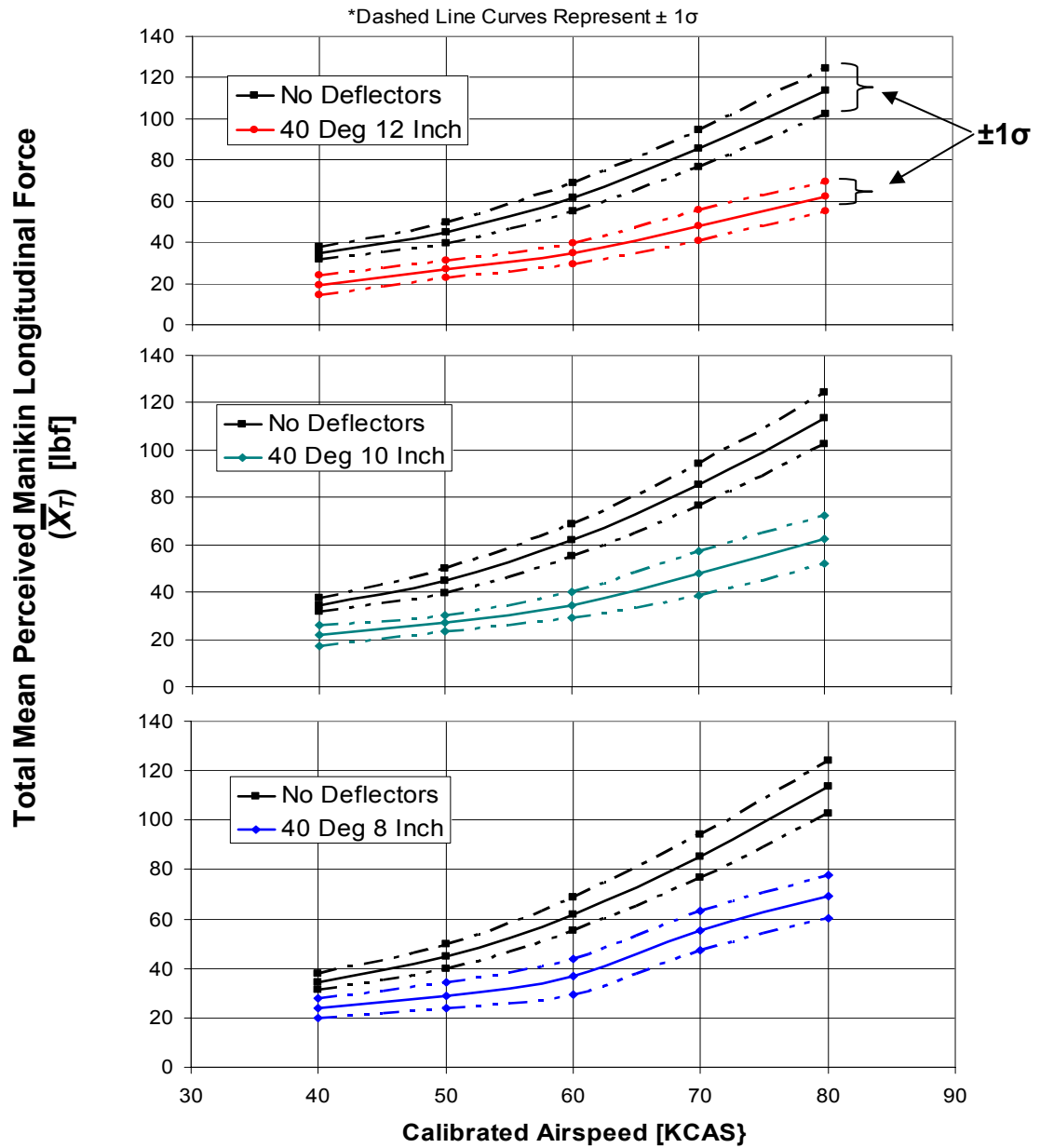


Figure 32. Calibrated Airspeed versus Total Mean Perceived Manikin Longitudinal Force - 40° Deflectors versus No Deflector.



## Airspeed vs. Total Manikin Force\* 50 Degree Deflectors

Configuration: 2 Manikins per side  
 Crew: Allison/Wright  
 Gross Weight: 2994 lb  
 Center of Gravity: 99.0 in

Pressure Alt: 850-1070 ft  
 OAT: 8-21 °C  
 Aircraft ID: N500VS  
 Aircraft Model: MD-500D

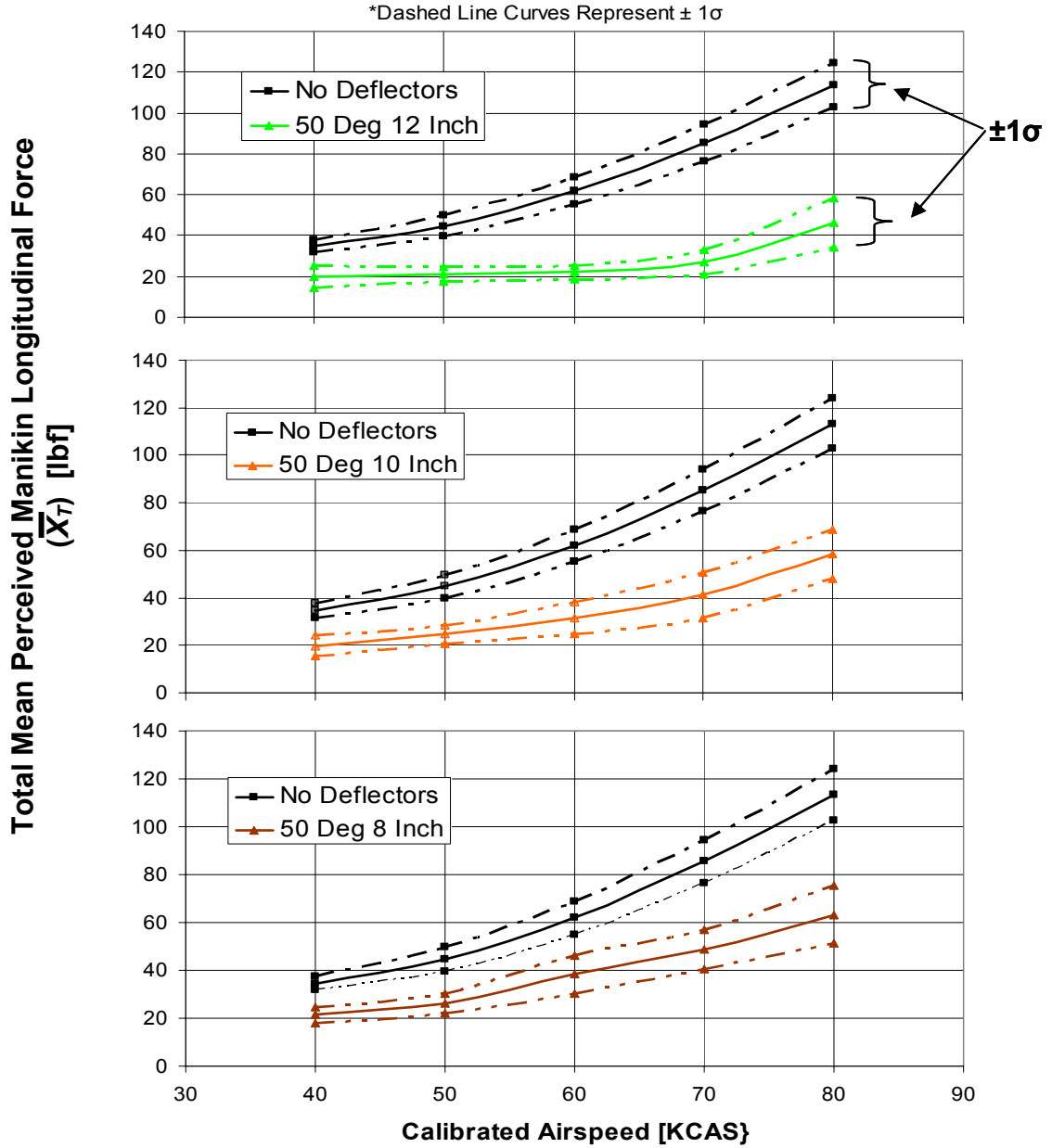


Figure 33. Calibrated Airspeed versus Total Mean Perceived Manikin Longitudinal Force - 50° Deflectors versus No Deflector.

sweep angle resulted in less FOV and egress obstruction suggested the 50° 8-inch deflector as the optimum unmodified deflector configuration.

The 50° 8-inch deflector was then modified with the 0.55-inch PVC plastic Gurney flap. Full flight envelope testing of this modified configuration was not completed at the time of this report's preparation, however preliminary data was available. The 50° 8-inch deflector with Gurney flap at 80 KCAS resulted in a 52% reduction in total perceived longitudinal manikin force, or 8% more than the unmodified 50° 8-inch deflector (Appendix A, Table 5). The Gurney flap also resulted in significantly reduced wind and noise in the cockpit compared to the unmodified 50° 8-inch deflector.

Photographs taken during tuft flights with the 50° 8-inch deflector with Gurney flap at 80 KCAS showed that the airflow across the deflector surface was being diverted as predicted to clear the flap height (Figure 34).

The performance of the 50° 8-inch deflector with Gurney flap was significantly better than the unmodified 50° 8-inch deflector in air load reduction on the manikins. While it did not achieve the air load reductions of the 50° 12-inch deflector, it did exceed the reductions of the 50° 10-inch deflector.

## **Helicopter Performance**

The second objective, to determine if the deflector could provide any performance enhancement via total parasite drag reduction, was also met, although less conclusively than the force reduction. A plot of CAS versus Main Rotor Torque (Q), showed that all deflector configurations resulted in

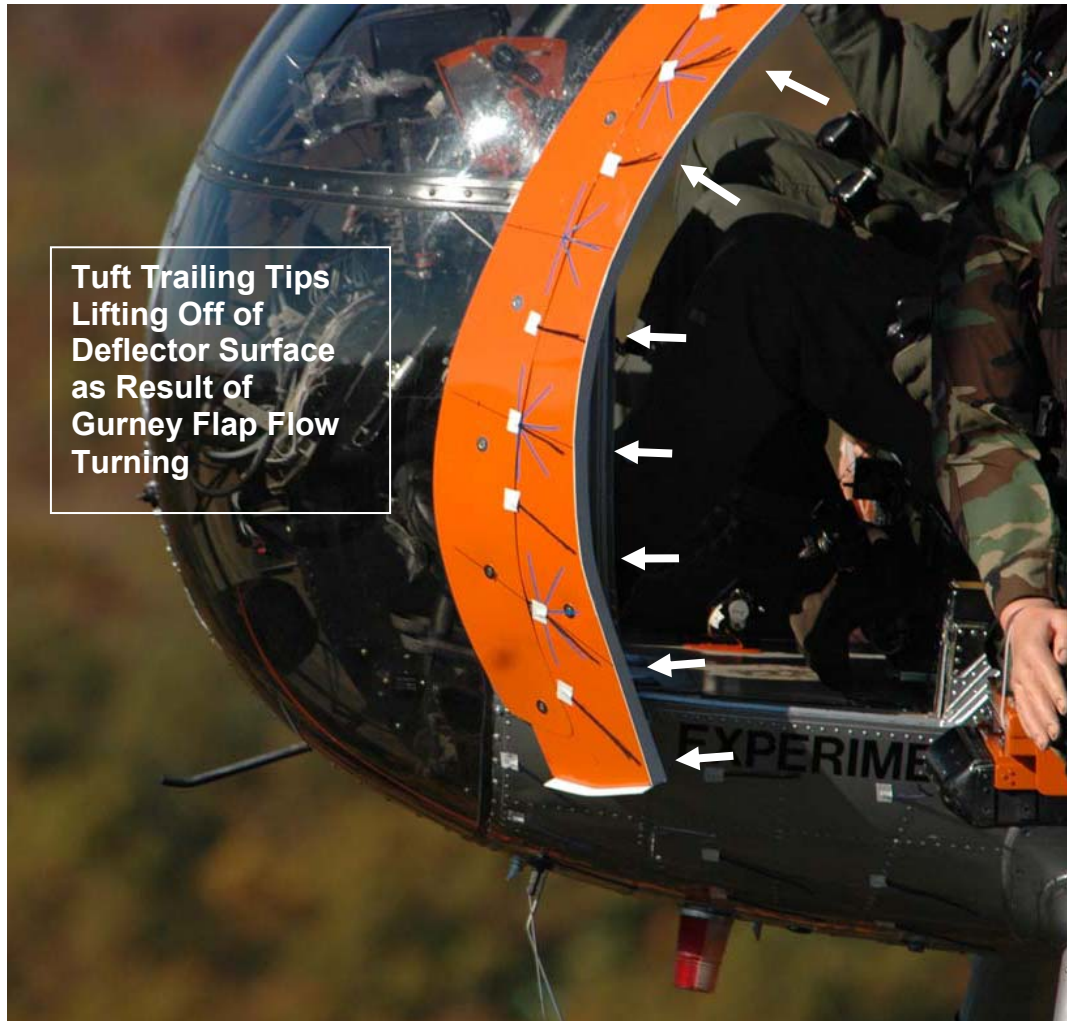


Figure 34. Tuft Flight Visualization of 50° 8-inch deflector with Gurney flap.

reduced torque required to maintain straight and level flight (Figure 35). The actual amount of torque reduction was not statistically significant in 5 of the 6 cases. The sixth configuration, 40° 10-inch deflector, however, had a significant torque reduction of 5 psi at 80 KCAS. Two independent data points were recorded at 80 KCAS during the one flight with this configuration and the value of 70 psi was repeated on each. Although this value at this point repeated, it was noted that in the curve describing the torque required for this deflector has a point of inflection at the 70 KCAS point which no other configuration experienced. For this reason, it was suspected that the torque value recorded for the 40° 10-inch deflector at 80 KCAS was inaccurate and would not receive undue consideration when determining the optimum deflector configuration.

The 50° 8-inch deflector with Gurney flap at 80 KCAS required 72 psi of main rotor torque, indicating a 3psi reduction in power required at that speed with respect to the no deflector baseline condition. While this reduction was potentially significant, there was insufficient data available at the time of report preparation to confirm the validity of this reduction.

### **Helicopter Handling Qualities**

A formal handling qualities evaluation was not conducted in the course of this investigation. The test plan build up test procedures were designed to identify any undesirable or unanticipated stability and control effects. No adverse

## Airspeed vs. Torque All Deflectors

Configuration: 2 Manikins per side  
Crew: Allison/Wright  
Gross Weight: 2994 lb  
Center of Gravity: 99.0 in

Pressure Alt: 850-1070 ft  
OAT: 8-21 °C  
Aircraft ID: N500VS  
Aircraft Model: MD-500D

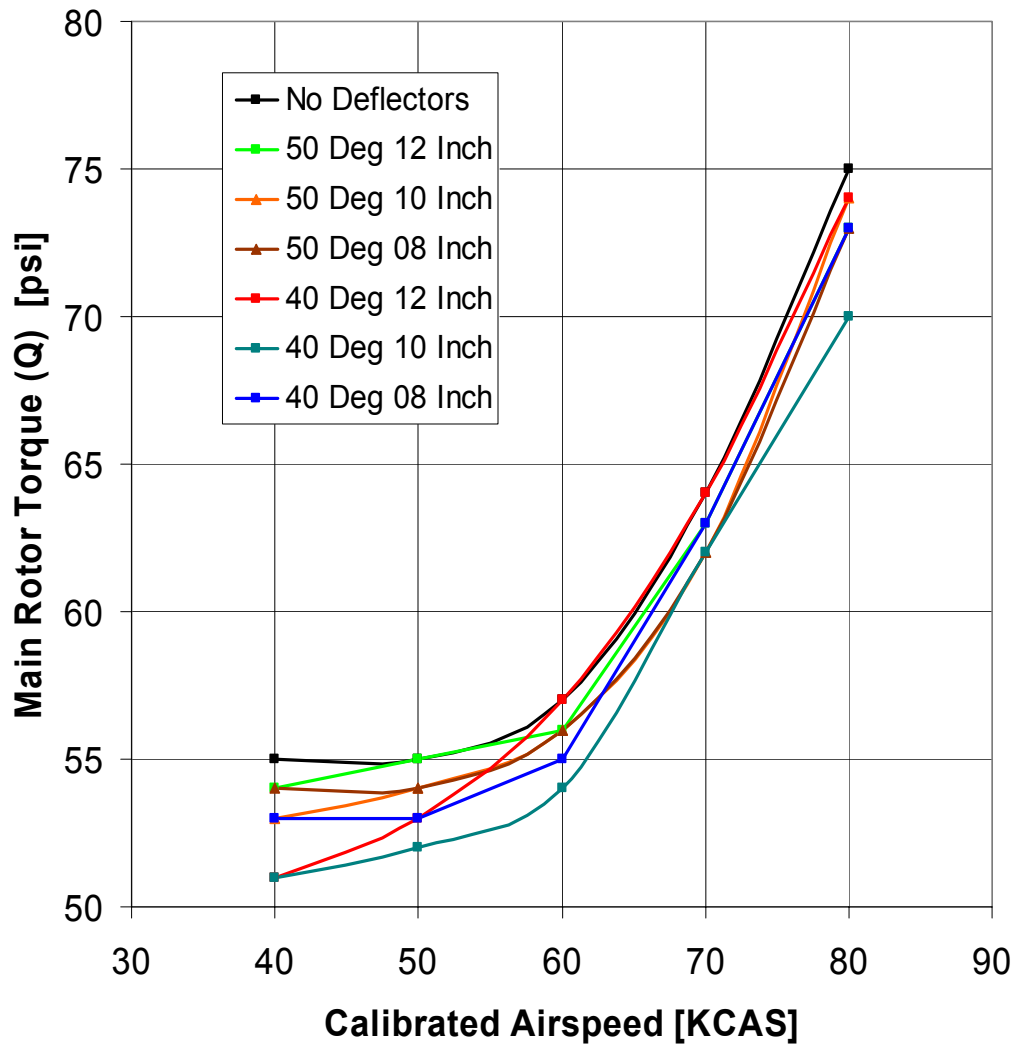


Figure 35. Calibrated Airspeed (CAS) versus Main Rotor Torque (Q) - All Deflector Configurations.

stability or control effects were noted throughout the execution of the 18 test flight sorties which were not present without deflectors installed.

### **Pitot Static System**

All deflector configurations caused ship static port interference in forward flight at all tested airspeeds. The cockpit indications were average altimeter fluctuations of  $\pm 30$  feet and increased pilot workload to maintain ship indicated airspeed. The interference effects were exacerbated by left sideslip and mitigated by right sideslip angles. This behavior was evident prior to installing any of the test equipment, but lesser magnitude. Altimeter fluctuations of  $\pm 10$  feet were observed prior to deflector installation.

The test aircraft was fitted with tufts for flow visualization and a flight was conducted with a photographic chase aircraft. The tufts revealed that airflow was smooth and oriented with the direction of flight on the right side of the fuselage adjacent to the static port location (Figure 36). The flow on the left side was highly turbulent and reverse flow condition in the area immediately forward and below the static port location (Figure 37).

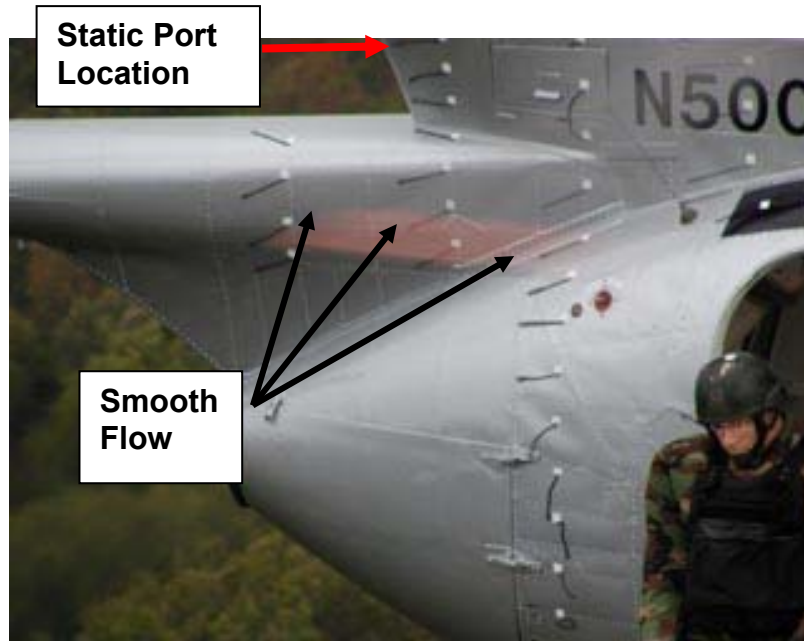


Figure 36. Airflow Visualization on Right Aft Fuselage.



Figure 37. Airflow Visualization on Left Aft Fuselage.

## **CHAPTER VI CONCLUSIONS AND RECOMMENDATIONS**

### **Conclusions**

#### ***Design Process***

The systems approach to material selection of the wind deflectors was highly successful. The functional breakdown allowed for a thorough understanding of the material requirements for each subsystem, creating a savings in both time and money.

#### ***Deflector Mounting System***

The attachment of the fiberglass deflector to the airframe using an aluminum leading edge fixture provided for strong, rigid attachment. This method allowed for direct lay up on the aircraft instead of manufacturing molds for that purpose.

#### ***Deflector Material Selection***

Although the materials used in the fabrication of the deflection devices met or exceeded all requirements for strength and stiffness, the safety concerns regarding field-of-view restrictions indicated that future production models cannot be of the same construction. Future deflectors for operational or test use must be transparent and optically sound.



### Optimum Deflector Configuration

The optimum configuration was initially defined as that deflector which possessed the greatest combination of *both* reduction in EP longitudinal force *and* enhancement in performance at a cruise airspeed of 80 KCAS. This was a purely objective process that required only the analysis of hard data. Each configuration was depicted on a scatter plot of EP Total Longitudinal Force ( $\bar{X}_T$ ) versus Main Rotor Torque ( $Q$ ). The optimum deflector configuration, in which both parameters carried equal weight, was that one which plotted closest to the origin (Figure 38). The optimum, based solely upon this non-weighted, objective method is the 50° 12 inch deflector.

This non-weighted, objective approach was considered insufficient in that it

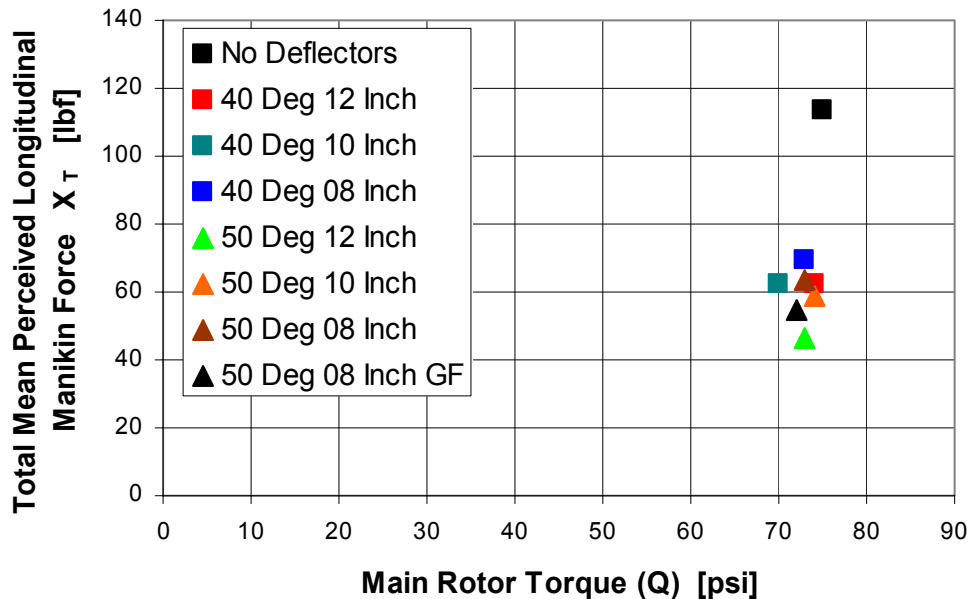


Figure 38. Deflector Optimization (Non-Weighted Objective).

did not take into consideration other factors. Principally, the 50° 12-inch deflector was an unacceptable obstruction to pilot field-of-view and egress. A portion of the FOV could be recovered by fabricating a future production deflector from a clear polycarbonate-type material, but the egress concern remained. Polycarbonate materials are also subject to scratching and crazing effects that degrade their optical qualities over time, thereby revisiting the FOV problem with a wide deflector.

The 50° 8-inch deflector with the 0.55-inch Gurney flap reduced the Total Perceived Force on the EP manikins by 52% (Table 5). The two unmodified configurations that achieved the best air load reductions were the 50° 12-inch

**Table 5: Deflector Summary 80 Knots [KCAS]**

Deflector Configuration		Total Mean Perceived Manikin Longitudinal Force			Main Rotor Torque	
Angle [deg]	Width [in]	$\bar{X}_T$ [lbf]	$\Delta\bar{X}_T$ [lbf]	$\Delta\bar{X}_T$ [%]	$Q$ [psi]	$\Delta Q$ [psi]
No Deflectors		113.4	0.00	0.0%	75	0
40	12	62.4	-51.0	-45.0%	74	-1
	10	62.2	-51.2	-45.1%	70	-5
	8	69.1	-44.3	-39.1%	73	-2
50	12	46.5	-66.9	-59.0%	74	-1
	10	58.6	-54.8	-48.3%	74	-1
	8	63.3	-50.1	-44.2%	73	-2
	8GF	54.4	-59.0	-52.0%	72	-3

deflector with a 59% reduction and the 50° 10-inch deflector with a 48% reduction. The effect of the Gurney flap allowed the 50° 8-inch deflector to achieve an EP air load reduction equivalent to a 50° deflector of approximately 11.2 inches, but without the accompanying egress and FOV penalties. Additionally, the 50° 8-inch deflector with Gurney flap produced a reduced 80 knot cruise torque requirement by 3 psi as compared to the no deflector baseline configuration. Detailed analysis of the deflector data is located in Appendix A.

The 50° 8-inch deflector with the 0.55-inch Gurney flap modification was selected from all test configurations as the optimum configuration based upon all available evaluation criteria (Figure 39).



Figure 39. Test Aircraft in Flight with 50° 8-inch deflector with Gurney Flap.

## Recommendations

Based upon the findings and conclusions of this design, prototyping and flight test investigation, the following recommendations are made:

1. Use the 50 degree 8 inch geometry with the 0.55-inch Gurney flap as the baseline for all future deflector testing.
2. Investigate a range of modifications to the existing prototype deflector, including but not limited to:
  - a. Vortex generators.
  - b. Tapering of deflectors above crew doors.
  - c. Flight with EP manikins removed.
3. Produce an airworthy prototype from clear polycarbonate.
4. Conduct a frequency response investigation of the deflector and external passenger system.
5. Conduct a full flight performance evaluation.
6. Conduct a full flight stability and control evaluation.

## **LIST OF REFERENCES**

## LIST OF REFERENCES

1. MD-500D, Rotorcraft Flight Manual Model 369D, MD Helicopters, Inc., Mesa, Arizona, August 1998.
2. Edwards, E., "Man and machine: Systems for Safety", Proceedings of British Airline Pilots Associations Technical Symposium, British Airline Pilots Associations, London, 1972, pp. 21-36.
3. Steinhoff, John S. "Application of Vorticity Confinement to the Prediction of the Flow over Complex Bodies," AIAA Journal, Vol. 41, No. 4, pp.809-816, May 2003.
4. Military Specification MIL-H-8501A, Helicopter Flying and Ground Handling Qualities, 7 September 1961.
5. Prouty, Raymond W. Helicopter Performance, Stability, and Control, Robert E. Krieger Publishing, Malabar, Florida, 1990.
6. USNTPS Flight Test Manual, Rotary Wing Performance, FTM 106, 31 December 1996.
7. USNTPS Flight Test Manual, Rotary Wing Stability and Control, FTM 107, 31 December 1995.
8. NASA Technical Note, NASA TN D-5153, Use of Pilot Rating in the Evaluation of Aircraft Handling Qualities, April 1969.
9. Hicks, Eric G. "Experimental Study of Alternative Flow Diverting Devices for the Modified MH-6J Helicopter." The University of Tennessee Space Institute, Tullahoma, Tennessee, November 1997.
10. McDougall, Kelly E. "Flight Testing Flow Diverting Devices on an OH-58A+ for Applications to an MH-6 Helicopter." The University of Tennessee Space Institute, Tullahoma, Tennessee, December 2000.
11. Mulnik, Matthew P. "Design of a Flow Diverting Device for OH-58A Helicopters." The University of Tennessee Space Institute, Tullahoma, Tennessee, December 2000.
12. Lewis, Richard L. "Wind Tunnel Investigation of Wind Deflectors for the MH-6M Mission-Enhanced Little Bird." The University of Tennessee Space Institute, Tullahoma, Tennessee, December 2005.

13. Liver, Peter A. "Roll-up of a Vortex Sheet Trailing from a Vortex Generator." The University of Tennessee Space Institute, Tullahoma, Tennessee, December 1987.
14. Hoerner Sighard F. *Fluid Dynamic Drag: Practical Information on Aerodynamic Drag and Hydrodynamic Resistance*, Hoerner Fluid Dynamics, Bakersfield, California 1965.
15. Dow Chemical Corp, "Performance of Styrofoam Products," October 2006. Available at <http://www.dow.com/styrofoam/na/corefoams/perf/>.
16. Hexcel, Inc., "Model 7725 Aerospace Fiberglass Fabric," September 2006. Available at <http://www.hexcel.com/NR/rdonlyres/EAA824B6-3AE3-4D5C-8EF2-BC548E2F8358/0/7725.pdf>.
17. Alcoa, Inc., "Alclad Alloy 2024 Sheet and Plate Techsheet," September 2006. Available at [http://www.alcoa.com/mill\\_products/catalog/pdf/alloy2024techsheet.pdf](http://www.alcoa.com/mill_products/catalog/pdf/alloy2024techsheet.pdf).
18. Fibre Glast Developments Corp., "EZ-Poxy 10/83 Material Properties," June 2006. Available at [www.matweb.com/search/SpecificMaterial.asp?bassnum=PFIBRE12](http://www.matweb.com/search/SpecificMaterial.asp?bassnum=PFIBRE12).
19. Raymer, Daniel P. *Aircraft Design: A Conceptual Approach*, AIAA, Education Series, AIAA, Boston, Massachusetts 1999.
20. Achenbach, E. And Heinecke, E. "On vortex shedding from smooth and rough cylinders in the range of Reynolds number  $6 \times 10^3$  and  $5 \times 10^6$ ." Journal of Fluid Mechanics 109, 239-252.
21. Federal Aviation Administration, *Advisor Circular (AC) 43.13-2A Acceptable Methods, Techniques, and Practices - Aircraft Alterations*, United States Department of Transportation, Washington, DC 1997.
22. Kentfield, J.A.C., "The Potential of Gurney Flaps for Improving the Aerodynamic Performance of Helicopter Rotors," AIAA International Powered Lift Conference, pp. 283-292, AIAA Paper 93-4883, 1993.
23. White, Frank M. *Viscous Fluid Flow 4th Edition*, McGraw Hill Science / Engineering / Math, New York, New York 1999.

## **APPENDICES**



## **APPENDIX A**

### **Data Tables**

**Table 6: Detailed Deflector Summary 80 Knots<sup>1</sup> [KCAS]**  
**Table 6: Detailed Deflector Summary 80kt<sup>1</sup> [KCAS]**

Deflector Configuration		Load Cell Force Left ( $X_L$ )		Load Cell Force Right ( $X_R$ )		Load Cell Force Left and Right ( $X_T$ )			Load Cell Force Change ( $\Delta X_T$ )		Main Rotor Torque ( $Q$ )	Main Rotor Torque Change ( $\Delta Q$ )	
Angle [deg]	Width [in]	$\bar{X}_L$ [lbf]	$\sigma_L$ [lbf]	$\bar{X}_R$ [lbf]	$\sigma_R$ [lbf]	$\bar{X}_T - (\sigma_L + \sigma_R)$ [lbf]	$\bar{X}_L + \bar{X}_R$ [lbf]	$\bar{X}_T + (\sigma_L + \sigma_R)$ [lbf]	$X_{T-Conf} - X_{T-BL}$ [lbf]	[%]	[psi]	$Q_{Conf} - Q_{BL}$ [psi]	[%]
No Deflectors		57.1	4.90	56.3	5.89	102.6	113.4	124.2	0.00	0.0%	75	0	0.0%
40	12	29.2	3.33	33.2	3.84	55.2	62.4	69.5	-51.0	-45.0%	74	-1	-1.4%
	10	29.4	4.74	32.8	5.38	52.1	62.2	72.3	-51.2	-45.1%	70	-5	-7.1%
	8	30.3	4.07	38.8	4.70	60.4	69.1	77.9	-44.2	-39.0%	73	-2	-2.7%
50	12	16.4	5.74	30.1	6.23	34.5	46.5	58.4	-66.9	-59.0%	74	-1	-1.4%
	10	23.8	4.92	34.8	5.39	48.3	58.6	68.9	-54.8	-48.3%	74	-1	-1.4%
	8	26.0	5.53	37.3	6.36	51.4	63.3	75.2	-50.1	-44.2%	73	-2	-2.7%
	8GF	23.6	2.00	30.8	2.50	49.9	54.4	58.9	-58.9	-52.0%	72	-3	-4.2%

1. Values derived from flight data point in specified configuration with highest pilot Confidence Value (CV) rating.

**Table 7: Detailed Deflector Summary 70 Knots<sup>1</sup> [KCAS]**

Deflector Configuration		Load Cell Force Left ( $X_L$ )		Load Cell Force Right ( $X_R$ )		Load Cell Force Left and Right ( $X_T$ )			Load Cell Force Change ( $\Delta X_T$ )		Main Rotor Torque ( $Q$ )	Main Rotor Torque Change ( $\Delta Q$ )	
Angle [deg]	Width [in]	$\bar{X}_L$ [lbf]	$\sigma_L$ [lbf]	$\bar{X}_R$ [lbf]	$\sigma_R$ [lbf]	$\bar{X}_T - (\sigma_L + \sigma_R)$ [lbf]	$\bar{X}_L + \bar{X}_R$ [lbf]	$\bar{X}_T + (\sigma_L + \sigma_R)$ [lbf]	$X_{T-Conf}$ [lbf]	$X_{T-BL}$ [%]	[psi]	$Q_{Conf} - Q_{BL}$ [psi]	[%]
No Deflectors		43.0	4.25	42.4	4.60	76.5	85.4	94.2	0.00	0.0%	64	0	0.0%
40	12	23.6	3.54	24.5	3.78	40.8	48.1	55.4	-37.3	-43.7%	64	0	0.0%
	10	22.1	4.40	25.6	4.91	38.4	47.7	57.0	-37.7	-44.1%	62	-2	-3.2%
	8	23.6	3.70	31.7	4.20	47.4	55.3	63.2	-30.1	-35.2%	63	-1	-1.6%
50	12	8.32	2.95	18.7	3.17	20.9	27.0	33.1	-58.4	-68.4%	63	-1	-1.6%
	10	15.7	4.52	25.5	5.07	31.7	41.3	50.8	-44.1	-51.7%	62	-2	-3.2%
	8	19.6	3.88	29.1	4.33	40.5	48.7	56.9	-36.7	-43.0%	62	-2	-3.2%

1. Values derived from flight data point in specified configuration with highest pilot Confidence Value (CV) rating.

**Table 8: Detailed Deflector Summary 60 Knots<sup>1</sup> [KCAS]**

Deflector Configuration		Load Cell Force Left ( $X_L$ )		Load Cell Force Right ( $X_R$ )		Load Cell Force Left and Right ( $X_T$ )			Load Cell Force Change ( $\Delta X_T$ )		Main Rotor Torque ( $Q$ )	Main Rotor Torque Change ( $\Delta Q$ )	
Angle [deg]	Width [in]	$\bar{X}_L$ [lbf]	$\sigma_L$ [lbf]	$\bar{X}_R$ [lbf]	$\sigma_R$ [lbf]	$\bar{X}_T - (\sigma_L + \sigma_R)$ [lbf]	$\bar{X}_L + \bar{X}_R$ [lbf]	$\bar{X}_T + (\sigma_L + \sigma_R)$ [lbf]	$X_{T-Conf}$ [lbf]	$X_{T-BL}$ [%]	[psi]	$Q_{Conf}$ [psi]	$Q_{BL}$ [%]
No Deflectors		30.9	3.40	31.0	3.42	55.1	61.9	68.7	0.00	0.0%	57	0	0.0%
40	12	16.2	2.61	18.2	2.71	29.1	34.4	39.8	-27.4	-44.4%	57	0	0.0%
	10	14.3	2.56	20.1	2.87	29.0	34.4	39.8	-27.5	-44.4%	54	-3	-5.6%
	8	15.0	3.17	21.7	4.22	29.3	36.7	44.1	-25.2	-40.7%	55	-2	-3.6%
50	12	6.19	1.70	15.8	1.74	18.6	22.0	25.5	-39.9	-64.4%	56	-1	-1.8%
	10	11.4	3.08	20.2	3.57	24.9	31.5	38.2	-30.3	-49.0%	56	-1	-1.8%
	8	15.7	3.89	22.7	4.02	30.5	38.4	46.3	-23.5	-37.9%	56	-1	-1.8%

1. Values derived from flight data point in specified configuration with highest pilot Confidence Value (CV) rating.

**Table 9: Detailed Deflector Summary 50 Knots<sup>1</sup> [KCAS]**

Deflector Configuration		Load Cell Force Left ( $X_L$ )		Load Cell Force Right ( $X_R$ )		Load Cell Force Left and Right ( $X_T$ )			Load Cell Force Change ( $\Delta X_T$ )		Main Rotor Torque ( $Q$ )	Main Rotor Torque Change ( $\Delta Q$ )	
Angle [deg]	Width [in]	$\bar{X}_L$ [lbf]	$\sigma_L$ [lbf]	$\bar{X}_R$ [lbf]	$\sigma_R$ [lbf]	$\bar{X}_T - (\sigma_L + \sigma_R)$ [lbf]	$\bar{X}_L + \bar{X}_R$ [lbf]	$\bar{X}_T + (\sigma_L + \sigma_R)$ [lbf]	$X_{T-Conf}$ [lbf]	$X_{T-BL}$ [%]	[psi]	$Q_{Conf} - Q_{BL}$ [psi]	[%]
No Deflectors		21.6	2.45	23.1	2.58	39.7	44.7	49.8	0.00	0.0%	55	0	0.0%
40	12	12.2	2.02	14.9	2.17	23.0	27.2	31.4	-17.6	-39.3%	53	-2	-3.8%
	10	11.9	1.64	14.9	1.73	23.5	26.9	30.2	-17.9	-39.9%	53	-2	-3.8%
	8	11.6	2.35	17.5	2.75	24.0	29.1	34.2	-15.6	-35.0%	53	-2	-3.8%
50	12	7.09	1.72	13.9	1.76	17.5	21.0	24.5	-23.7	-53.0%	55	0	0.0%
	10	8.52	1.92	16.1	2.01	20.7	24.6	28.6	-20.1	-44.9%	55	0	0.0%
	8	8.01	1.92	17.9	2.15	21.9	26.0	30.0	-18.8	-42.0%	54	-1	-1.9%

1. Values derived from flight data point in specified configuration with highest pilot Confidence Value (CV) rating.

**Table 10: Detailed Deflector Summary 40 Knots<sup>1</sup> [KCAS]**

Deflector Configuration		Load Cell Force Left ( $X_L$ )		Load Cell Force Right ( $X_R$ )		Load Cell Force Left and Right ( $X_T$ )			Load Cell Force Change ( $\Delta X_T$ )		Main Rotor Torque ( $Q$ )	Main Rotor Torque Change ( $\Delta Q$ )	
Angle [deg]	Width [in]	$\bar{X}_L$ [lbf]	$\sigma_L$ [lbf]	$\bar{X}_R$ [lbf]	$\sigma_R$ [lbf]	$\bar{X}_T - (\sigma_L + \sigma_R)$ [lbf]	$\bar{X}_L + \bar{X}_R$ [lbf]	$\bar{X}_T + (\sigma_L + \sigma_R)$ [lbf]	$X_{T-Conf}$ [lbf]	$X_{T-BL}$ [%]	[psi]	$Q_{Conf} - Q_{BL}$ [psi]	[%]
No Deflectors		16.8	1.58	17.8	1.46	31.6	34.6	37.6	0.00	0.00	55	0	0.0%
40	12	8.43	2.28	10.7	2.39	14.5	19.1	23.8	-15.5	-44.7%	47	-8	-17.0%
	10	8.15	2.05	13.5	2.26	17.3	21.6	25.9	-13.0	-37.5%	51	-4	-7.8%
	8	9.01	1.86	14.8	2.11	19.8	23.8	27.8	-10.8	-31.2%	53	-2	-3.8%
50	12	5.66	2.58	14.0	2.92	14.2	19.7	25.2	-14.9	-43.2%	54	-1	-1.9%
	10	6.29	2.20	13.4	2.13	15.4	19.7	24.0	-14.9	-43.1%	53	-2	-3.8%
	8	8.74	1.48	12.6	1.69	18.2	21.4	24.5	-13.2	-38.3%	54	-1	-1.9%

1. Values derived from flight data point in specified configuration with highest pilot Confidence Value rating.

**Table 11: Flight Test Data Card No Deflectors 2 Manikins per Side (Baseline).**

Test Aircraft		ID	DATE		Purpose		
MD-500D		N500VS	20061011		No Deflector / 4 Manikin Baseline		
CREW	TIME		FUEL		Method		
Allison Wright	T/O <b>0707</b>	LDG <b>0745</b>	T/O <b>31.5</b>	LDG <b>11.8</b>	Straight and Level 40-80 KIAS		
AWOS/REMARKS- <b>WIND 210-13 / VIS 10+ / SKY Cir / TEMP/DP 13/5 / ALT 29.77</b>							
H <sub>PO</sub> [ft]	<b>+865</b>		OAT [°C]	<b>+11</b>	N <sub>R</sub> [%]	<b>102</b>	
V <sub>ref</sub> [kt]	Event	V <sub>I</sub> [kt]	Q [psi]	N <sub>1</sub> [%]	TGT [deg]	FC [gal]	CV [1-5]
FPI	<b>0</b>	<b>0</b>					
FPOD	<b>1</b>	<b>0</b>	<b>26</b>	<b>82.6</b>	<b>540</b>		
HVR	<b>2</b>	<b>0</b>	<b>74</b>	<b>96.6</b>	<b>700</b>		<b>4</b>
40	<b>8</b>	<b>40</b>	<b>55</b>	<b>91.5</b>	<b>605</b>		<b>4</b>
40	<b>9</b>	<b>40</b>	<b>55</b>	<b>91.5</b>	<b>605</b>		<b>3</b>
50	<b>10</b>	<b>51</b>	<b>55</b>	<b>91.5</b>	<b>605</b>		<b>4</b>
50	<b>11</b>	<b>50</b>	<b>54</b>	<b>91.7</b>	<b>605</b>		<b>3</b>
60	<b>12</b>	<b>60</b>	<b>56</b>	<b>93.5</b>	<b>605</b>		<b>5</b>
60	<b>13</b>	<b>61</b>	<b>56</b>	<b>93.5</b>	<b>610</b>		<b>4</b>
70	<b>14</b>	<b>70</b>	<b>64</b>	<b>94.5</b>	<b>650</b>		<b>3</b>
70	<b>15</b>	<b>71</b>	<b>63</b>	<b>94.0</b>	<b>640</b>		<b>4</b>
70	<b>19</b>	<b>70</b>	<b>75</b>	<b>97.0</b>	<b>700</b>		<b>4</b>
70	<b>20</b>	<b>80</b>	<b>74</b>	<b>96.5</b>	<b>690</b>		<b>5</b>
80	<b>16</b>	<b>81</b>	<b>75</b>	<b>97.0</b>	<b>700</b>		<b>4</b>
80	<b>17</b>	<b>80</b>	<b>74</b>	<b>96.5</b>	<b>690</b>		<b>5</b>
80	<b>18</b>	<b>80</b>	<b>75</b>	<b>97.0</b>	<b>700</b>		<b>4</b>

**Table 12: Flight Test Data Card 40 Degree 12 Inch Deflector**

Test Aircraft		ID	DATE		Purpose		
MD-500D		N500VS	20061009		Deflector Test 40° / 12"		
CREW	TIME		FUEL		Method		
Allison Wright	T/O <b>1022</b>	LDG <b>1051</b>	T/O <b>28.9</b>	LDG <b>15.2</b>	Straight and Level 40-80 KIAS		
AWOS/REMARKS- <b>WIND 290-3 / VIS 10+ / SKY Clr / TEMP/DP 21/15 / ALT 30.15</b>							
H <sub>PO</sub> [ft]	<b>+930</b>		OAT [°C]	<b>+19</b>	N <sub>R</sub> [%]	<b>102</b>	
V <sub>ref</sub> [kt]	Event	V <sub>I</sub> [kt]	Q [psi]	N <sub>1</sub> [%]	TGT [deg]	FC [gal]	CV [1-5]
FPI	<b>0</b>	<b>0</b>	<b>18</b>	<b>63.8</b>	<b>450</b>	<b>28.5</b>	
FPOD	<b>1</b>	<b>0</b>	<b>26</b>	<b>83.7</b>	<b>535</b>	<b>28.2</b>	
HVR	<b>2</b>	<b>0</b>	<b>73</b>	<b>93.7</b>	<b>700</b>	<b>27.7</b>	<b>4</b>
40	<b>3</b>	<b>42</b>	<b>54</b>	<b>92.5</b>	<b>620</b>	<b>25.4</b>	<b>3</b>
40	<b>4</b>						<b>4</b>
50	<b>5</b>	<b>49</b>	<b>54</b>	<b>92.1</b>	<b>625</b>	<b>24.3</b>	<b>4</b>
50	<b>6</b>						<b>3</b>
60	<b>7</b>	<b>60</b>	<b>58</b>	<b>92.6</b>	<b>625</b>	<b>24.0</b>	<b>2</b>
60	<b>8</b>	<b>60</b>					<b>3</b>
70	<b>9</b>	<b>70</b>	<b>63</b>	<b>93.7</b>	<b>640</b>	<b>22.6</b>	<b>2</b>
70	<b>10</b>						<b>3</b>
80	<b>11</b>	<b>70</b>	<b>71</b>	<b>96.7</b>	<b>675</b>	<b>22.0</b>	<b>3</b>
80	<b>12</b>						<b>3</b>
80	<b>13</b>	<b>81</b>	<b>72</b>	<b>95.9</b>	<b>705</b>	<b>21.2</b>	<b>3</b>
80	<b>14</b>	<b>81</b>	<b>73</b>	<b>96.0</b>	<b>710</b>	<b>20.9</b>	<b>3</b>
FPOD	<b>15</b>						



**Table 13: Flight Test Data Card 40 Degree 10 Inch Deflector (Flight 1)**

Test Aircraft		ID	DATE		Purpose		
MD-500D		N500VS	20061010		Deflector Test 40° / 10"		
CREW	TIME		FUEL		Method		
Allison Wright	T/O <b>0816</b>	LDG <b>0840</b>	T/O <b>27.4</b>	LDG <b>18.2</b>	Straight and Level 40-80 KIAS		
AWOS/REMARKS-							
WIND 090-2 / VIS 10+ / SKY Clr / TEMP/DP 16/13 / ALT 30.10							
H <sub>PO</sub> [ft]	<b>+1050</b>		OAT [°C]	<b>+14</b>	N <sub>R</sub> [%]	<b>102</b>	
V <sub>ref</sub> [kt]	Event	V <sub>I</sub> [kt]	Q [psi]	N <sub>1</sub> [%]	TGT [deg]	FC [gal]	CV [1-5]
FPI	<b>0</b>	<b>0</b>					
FPOD	<b>1</b>	<b>0</b>	<b>26</b>	<b>83.0</b>	<b>535</b>	<b>27.6</b>	
HVR	<b>2</b>	<b>0</b>	<b>75</b>	<b>98.0</b>	<b>700</b>	<b>26.3</b>	<b>5</b>
40	<b>3</b>	<b>40</b>	<b>53</b>	<b>91.0</b>	<b>610</b>	<b>25.8</b>	<b>5</b>
40	<b>4</b>	<b>50</b>	<b>53</b>	<b>91.0</b>	<b>615</b>	<b>25.4</b>	<b>4</b>
50	<b>5</b>	<b>50</b>	<b>55</b>	<b>92.0</b>	<b>610</b>	<b>24.8</b>	<b>5</b>
50	<b>6</b>		<b>55</b>	<b>92</b>		<b>25.4</b>	<b>4</b>
60	<b>7</b>	<b>50</b>	<b>56</b>	<b>92.5</b>	<b>615</b>	<b>24.7</b>	<b>5</b>
60	<b>8</b>	<b>58</b>	<b>56</b>	<b>93.0</b>	<b>615</b>	<b>24.1</b>	<b>4</b>
70	<b>9</b>	<b>58</b>	<b>62</b>	<b>93.0</b>	<b>615</b>	<b>23.8</b>	<b>5</b>
70	<b>10</b>	<b>71</b>	<b>63</b>	<b>95.0</b>	<b>625</b>	<b>23.4</b>	<b>4</b>
80	<b>11</b>	<b>70</b>	<b>69</b>	<b>95.0</b>	<b>630</b>	<b>23.1</b>	<b>4</b>
80	<b>12</b>	<b>80</b>	<b>70</b>	<b>97.0</b>	<b>680</b>	<b>22.7</b>	<b>4</b>
80	<b>13</b>	<b>81</b>	<b>71</b>	<b>96.5</b>	<b>685</b>	<b>22.5</b>	<b>5</b>
FPOD	<b>14</b>	<b>80</b>	<b>25</b>	<b>97.0</b>	<b>670</b>	<b>22.1</b>	<b>5</b>

**Table 14: Flight Test Data Card 40 Degree 10 Inch Deflector (Flight 2)**

Test Aircraft		ID	DATE		Purpose		
MD-500D		N500VS	20061011		Deflector Test 40° / 10"		
CREW	TIME		FUEL		Method		
Allison Wright	T/O <b>0803</b>	LDG <b>0831</b>	T/O <b>27.7</b>	LDG <b>19.6</b>	Straight and Level 40-80 KIAS		
AWOS/REMARKS- <b>WIND 190-7 / VIS 10+ / SKY 090 BKN / TEMP/DP 18/16 / ALT 29.78</b>							
H <sub>PO</sub> [ft]	<b>+875</b>		OAT [°C]	<b>+14</b>	N <sub>R</sub> [%]	<b>102</b>	
V <sub>ref</sub> [kt]	Event	V <sub>I</sub> [kt]	Q [psi]	N <sub>1</sub> [%]	TGT [deg]	FC [gal]	CV [1-5]
FPI	<b>0</b>	<b>0</b>					
FPOD	<b>1</b>	<b>0</b>	<b>26</b>	<b>93.2</b>	<b>575</b>	<b>27.9</b>	
HVR	<b>2</b>	<b>0</b>	<b>75</b>	<b>97.5</b>	<b>705</b>	<b>27.2</b>	
40	<b>3</b>	<b>40</b>	<b>53</b>	<b>93.5</b>	<b>610</b>	<b>26.3</b>	<b>5</b>
40	<b>4</b>	<b>40</b>	<b>53</b>		<b>605</b>	<b>25.9</b>	<b>4</b>
50	<b>5</b>	<b>50</b>	<b>55</b>	<b>92.5</b>	<b>615</b>	<b>25.7</b>	<b>4</b>
50	<b>6</b>	<b>50</b>	<b>55</b>		<b>600</b>	<b>25.5</b>	<b>4</b>
60	<b>7</b>	<b>60</b>	<b>56</b>	<b>92.5</b>	<b>620</b>	<b>25.2</b>	<b>4</b>
60	<b>8</b>	<b>60</b>	<b>56</b>			<b>24.8</b>	<b>4</b>
70	<b>9</b>	<b>71</b>	<b>62</b>	<b>94.2</b>	<b>635</b>	<b>24.4</b>	<b>3</b>
70	<b>10</b>	<b>69</b>	<b>63</b>			<b>24.1</b>	<b>1</b>
70	<b>11</b>						
80	<b>12</b>	<b>79</b>	<b>70</b>	<b>97.0</b>	<b>690</b>	<b>22.7</b>	<b>4</b>
80	<b>13</b>	<b>80</b>	<b>71</b>	<b>97.0</b>	<b>705</b>		
80	<b>14</b>					<b>21.7</b>	<b>3</b>
FPOD	<b>15</b>	<b>0</b>	<b>25</b>			<b>22.1</b>	

**Table 15: Flight Test Data Card 40 Degree 8 Inch Deflector (Flight 1)**

Test Aircraft		ID	DATE		Purpose		
MD-500D		N500VS	20061011		Deflector Test 40° / 8"		
CREW	TIME		FUEL		Method		
Allison Wright	T/O <b>0945</b>	LDG <b>1011</b>	T/O <b>28.5</b>	LDG <b>18.5</b>	Straight and Level 40-80 KIAS		
AWOS/REMARKS- <b>WIND 210-13 / VIS 10+ / SKY Clr / TEMP/DP 21/16 / ALT 29.77</b>							
H <sub>PO</sub> [ft]	<b>+1030</b>		OAT [°C]	<b>+18</b>	N <sub>R</sub> [%]	<b>102</b>	
V <sub>ref</sub> [kt]	Event	V <sub>I</sub> [kt]	Q [psi]	N <sub>1</sub> [%]	TGT [deg]	FC [gal]	CV [1-5]
FPI	<b>0</b>	<b>0</b>					
FPOD	<b>1</b>	<b>0</b>	<b>26</b>	<b>93.2</b>	<b>565</b>	<b>28.1</b>	
HVR	<b>2</b>	<b>0</b>	<b>73</b>	<b>96.0</b>	<b>700</b>	<b>27.7</b>	<b>2</b>
40	<b>3</b>	<b>40</b>	<b>54</b>	<b>91.5</b>	<b>610</b>	<b>25.4</b>	<b>4</b>
40	<b>4</b>	<b>40</b>	<b>54</b>	<b>91.7</b>	<b>615</b>	<b>24.7</b>	<b>2</b>
50	<b>5</b>	<b>48</b>	<b>54</b>	<b>91.8</b>	<b>610</b>	<b>24.3</b>	<b>3</b>
50	<b>6</b>	<b>50</b>	<b>52</b>				<b>3</b>
60	<b>7</b>	<b>61</b>	<b>57</b>	<b>92.0</b>	<b>615</b>	<b>24.0</b>	<b>1</b>
60	<b>8</b>	<b>60</b>	<b>56</b>	<b>91.5</b>	<b>615</b>	<b>23.0</b>	<b>3</b>
70	<b>9</b>	<b>70</b>	<b>63</b>	<b>92.0</b>	<b>615</b>	<b>22.6</b>	<b>3</b>
70	<b>10</b>	<b>71</b>	<b>64</b>	<b>93.5</b>	<b>625</b>	<b>22.2</b>	<b>2</b>
80	<b>11</b>	<b>81</b>	<b>74</b>	<b>93.0</b>	<b>630</b>	<b>22.0</b>	<b>2</b>
80	<b>12</b>	<b>80</b>	<b>73</b>				<b>3</b>

**Table 16: Flight Test Data Card 40 Degree 8 Inch Deflector (Flight 2)**

Test Aircraft		ID	DATE		Purpose		
MD-500D		N500VS	20061012		Deflector Test 40° / 8"		
CREW	TIME		FUEL		Method		
Allison Wright	T/O <b>0801</b>	LDG <b>0820</b>	T/O <b>27.6</b>	LDG <b>19.7</b>	Straight and Level 40-80 KIAS		
AWOS/REMARKS- <b>WIND 350-6/ VIS 10+ / SKY Clr / TEMP/DP 8/5 / ALT 29.93</b>							
H <sub>PO</sub> [ft]	<b>+920</b>		OAT [°C]	<b>+8</b>	N <sub>R</sub> [%]	<b>102</b>	
V <sub>ref</sub> [kt]	Event	V <sub>I</sub> [kt]	Q [psi]	N <sub>1</sub> [%]	TGT [deg]	FC [gal]	CV [1-5]
FPI	<b>0</b>	<b>0</b>					
FPOD	<b>1</b>	<b>0</b>	<b>26</b>	<b>82.5</b>	<b>540</b>	<b>27.2</b>	
HVR	<b>2</b>	<b>0</b>	<b>73</b>	<b>96.0</b>	<b>695</b>	<b>26.8</b>	
40	<b>3</b>	<b>40</b>	<b>52</b>	<b>91.0</b>	<b>605</b>	<b>26.1</b>	<b>3</b>
40	<b>4</b>	<b>40</b>	<b>52</b>	<b>91.0</b>	<b>600</b>	<b>26.3</b>	<b>4</b>
50	<b>5</b>	<b>50</b>	<b>54</b>	<b>92.0</b>	<b>605</b>	<b>25.5</b>	<b>4</b>
50	<b>6</b>	<b>50</b>	<b>53</b>		<b>605</b>	<b>25.3</b>	<b>3</b>
60	<b>7</b>	<b>60</b>	<b>56</b>	<b>92.0</b>	<b>610</b>	<b>24.6</b>	<b>4</b>
60	<b>8</b>	<b>60</b>	<b>56</b>		<b>610</b>	<b>23.5</b>	<b>4</b>
70	<b>9</b>	<b>70</b>	<b>63</b>	<b>94.0</b>	<b>635</b>	<b>22.7</b>	<b>3</b>
70	<b>10</b>	<b>70</b>	<b>64</b>		<b>630</b>	<b>22.5</b>	<b>4</b>
80	<b>11</b>	<b>81</b>	<b>74</b>	<b>96.0</b>	<b>675</b>	<b>21.7</b>	<b>3</b>
80	<b>12</b>	<b>80</b>	<b>75</b>		<b>675</b>	<b>21.5</b>	<b>4</b>
80	<b>13</b>	<b>80</b>	<b>75</b>			<b>21.3</b>	<b>4</b>

**Table 17: Flight Test Data Card 50 Degree 12 Inch Deflector**

Test Aircraft		ID	DATE		Purpose		
MD-500D		N500VS	20061013		Deflector Test 50° / 12"		
CREW	TIME		FUEL		Method		
Allison Wright	T/O <b>0745</b>	LDG <b>0805</b>	T/O <b>28.1</b>	LDG <b>21.4</b>	Straight and Level 40-80 KIAS		
AWOS/REMARKS- <b>WIND Calm / VIS 10+ / SKY Clr / TEMP/DP 0/-2 / ALT 30.03</b>							
H <sub>PO</sub> [ft]	<b>+1000</b>		OAT [°C]	<b>+2</b>	N <sub>R</sub> [%]	<b>102</b>	
V <sub>ref</sub> [kt]	Event	V <sub>I</sub> [kt]	Q [psi]	N <sub>1</sub> [%]	TGT [deg]	FC [gal]	CV [1-5]
FPI	<b>0</b>	<b>0</b>	<b>18</b>	<b>63.8</b>	<b>450</b>	<b>28.8</b>	
FPOD	<b>1</b>	<b>0</b>	<b>27</b>	<b>75.0</b>	<b>515</b>	<b>28.1</b>	
HVR	<b>2</b>	<b>0</b>	<b>73</b>	<b>92.0</b>	<b>670</b>	<b>27.6</b>	<b>4</b>
40	<b>3</b>	<b>40</b>	<b>53</b>	<b>90.0</b>	<b>570</b>	<b>26.9</b>	<b>3</b>
40	<b>4</b>	<b>40</b>	<b>53</b>	<b>90.5</b>	<b>580</b>	<b>26.7</b>	<b>4</b>
50	<b>5</b>	<b>50</b>	<b>55</b>	<b>90.5</b>	<b>580</b>	<b>26.1</b>	<b>4</b>
50	<b>6</b>	<b>50</b>	<b>55</b>	<b>90.5</b>		<b>25.9</b>	<b>4.5</b>
60	<b>7</b>	<b>60</b>	<b>65</b>	<b>92.0</b>	<b>595</b>	<b>25.6</b>	<b>5</b>
60	<b>8</b>	<b>60</b>	<b>56</b>	<b>91.5</b>	<b>600</b>	<b>25.3</b>	<b>4</b>
70	<b>9</b>	<b>70</b>	<b>62</b>	<b>93.0</b>	<b>605</b>	<b>24.9</b>	<b>4</b>
70	<b>10</b>	<b>69</b>	<b>63</b>	<b>93.0</b>	<b>605</b>	<b>24.7</b>	<b>4</b>
80	<b>11</b>	<b>80</b>	<b>74</b>	<b>95.0</b>	<b>625</b>	<b>24.7</b>	<b>4</b>
80	<b>12</b>	<b>80</b>	<b>75</b>	<b>95.5</b>	<b>625</b>	<b>24.0</b>	<b>4</b>
80	<b>13</b>	<b>80</b>	<b>74</b>	<b>95.0</b>	<b>624</b>	<b>23.6</b>	<b>5</b>
RSS	<b>14</b>	<b>60</b>					<b>4</b>
LSS	<b>15</b>	<b>60</b>					<b>4</b>
FPOD	<b>16</b>	<b>0</b>	<b>26</b>			<b>21.5</b>	

**Table 18: Flight Test Data Card 50 Degree 10 Inch Deflector**

Test Aircraft		ID	DATE		Purpose		
MD-500D		N500VS	20061013		Deflector Test 50° / 10"		
CREW	TIME		FUEL		Method		
Allison Wright	T/O <b>0915</b>	LDG <b>0935</b>	T/O <b>28.3</b>	LDG <b>21.0</b>	Straight and Level 40-80 KIAS		
AWOS/REMARKS- <b>WIND Calm / VIS 10+ / SKY Clr / TEMP/DP 10/-1 / ALT 30.06</b>							
H <sub>PO</sub> [ft]	<b>+100</b>		OAT [°C]	<b>+8</b>	N <sub>R</sub> [%]	<b>102</b>	
V <sub>ref</sub> [kt]	Event	V <sub>I</sub> [kt]	Q [psi]	N <sub>1</sub> [%]	TGT [deg]	FC [gal]	CV [1-5]
FPI	<b>0</b>	<b>0</b>					
FPOD	<b>1</b>	<b>0</b>	<b>27</b>	<b>85.5</b>	<b>515</b>	<b>28.2</b>	
HVR	<b>2</b>	<b>0</b>	<b>74</b>	<b>96.0</b>	<b>685</b>	<b>27.2</b>	
40	<b>3</b>	<b>40</b>	<b>55</b>	<b>91.0</b>	<b>590</b>	<b>26.8</b>	<b>4</b>
40	<b>4</b>	<b>40</b>	<b>54</b>	<b>91.0</b>	<b>595</b>	<b>26.6</b>	<b>3</b>
50	<b>5</b>	<b>50</b>	<b>55</b>	<b>92.0</b>	<b>600</b>	<b>26.0</b>	<b>4</b>
50	<b>6</b>	<b>50</b>	<b>56</b>	<b>92</b>	<b>605</b>	<b>25.7</b>	<b>4</b>
60	<b>7</b>	<b>59</b>	<b>56</b>	<b>92.0</b>	<b>605</b>	<b>25.5</b>	<b>2</b>
60	<b>8</b>	<b>60</b>	<b>56</b>	<b>92.0</b>	<b>610</b>	<b>25.1</b>	<b>3</b>
60	<b>9</b>	<b>60</b>	<b>56</b>	<b>92.5</b>	<b>610</b>	<b>24.8</b>	<b>4</b>
70	<b>10</b>	<b>70</b>	<b>61</b>	<b>93.0</b>	<b>615</b>	<b>24.0</b>	<b>4</b>
70	<b>11</b>	<b>69</b>	<b>62</b>	<b>93.0</b>	<b>615</b>	<b>23.7</b>	<b>3</b>
80	<b>12</b>	<b>80</b>	<b>73</b>	<b>95.5</b>	<b>650</b>	<b>23.3</b>	<b>4</b>
80	<b>13</b>	<b>80</b>	<b>72</b>	<b>96.0</b>	<b>650</b>	<b>23.0</b>	<b>3</b>
80	<b>14</b>	<b>81</b>	<b>74</b>	<b>96.0</b>	<b>665</b>	<b>22.6</b>	<b>3</b>
80	<b>15</b>	<b>81</b>	<b>74</b>	<b>96.2</b>	<b>660</b>	<b>22.2</b>	<b>4</b>
FPOD	<b>16</b>	<b>0</b>	<b>26</b>	<b>91.5</b>	<b>520</b>	<b>21.1</b>	

**Table 19: Flight Test Data Card 50 Degree 8 Inch Deflector**

Test Aircraft		ID	DATE		Purpose		
MD-500D		N500VS	20061013		Deflector Test 50° / 8"		
CREW	TIME		FUEL		Method		
Allison Wright	T/O <b>1050</b>	LDG <b>1115</b>	T/O <b>28.1</b>	LDG <b>18.5</b>	Straight and Level 40-80 KIAS		
AWOS/REMARKS- <b>WIND Calm / VIS 10+ / SKY Clr / TEMP/DP 10/-1 / ALT 30.06</b>							
H <sub>PO</sub> [ft]			OAT [°C]	<b>+9</b>	N <sub>R</sub> [%]	<b>102</b>	
V <sub>ref</sub> [kt]	Event	V <sub>I</sub> [kt]	Q [psi]	N <sub>1</sub> [%]	TGT [deg]	FC [gal]	CV [1-5]
FPI	<b>0</b>	<b>0</b>	<b>18</b>	<b>63.8</b>	<b>450</b>	<b>28.5</b>	
FPOD	<b>1</b>	<b>0</b>	<b>26</b>	<b>92.2</b>	<b>535</b>	<b>28.2</b>	
HVR	<b>2</b>	<b>0</b>	<b>73</b>	<b>96.0</b>	<b>700</b>	<b>27.7</b>	<b>4</b>
40	<b>3</b>	<b>40</b>	<b>55</b>	<b>91.5</b>	<b>610</b>	<b>25.4</b>	<b>3</b>
50	<b>4</b>	<b>50</b>	<b>54</b>	<b>91.7</b>	<b>615</b>	<b>24.7</b>	<b>3</b>
50	<b>5</b>	<b>50</b>	<b>54</b>	<b>91.8</b>	<b>610</b>	<b>24.3</b>	<b>4</b>
50	<b>6</b>						<b>0</b>
50	<b>7</b>	<b>50</b>	<b>54</b>	<b>92.0</b>	<b>615</b>	<b>24.0</b>	<b>2</b>
60	<b>8</b>	<b>58</b>	<b>56</b>	<b>91.5</b>	<b>615</b>	<b>23.0</b>	<b>2</b>
60	<b>9</b>	<b>58</b>	<b>54</b>	<b>92.0</b>	<b>615</b>	<b>22.6</b>	<b>1</b>
70	<b>10</b>	<b>71</b>	<b>61</b>	<b>93.5</b>	<b>625</b>	<b>22.2</b>	<b>2</b>
70	<b>11</b>	<b>70</b>	<b>62</b>	<b>93.0</b>	<b>630</b>	<b>22.0</b>	<b>3</b>
80	<b>12</b>	<b>80</b>	<b>73</b>	<b>96.0</b>	<b>680</b>	<b>21.5</b>	<b>2</b>
80	<b>13</b>	<b>81</b>	<b>74</b>	<b>96.2</b>	<b>685</b>	<b>21.2</b>	<b>3</b>
80	<b>14</b>	<b>80</b>	<b>73</b>	<b>96.0</b>	<b>670</b>	<b>20.9</b>	<b>3</b>
80	<b>15</b>	<b>80</b>	<b>73</b>	<b>96.2</b>	<b>685</b>	<b>20.5</b>	<b>4</b>
RSS	<b>16</b>	<b>60</b>					<b>4</b>
LSS	<b>17</b>	<b>60</b>					<b>4</b>
FPOD	<b>18</b>	<b>0</b>	<b>26</b>	<b>92.0</b>	<b>520</b>	<b>18.9</b>	

## **APPENDIX B**

### **Figures**



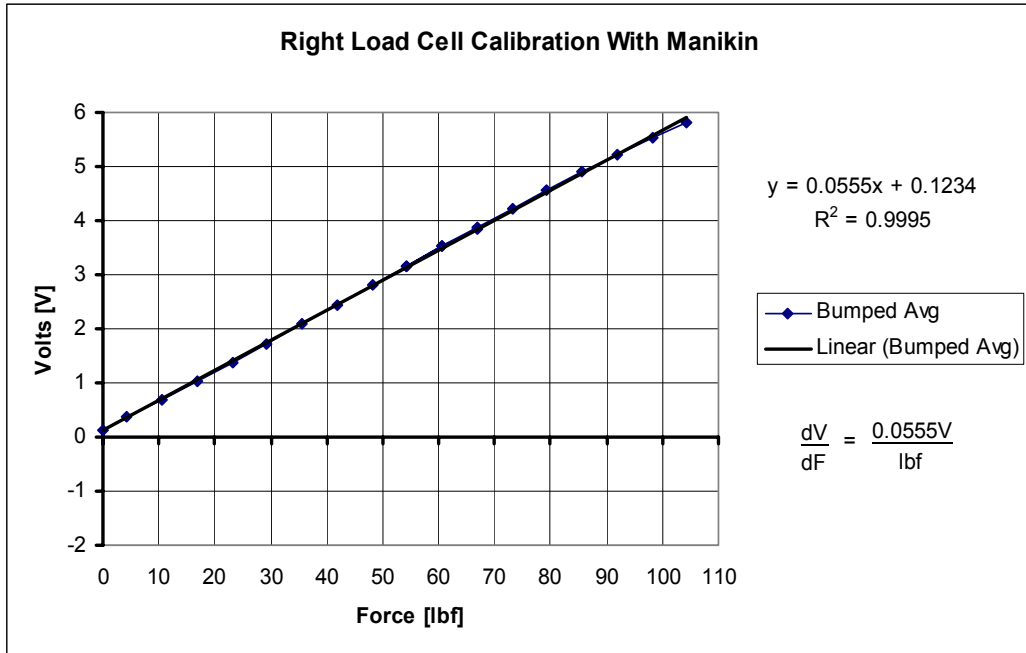


Figure 41. Right Manikin Load Force Calibration.

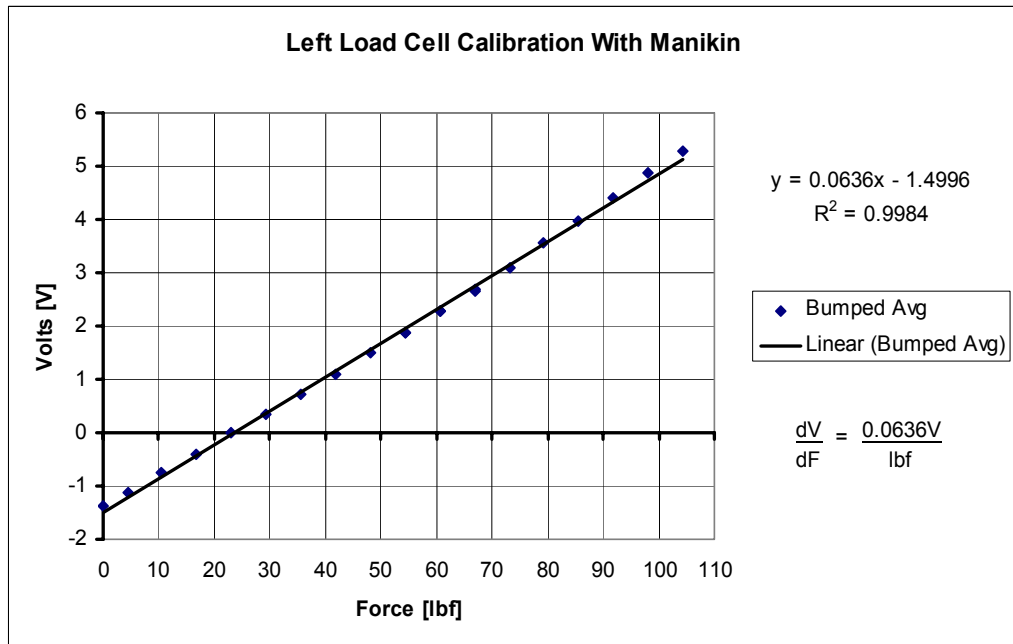


Figure 42. Left Manikin Load Cell Calibration.



Figure 43. Fuselage Sweep Angle Measurement Protractor (Installed).

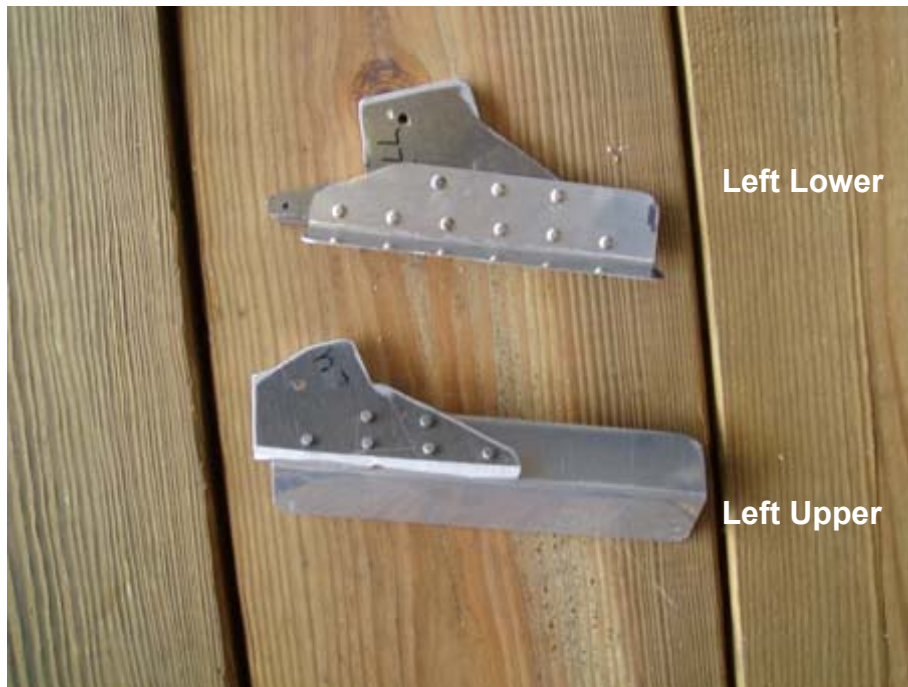


Figure 44. Left Upper and Lower Hinge Brace Assembly (Not installed).

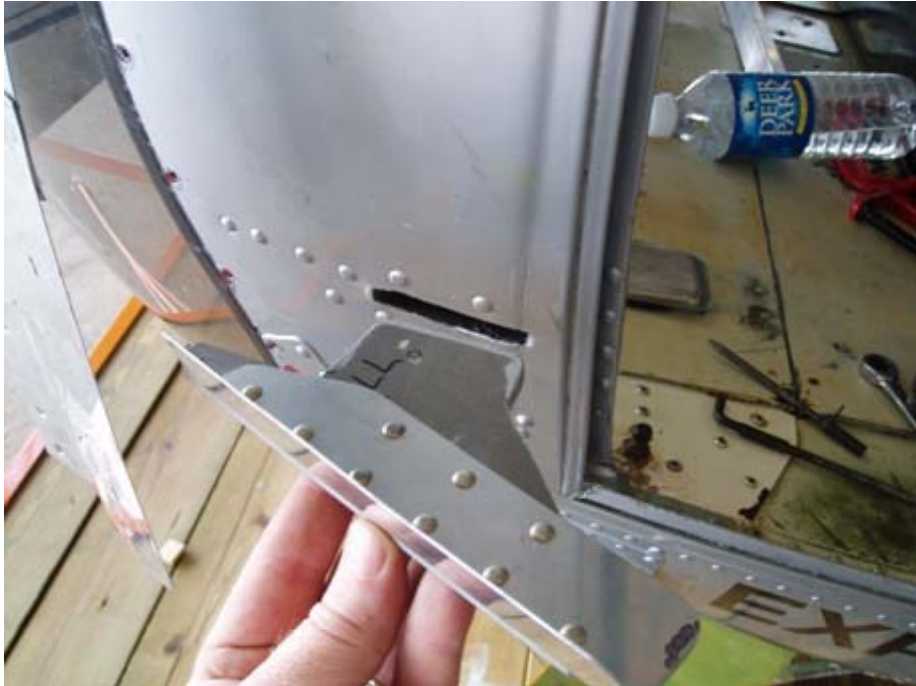


Figure 45. Lower Hinge Brace (Installation).



Figure 46. Lower Hinge Brace (Installed).



Figure 47. Upper Hinge Brace (Installed).



Figure 48. Leading Edge Metal Fixture with Hinge Braces (Installed, Complete).



Figure 49. Deflector Edge Filling.



Figure 50. Deflector Attached to Full Leading Edge Fixture



Figure 51. External Passenger Bench System.



Figure 52. Deflector Installed on Right Side...



Figure 53. Pilot Field-of-View with 40 Degree 12 Inch Deflector Installed (Left)



Figure 54. Pilot Field-of-View with 40 Degree 12 Inch Deflector Installed (Right).



Figure 55. Deflector Material Test Section (Bending).



Figure 56. Deflector Test Section Bending Test.





Figure 57. Deflector Material Test Section (Tear Out).



Figure 58. Deflector Test Section Tear Out Test.



Figure 59. Static Load Testing of Installed Deflector (1).



Figure 60. Static Load Testing of Installed Deflector (2).



Figure 61. Manikin Longitudinal Force Load Cell.



Figure 62. Manikin Roller Seat Assembly with Load Cell Location.



Figure 63. Manikin Roller Seat Assembly (Front, Installed).



Figure 64. Manikin Roller Seat Assembly (Oblique, Installed).



Figure 65. External Passenger Bench with Manikins Installed.



Figure 66. MD-500 Aircraft Configured for Deflector Flight.



Figure 67. 40 Degree 12 Inch Deflector (Installed).



Figure 68. 40 Degree 10 Inch Deflector (Installed).



Figure 69. 40 Degree 8 Inch Deflector (Installed).



Figure 70. 50 Degree 10 Inch Deflector (Installed).



Figure 71. 50 Degree 8 Inch Deflector (Installed).



Figure 72. 50 Degree 8 Inch Deflector with Flow Visualization Tufts.





Figure 73. 50 Degree 8 Inch In-flight Flow Visualization (Right Front View).



Figure 74. 50 Degree 8 Inch In-flight Flow Visualization (Right Close-Up).



Figure 75. 50 Degree 8 Inch In-flight Flow Visualization (Left Front)



Figure 76. 50 Degree 8 Inch Deflector Flow Visualization Flight (Left Upper).



Figure 77. 50 Degree 8 Inch in-flight Flow Visualization (Left Close-Up).



Figure 78. 50 Degree 8 Inch In-flight Flow Visualization (Front).

## **APPENDIX C**

### **Flight Permit and Safety/Hazard Review**


AVIATION SYSTEMS AND FLIGHT RESEARCH DEPARTMENT		
FLIGHT PERMIT		
<b>Aircraft</b> MD500 / N500VS	<b>Research/Training Program</b> Wind Deflector	<b>Date</b> 17 Aug 2006
<b>Flight activity (Type of operation – research, training, support)</b>  Test flight in support of Wind Deflector research project. First test flight with composite wind deflectors attached (“clean” benches and air data boom attached also).		
<b>Limitations (Aircraft limitations due to experimental hardware, software, weather conditions, pilot qualification and allowable aircrew)</b>  1. CONFIGURATION: 1.1. Flight configuration limited to left and/or right wind deflector, “clean” benches (no load cell seats or dummy supports), and air data boom attached. 1.2. Gross weight and center of gravity within normal limits.  2. FLIGHT CONDITIONS: 2.1. Day VFR flight only, wind < 15 kts. 2.2. Maximum airspeed and altitude of 85 KIAS and 1,000 ft AGL, respectively. 2.3. Normal acceleration limits of 0 to 2 g.  3. TEST MANEUVERS: 3.1. Level flight from hover to 85 KIAS maximum. 3.2. Steady heading sideslips (SHSS) to maximum 1 “trim ball” deflection.  4. AIRCREW: 4.1. Minimum crew of one test pilot and one Flight Test Engineer.  5. TEST AREA: 5.1. All tests to be flown within Tullahoma (THA) airport local area. 5.2. Flight over populated areas will be avoided.		
<b>Contacts (Personnel responsible for engineering and operation)</b>  Rodney Allison, Aircraft Operations , 931-393-7411 Greg Heatherly, Aircraft Maintenance, 931-393-7415 Michael Leigh, Instrumentation Technician, 931-393-7415		
<b>Name/Date/Signature</b>  Stephen Corda / 17 Aug 2006 		

Figure 79. Wind Deflector Test Program Flight Permit.

Aircraft MD369D/N500VS	Research or Training Program Wind Deflector Project	Date 15 Aug 06
<b>Hazard (Describe the event that will directly produce the injury or damage. Describe the nature and extent of the injury or damage)</b> Rotor System or flight control surface failure resulting in forced autorotation and landing.		
<b>Causes (Describe the circumstances and events leading up to the hazard)</b> The following equipment separating from the aircraft: 1) Deflector as a result of structural failure 2) Manikin or part of manikin/equipment 3) Instrumentation		
<b>Mitigation and controls (Describe the design features and procedures that will be used to mitigate the risk. List any testing that has been or will be performed to verify risk mitigation procedures and controls)</b>  1) Detailed static testing will be accomplished in accordance with AC 43.13-2A chapter 1 Deflectors were tested IAW AC 43.13-2A. Additionally, the deflectors were tested by applying point loads at mid span points at 8 locations. 50 lbs. applied, deflection <1/4 inch over all frontal surface areas (push and pull) Tear out testing – exceeded 100 lbs per hole, no elongation (19 holes) Tap testing indicates no natural freq < 250 Hz Incremental build-up flight will be accomplished without manikins Detailed pre- and post-flight inspections In the event of a structural vibration that appears to be divergent, the pilot flying will immediately slow the aircraft while the non-flying pilot will attempt to damp the mode by applying pressure against the inner surface of the deflector. 2) The manikins designed to sustain high loads and roller system will be static load tested per AC43.13-2A The manikins will be secured to the EPS with a minimum of 3 straps. As a final retention device, the manikins will have a safety line attached between themselves and a fixed ring on the EPS. The helmets and all other worn gear will be secured with safety wire or equivalent. 3) The instrumentation pallet was static load tested. Additionally, the equipment will be pre- and post- flight inspected.		
<b>Risk Assessment (Provide the risk assessment after mitigation or controls are established)</b>  Severity <u>  I  </u> Probability of Occurrence <u>  E  </u> Risk Assessment Code <u>  R3  </u>		
Prepared by/Date R. Allison / 15Aug 06	Committee Review/Date <i>R. J. Canardo</i> 17 Aug 06	Chairman Review/Date <i>Stacy Coyle</i> 8/17/06

*W. Soler*  
*Roy J. Schuch*  
*MS*

Figure 80. Safety/Hazard Review Sheet 1 of 5.

Aircraft MD369D/N500VS	Research or Training Program Wind Deflector Project	Date 15 Aug 06
<b>Hazard</b> (Describe the event that will directly produce the injury or damage. Describe the nature and extent of the injury or damage) Electrical Fire resulting in forced landing.		
<b>Causes</b> (Describe the circumstances and events leading up to the hazard) Short circuit		
<b>Mitigation and controls</b> (Describe the design features and procedures that will be used to mitigate the risk. List any testing that has been or will be performed to verify risk mitigation procedures and controls) Pilot accessible master instrumentation switch installed Circuit breakers are installed as required. Wire to fuse compatibility checked Conducted a thorough load analysis		
<b>Risk Assessment</b> (Provide the risk assessment after mitigation or controls are established) Severity <u>I</u> Probability of Occurrence <u>E</u> Risk Assessment Code <u>R3</u>		
Prepared by/Date R. Allison / 15 Aug 06	Committee Review/Date R. Remond 17 Aug 06	Chairman Review/Date Steph Conda 8/17/06

Boles Roy J. Schuy  
 [Signature]

Figure 81. Safety/Hazard Review Sheet 2 of 5.

Aircraft MD369D/N500VS	Research or Training Program Wind Deflector Project	Date 15 Aug 06
<b>Hazard</b> (Describe the event that will directly produce the injury or damage. Describe the nature and extent of the injury or damage) Third party injury on the ground.		
<b>Causes</b> (Describe the circumstances and events leading up to the hazard) 1.) Equipment or equipment fixture failure, resulting in test equipment departing aircraft in flight. 2.) Crew, ground maintenance, university employee, or project observer injury due to aircraft exhaust, main rotor, tail rotor, and high noise level		
<b>Mitigation and controls</b> (Describe the design features and procedures that will be used to mitigate the risk. List any testing that has been or will be performed to verify risk mitigation procedures and controls)  1.) Flight will be conducted on predetermined route over an unpopulated area. All test equipment fixtures static tested in accordance with AC43.13-2A Complete pre-post-flight inspections conducted on test equipment for each flight 2.) Personnel directly involved with flight test operations briefed prior to first flight. Safety observer posted at aircraft for all ground operations with engine operating No major maintenance on test configuration changes with engines operating.		
<b>Risk Assessment</b> (Provide the risk assessment after mitigation or controls are established)  Severity <u>  I  </u> Probability of Occurrence <u>  E  </u> Risk Assessment Code <u>  R3  </u>		
Prepared by/Date R. Allison / 15 Aug 06	Committee Review/Date R.J. Ranaudo 17 Aug 06	Chairman Review/Date Steph Conda 8/17/06

*R. Allison*  
*Steph Conda*  
*Roy J. Schuch*  
*N.R.*

Figure 82. Safety/Hazard Review Sheet 3 of 5.



Aircraft MD369D/N500VS	Research or Training Program Wind Deflector Project	Date 15 Aug 06
<b>Hazard</b> (Describe the event that will directly produce the injury or damage. Describe the nature and extent of the injury or damage) Loss of Aircraft Control		
<b>Causes</b> (Describe the circumstances and events leading up to the hazard) Instrumentation string pots jam the flight controls		
<b>Mitigation and controls</b> (Describe the design features and procedures that will be used to mitigate the risk. List any testing that has been or will be performed to verify risk mitigation procedures and controls) Weak link installed in-line with the string pots.		
<b>Risk Assessment</b> (Provide the risk assessment after mitigation or controls are established) Severity <u>I</u> Probability of Occurrence <u>E</u> Risk Assessment Code <u>R3</u>		
Prepared by/Date R. Allison / 15 Aug 06	Committee Review/Date R.J. Rancards 17 Aug 06	Chairman Review/Date Stiglitz 8/17/06

*Roy J. Schulz*  
*NO*

Figure 83. Safety/Hazard Review Sheet 4 of 5.

SAFETY FINDING

Conclusions and Recommendations:

The Safety Committee consisted of the following personnel.

- Richard Ranaudo - Committee Head
- Peter Salies - Aerodynamics and Structures
- Roy Shuly - Aerodynamics
- Mike Leigh - Electrical and Instrumentation
- Greg Heatherly - Mechanical and Aircraft Systems
- Rodney Altison - Project Team Lead and Test Pilot
- James Wright - Flight Test Engineer and Test Pilot
- Nate Palumbo - Aerodynamics & Structures (Ad Hoc).

The committee has reviewed the safety risk assessment and is in agreement with the final analysis of risk after ground testing and procedural test conditions were implemented. Flight test of the deflectors will proceed in a build up fashion, with incremental changes in speed and sideslip. The flight test will consist of two flights, the first with only the right deflector installed, and the second with the left and right deflectors installed. During build up maneuvers in each test, the flight crew will discontinue envelope expansion if any potentially hazardous characteristics are noted, either in the structural integrity of the deflectors, or in aircraft handling. The fire station will be alerted when the test is planned, and the test aircraft will remain in contact with a UTSI ground station at all times. The committee recommends that the test proceed as planned.

Richard Ranaudo  
Signature and date Aug 17, 2006

Figure 84. Safety/Hazard Review Sheet 5 of 5.

## **APPENDIX D**

### **Test Plan**

**TEST PLAN**  
**for**  
**AIRCRAFT WIND DEFLECTOR**

**Prepared by**  
**Professor Rodney Allison**  
**James J. Wright**

**University of Tennessee Space Institute**  
**Tullahoma, TN 37388-9700**

**May 24, 2006**

## UTSI TEST PLAN

**Test Plan: Wind Deflector Study**  
**Risk Category / Categories: B**  
**Test Plan Expiration Date: NA**

<b>PROJECT TITLE: Wind Deflector Project</b>		<b>DATE: 24 May 06</b>	
<b>Project Officer / Telephone: Rodney Allison / 931-393-7411</b>		<b>Project Officer / Telephone:</b>	
<b>Funding Expiration: N/A</b>	<b>Chargeable Object:</b>		
<b>Est. Date of 1<sup>st</sup> Grnd/Flt Event: 17 July 2006</b>	<b>Est. Date of Last Grnd/Flt Event: 1 Oct 2006</b>	<b>Est. Date of Test Program Completion: 31 Dec 2006</b>	
<b>Est. Ground Test Hrs: 2.0</b>	<b>Est. Flight Test Hrs: 75</b>	<b>Est. Total Sorties Req'd: 50</b>	

**TEST TEAM SIGNATURES**

The following individuals have read the test plan, understand the planned tests and acknowledge their roles and responsibilities for this project.

(SIGNATURE)	(DATE)	(PRINCIPAL INVESTIGATOR/PROJECT (PILOT)
(Signature)	(Date)	RODNEY ALLISON (PILOT/FTE)
(Signature)	(Date)	RALPH KIMBERLIN (PILOT/FTE)
(Signature)	(Date)	STEPHEN CORDA (PILOT/FTE)
(Signature)	(Date)	JIM WRIGHT (Pilot/FTE)
(Signature)	(Date)	Kim Elsholz (Mechanic/FTE)
(Signature)	(Date)	Greg Heatherly (Mechanic/FTE)
(Signature)	(Date)	Mark Blanks (Instrumentation/FTE)
(Signature)	(Date)	Mike Leigh (Instrumentation)
		Brandon Sirbaugh

**TABLE OF CONTENTS**

1.0 BACKGROUND..... 1

2.0 PURPOSE..... 1

3.0 DESCRIPTION OF TEST AIRCRAFT AND EQUIPMENT

    3.1 Basic Aircraft..... 1

    3.2 Test Aircraft Modification ..... 2

    3.3 Test Items ..... 2

    3.4 Test Instrumentation ..... 2

4.0 SCOPE OF TESTS

    4.1 Test Envelope..... 3

    4.2 Flight Clearance..... 3

    4.3 Tests and Test Conditions ..... 3

    4.4 Test Loadings ..... 4

    4.5 Test Configurations..... 4

    4.6 Test Criteria ..... 4

    4.7 Limitations to Scope ..... 4

5.0 METHOD OF TESTS

    5.1 Test Method and Procedures..... 4

    5.2 Instrumentation and Data Extraction..... 4

    5.3 Support Requirements ..... 5

    5.4 Personnel Requirements ..... 5

6.0 RISK MANAGEMENT

    6.1 Safety Checklist..... 5

    6.2 Test Hazard Analysis..... 6

    6.3 Firebreaks..... 6

    6.4 Hazard Pattern..... 6

    6.5 Environmental Analysis ..... 6

    6.6 Risk Category ..... 7

    6.7 Real-Time Data Monitoring..... 7

    6.8 Additional Special Precautions ..... 7

7.0 PROJECT MANAGEMENT

    7.1 Funding/Manpower Requirements..... 7

    7.2 Schedule/Milestones..... 7

    7.3 Reports ..... 7

    7.4 Project Security..... 8

REFERENCES..... 9

APPENDICES

    Appendix A: FIGURES ..... 10

    Appendix B: TABLES ..... 16

    Appendix C: SAFETY CHECKLIST ..... 20

    Appendix D: TEST HAZARD ANALYSIS..... 22

    Appendix E: TEST REPORTS/DELIVERABLES PLAN (TRDP) ..... 29

## **1.0 BACKGROUND**

Numerous rotary wing operators perform missions which require flight with personnel seated outside of the fuselage or with doors off. This investigation is specific to the round nose configured MD-500 series aircraft due to test aircraft availability and the wide range of missions it conducts worldwide. During cruise flight, personnel exposed to the aircraft slipstream are subject to high wind loads and extreme wind chill effects, compromising their ability to perform required tasks at destination. External passengers also add to the overall helicopter parasite drag, decreasing performance as well as interfering with the crew through increased noise and turbulence in the cockpit. Prior research indicates that attachment of wind deflectors to the helicopter forward fuselage diverts the wind away from the fuselage. This flow diversion reduces total parasite drag, slipstream effects on external passengers and fuselage entrained flow effects on internal passengers and crew.

Prior research indicated that the wind may be diverted away from the external personnel, to some degree, by attaching wind deflectors to the helicopter forward fuselage. This research explored the effects of various wind deflector designs in water tunnel (ref 1), wind tunnel (ref 9) and in-flight test (ref 7, 8). The tunnel experiments were conducted on a round nose MD500D (1/8 scale) half model, the flight tests were on an OH-58A+. Due to scaling considerations coming from the tunnels and the dissimilarity of the OH-58 and



the MD-500D fuselage and windscreen, it is anticipated that the previous flight test data may be of limited use, and will therefore be used only as a guide.

## **2.0 PURPOSE OF TEST**

The purpose of this effort is to determine if a wind deflector can be designed that will deflect a large amount of air from the personnel sitting outside the aircraft without adversely affecting the performance, handling qualities and field-of-view (FOV) of the MD-500D aircraft. To evaluate this effort, UTSI will lease a civil MD-500D and install with an external passenger seating system.

The requirements are as follows:

- a. Optimize air load reduction on first mock personnel on plank.  
Decrease overall aircraft drag or only increase it by 10 percent.
- b. Little to no impact on aircraft handling qualities.

UTSI will design, build and flight-test a minimum of five wind deflector configurations and select instruments to measure results against the objectives above. Baseline flight-test a fully configured MD-500 series aircraft (round nose), brief select configuration prior to flight testing, brief the flight test results, and report finding in a formal written report.

## **3.0 DESCRIPTION OF TEST AIRCRAFT OR EQUIPMENT**

### **3.1 Test Aircraft**

#### **General.**

The test aircraft MD-500D (Model 369D, Registration Number N500VS) (Figure A-1) is production representative, with the exception of an installed instrumented air data boom and sensitive test instrumentation package for recording aircraft parameters. It is a 5 place, turbine powered, rotary wing aircraft. The main rotor is a fully articulated five-bladed system, with anti-torque provided by a 2-bladed semi-rigid type tail rotor. Power from the turboshaft engine is transmitted through the main drive shaft to the main rotor transmission, and from the main rotor transmission through a drive shaft to the tail rotor. An overrunning (one way) clutch, placed between the engine and the main rotor transmission permits free-wheeling of the rotor system during autorotation.

### **3.2 Test Aircraft Modifications**

The MD-500D will be retrofitted with a government surplus external passenger seating system loaded with four (4) manikins, a flight test instrumentation package (see paragraph 3.4), and various Wind Deflectors (see paragraph 3.3).

### **3.3 Test Items**

Wind Deflector. A minimum of five (5) deflector configurations will be fabricated and tested. Construction should be of mixed aluminum and composite for speed and ease of manufacture, and will be opaque. Configurations will consist of two different sweep angles, and variations on vortex generator (VG) form, number and location. The angles and VG configurations will be based upon recommendations and estimates as published by Hicks/McDougall/Lewis (ref 6, 7, & 9). The Wind Deflectors may be tufted as required to aid in determining the optimum VG placement.

Manikins. The manikins being used for the forward plank-mounted personnel are the Rescue Randy Fire Fighter Combat Challenge manufactured by Simulaid, Incorporated. These manikins are manufactured from high impact ABS plastics, have interior weights bonded and riveted to the shell structure to give a representative weight distribution through the body, and all points of articulation are interconnected with steel cable rated to 4100 pounds. All manikins used will be approximately six foot height, to approximate the drag area representative of the customer's usage. The manikins will be equipped with clothing and minimal tactical gear. Due to availability of these devices, three will be Model 1435 and one is Model 1432. The difference is in the naked weight, the Model 1435 is 170 pounds and the 1432 weighs 135 pounds. The 170 pound manikins will be used in the forward EPS position,

and will be instrumented for capture of total drag. The aft mounted manikins will not be instrumented.

### **3.4 Test Instrumentation**

The test aircraft is equipped with a flight test instrumentation package to include an external sensitive air data boom, a multifunction display (MFD), and an internally mounted instrumentation pallet capable of recording the below listed parameters. Additional equipment will include a stopwatch, digital camera, and a cyclic control fixture. The following parameters will be recorded from the onboard instrumentation or by hand as required for the specific tests:

- Pitch Attitude (deg  $\theta$ )
- Roll Attitude (deg  $\phi$ )
- Side Slip (degrees  $\beta$ )
- Heading (deg  $\varphi$ )
- Calibrated Airspeed (KCAS)
- Pressure Altitude ( $H_P$  ft)
- GPS Altitude (ft)
- Ground Track (deg)
- Engine Gas Generator Speed ( $N_G$  %)
- Exhaust Gas Temperature (deg C)
- Outside Air Temperature (deg C)
- Ground Speed (kts)
- Engine Torque (Q psi)
- Rotor Speed ( $N_r$  %)
- Fuel Quantity (gallons)
- Fuel Flow (gpm)
- Drag on Forward Manikins (lbf)

## **4.0 SCOPE OF TESTS**

### **4.1 Test Envelope**

Tests will be conducted within the limits of reference 1. Test envelope parameters are presented in table 1.

## 4.2 Flight Clearance

Approval of this test plan will constitute flight clearance for the evaluation.

## 4.3 Tests and Test Conditions

The evaluation will include ground and flight testing. The ground test will consist of a cockpit field-of-view (FOV) evaluation. Flight testing will occur during approximately 30 flights totaling 45 hours in day visual meteorological conditions (VMC) in the local flying area of Tullahoma, Tennessee. The 30 flights will include continued evaluation of cockpit FOV and evaluation of performance and handling qualities for day VMC operations. A detailed test and test conditions table is presented in table B-1.

Table 1

TEST ENVELOPE PARAMETERS

Parameter	Test Limit
Maximum Cyclic Displacement on Ground	1 in.
Maximum Pedal Displacement on Ground	½ IN.
Maximum Step Input Size	1 IN.
Maximum Step Increment Size	¼ in.
Maximum Pitch Attitude	± 45°
Maximum Roll Attitude	± 60°
Maximum Sideslip (80 KCAS)	2 ball width from trim
Maximum Yaw Rate	45°/sec
Maximum Sideward Airspeed	35 kts
Maximum Rearward Airspeed	35 kts
Minimum N <sub>z</sub>	-0.5g
Maximum N <sub>z</sub>	+3.0g

#### **4.4 Test Loadings**

Flight operations will be conducted within the weight and center of gravity (CG) limits published in reference 1. Crew will consist of a minimum of one qualified Pilot in a pilot station.

#### **4.5 Test Configurations**

The test aircraft will be operated at 94-104% Nr. Engine bleed air will be off. All doors will be removed and the fresh air vent will remain closed. Baseline configuration will consist of the production MD-500D; Model 369D, with external passenger planks installed and four (4) full-scale manikins.

#### **4.6 Test Criteria**

Each wind deflector configuration will be tested against data derived from the baseline flight test of the test aircraft.

#### **4.7 Limitations to Scope**

There will be insufficient flight time and resources available to evaluate multiple aircraft weight and CG combinations. External loads will be conducted with manikins onboard the EPS for all actual flight test. The manikins and/or EPS may be removed for maintenance or pilot proficiency flights at the discretion of the project pilot. Flight tests will be restricted to the Tullahoma local flying area and test day environmental conditions. Night

operations will not be evaluated. Pitot static system calibration will be conducted prior to baseline of wind deflector evaluations.

## **5.0 METHOD OF TEST**

### **5.1 Test Method and Procedures**

All maneuvers are detailed by phase of flight in the Test Plan Matrix, table B-1. Performance tests will be conducted in accordance with USNTPS FTM 106, Rotary Wing Performance (ref 2). Stability and Control tests will be conducted in accordance with USNTPS FTM 107, Rotary Wing Stability and Control (ref 3). Amplifying information about specific procedures not covered in the FTM's and Operating Manual is provided in the remarks section of table B-1. Mission tasks will be assessed and handling quality ratings will be assigned using the Cooper-Harper Rating scale (HQR) from NASA TN 5153, (reference5). The Vibration Assessment Rating (VAR), Pilot Induced Oscillation (PIO), and turbulence rating scales will be used as necessary in accordance with reference 4. Bedford Workload Rating and the Modified Cooper-Harper scales are presented in figures A-2 and A-3 and will be used as necessary during systems evaluations.

#### ***5.1.1 Flight Preparation and/or Ground Checks***

All normal ground and pre-flights checks will be conducted in accordance with the aircraft operator's manual. The cockpit evaluation will be conducted at

the Tullahoma Regional Airport at the UTSI Flight Research Facility in accordance with table B-1.

### **5.1.2 Operational Procedures**

- a. Operational Countdown: N/A
- b. Switchology: N/A
- c. Aircraft Maneuvers: Will be conducted IAW reference 1 and table B-1.
  - i. Mission tasks will include: hover taxi, rearward flight, sideward flight, normal confined area type approach, normal confined area departure.
  - ii. Ground testing will include a cockpit evaluation of the pilot's FOV.
  - iii. Aircraft performance evaluation will include: engine assessment; IGE/OGE hover performance and vertical climb performance; level flight performance. No inlet recovery data is available for engine assessment. Pressure recovery will be assumed to be 1 and the temperature correction will be assumed zero.
  - iv. Aircraft stability and control evaluation will include mechanical characteristics in flight, trimmed flight control positions, control response, apparent longitudinal static stability, apparent maneuver stability, apparent spiral stability, apparent directional stability,



apparent short-term response, and gust response. Low airspeed specific tests will include trimmed flight control positions, longitudinal and lateral static stability.

- d. Test Specific Range Safety: NA.
- e. Changes to Aircraft Operating Manual or Emergency Procedures: Wind deflector installation has the potential to restrict crew egress. Emergency egress with deflectors installed will be rehearsed prior to first flight.
- f. Aircraft/Test Item discrepancy review procedures. The Aircraft Discrepancy Book will be reviewed by the project pilot prior to flight. The test team will review known aircraft discrepancies and their potential effect(s) on the safe conduct and completion of the test flights.
- g. The Pre-Test Brief: Conducted in accordance with the appropriate briefing guides and organizational SOP. All members will be required for the pre-test safety briefs.
- h. Test Specific Preflight/post-flight procedures for aircraft, instrumentation or test equipment: Instrumentation will be operationally checked 1 hour prior to the schedule departure time
- i. Test Specific Go/No-Go Criteria:
  - a. Weather Requirements:
    - i. Terminal: 100 ft ceiling/1/2 sm visibility.

- ii. Area: Ceiling no lower than 500 ft above highest planned test altitude and 3 sm visibility. A visible horizon is required.
- b. Chase Requirements: Initial fully configuration flight may require a chase aircraft as directed by the project pilot.
- c. Instrumentation Requirements: The No-Go instrumentation criteria for this evaluation; Manikin drag measurement devices, Normal aircraft engine instruments (N1, N2, NR, Oil Pressure, Oil Temp, Fuel Quantity), Fuel flow (or accurate and calibrated quantity measurement), Hp, OAT, and Calibrated Airspeed. Time histories are highly desirable for control response testing.
- d. Aircraft System Requirements: IAW operators manual.
- e. Additional Go/No-Go Criteria: none

## **5.2 Instrumentation and Data Extraction/Processing**

Data will be recorded on a laptop computer and kneeboard data cards. Flight data will be reduced using Microsoft Excel, MATLAB and the USNTPS Helicopter Performance software as appropriate.

## **5.3 Support Requirements**

- a. Support Aircraft. OH-58A+ chase aircraft.
- b. Unique ground support equipment. None.
- c. Laboratory. None.
- d. Remote site testing. None

e. Data services and photo support. Data will be reduced locally; no support required.

As required, video of test flights will be recorded from OH-58A+ pace aircraft.

f. Flight gear. Nomex flight suit and helmet will be worn for all flight tests.

#### **5.4 Personnel Requirements**

The Project Pilot must be current, qualified, and proficient in the test aircraft type prior to commencing the flight test.

### **6.0 RISK MANAGEMENT**

#### **6.1 Safety Checklist**

A safety checklist is presented in appendix C.

#### **6.2 Test Hazard Analysis**

A test hazard analysis is presented in appendix D.

#### **6.5 Environmental**

This proposed action is viewed as being a continuing test activity that posed no adverse threat to the environment; no substantial change is occurring to the continuing test action performed. No significant environmental degradation or effect is known to be occurring as a result of the test procedures; therefore, this action is considered not significant and requires no further environmental documentation.

## **6.6 Risk Category**

Risk Category B.

## **6.7 Real-Time Data Monitoring**

No real-time ground telemetry and data monitoring will occur during the flights.

## **6.8 Special Precaution**

The Project Pilot will ensure that the all crewmembers are aware of and understand all test particular maneuvers and procedures prior to flight. The team will observe normal operating limits, with special emphasis on flight control and power margins. Any violation of test limits will result in a “TERMINATE” call that will suspend the testing. The pilots will determine if testing can be continued or if the test event should be repeated. Recovery from maneuvers will be initiated in sufficient time to prevent exceeding an operating or test limit. Buildup procedures will begin with normal procedures, progress to emergency procedure training. Build-up is built into the test matrix to ensure the test team incrementally approaches any limits, starting tests from known conditions, conducting static tests prior to dynamic tests, and increasing speeds, accelerations, and larger attitude deviations. A “KNOCK IT OFF” call will be used to terminate the maneuver if aircraft limitations will be exceeded. If an emergency situation arises, an “ABORT” call will be used. A safety checklist is included as appendix C, and a hazard matrix is presented in table D-1.

## **7.0 PROJECT MANAGEMENT**

### **7.1 Funding and Manpower Requirements**

In place through UTSI.

### **7.2 Schedule/Milestones**

The schedule for this evaluation is presented on the Project Data/Signature sheet of this test plan.

### **7.3 Test Plan Change Procedure**

Changes will be submitted to the Project Pilot as they arise.

### **7.4 Reports**

A report of test results (RTR) is due no later than 31 December 2006.

## REFERENCES

1. MD-500D, Rotorcraft Flight Manual Model 369D, MD Helicopters, Inc., Mesa, Arizona, August 1998.
2. Military Specification MIL-H-8501A, Helicopter Flying and Ground Handling Qualities, 7 September 1961.
3. USNTPS Flight Test Manual, Rotary Wing Performance, FTM 106, 31 December 1996.
4. USNTPS Flight Test Manual, Rotary Wing Stability and Control, FTM 107, 31 December 1995.
5. NASA Technical Note, NASA TN D-5153, Use of Pilot Rating in the Evaluation of Aircraft Handling Qualities, April 1969.
6. Hicks, Eric G. "Experimental Study of Alternative Flow Diverting Devices for the Modified MH-6J Helicopter." The University of Tennessee Space Institute, Tullahoma, Tennessee, November 1997.
7. McDougall, Kelly E. "Flight Testing Flow Diverting Devices on an OH-58A+ for Applications to an MH-6 Helicopter." The University of Tennessee Space Institute, Tullahoma, Tennessee, December 2000.
8. Mulnik, Matthew P. "Design of a Flow Diverting Device for OH-58A Helicopters." The University of Tennessee Space Institute, Tullahoma, Tennessee, December 2000.
9. Lewis, Richard. "Wind Tunnel Investigation of Wind Deflectors for the MH-6M Mission-Enhanced Little Bird." The University of Tennessee Space Institute, Tullahoma, Tennessee, December 2005.

## DESCRIPTION OF MD-500D AIRCRAFT

### **General.**

The aircraft MD-500D is a 5 place, turbine powered, rotary wing aircraft constructed primarily of aluminum alloy. The main rotor is a fully articulated five-bladed system, with anti-torque provided by a 2-bladed semi-rigid type tail rotor.

### **Airframe.**

The airframe structure is egg-shaped and provides very clean aerodynamic lines. The rigid, three-dimensional truss type structure increases crew safety by means of its roll bar design, and by reduction in the number of potential sources of failure. The airframe structure is designed to be energy absorbing and fails progressively in the event of impact. The fuselage is a semi-monocoque structure that is divided into three main sections. The forward section is comprised of a pilot compartment and, directly aft separated by a bulkhead, a passenger/cargo compartment. The pilot compartment is equipped with seats for the pilot and either one or two passengers. A canopy of transparent tinted acrylic panels provides excellent visibility. The left seat in the pilot's compartment (looking forward) is the pilot's seat (command position); in special military version helicopters, the pilot's seat is on the right side. The lower fuselage structure beneath the pilot/passenger floor contains compartment space for the aircraft battery and

provision for small cargo storage or installation of avionics equipment. Access to the compartments is through two floor door plates. The cargo compartment in the center of the aircraft contains provisions for installation of a bench or individual folding type seats for two passengers, which are adjustable in height. The aft section includes the structure for the tailboom attachment and engine compartment. Access to the engine compartment is provided through clamshell doors contoured to the shape the fuselage. The lower section is divided by the center beam and provides housing for the two fuel cells. Provisions for the attachment of a cargo hook are located on the bottom of the fuselage in line with the center beam. The tailboom is a monocoque structure of aluminum alloy frames and skin. The tailboom is the supporting attachment structure for the stabilizers, tail rotor transmission and tail rotor. The tailboom also houses the tail rotor transmission drive shaft; the one-piece dynamically balanced shaft requires no intermediate couplings or bearings.

### **Landing Gear:**

The landing gear is a skid-type attached to the fuselage at 12 points and is not retractable. Aerodynamic fairings cover the struts. Nitrogen charged landing gear dampers act as springs and shock absorbers to cushion landings and provide ground resonance stability. Provisions for ground handling wheels are incorporated on the skid tubes.



**Helicopter Interior:**

The standard MD 500D requires a minimum crew of one pilot seated on the left side of the cockpit. The passengers sit to the right, abreast of the pilot. Seatbelts are provided for all positions. In the military version, the center seat is eliminated. An instrument panel is located forward of the seat at the aircraft centerline. The panel incorporates standard flight and engine instruments in addition to warning and caution lights. The panel also contains adequate space provisions for various arrangements of communication and navigation equipment. Seat belts are provided with several styles being offered. The seats and belts are easily removed. Cargo compartment bench-type seats may be easily folded out of the way or completely removed for accommodating cargo. During cargo carrying operations, the compartment floor serves as the cargo deck. Removable and interchangeable cargo tiedown fittings are available. Four doors are installed on the helicopter-two on each side. The two forward doors permit access to the forward compartment for pilot and passengers. The two aft doors allow entry to the passenger/cargo compartment. Transparent tinted windows are contained in the doors.

**Powerplant:**

The power plant used is either the Allison Model 250-C20B or 250-C20R/2 gas turbine engine with a takeoff power rating of 420shp for the C20B and 450shp for the C20R/2. Only 375 shp at 103 percent N2 RPM is used for

takeoff; 350 maximum continuous shp provides sufficient power for all other flight modes. Limiting the maximum power to less than the maximum rated power provides a higher engine critical altitude. The power turbine governor provides automatic constant speed control of rotor RPM.

### **Drive System:**

The overrunning clutch transmits power from the engine to the main drive shaft. The clutch has no external controls and disengages automatically during autorotation and engine shutdown. The main drive shaft connects to the main rotor transmission input shaft. The engine oil cooler blower is belt driven off the main drive shaft. The oil cooler blower draws cooling air from the air inlet fairing to supply ambient air to the engine and transmission oil coolers and to the engine compartment. The main rotor transmission is mounted on the basic airframe structure above the passenger/cargo compartment. The transmission is lubricated by its own air-cooled lubrication system. The main rotor static mast is non-rotating and is rigidly mounted to the mast support structure. The rotor hub is supported by the rotor mast. Torque is transmitted independently to the rotor through the main rotor drive shaft. Lifting loads are prevented from being imposed onto the main transmission eliminating thrust loading of transmission parts. The tail rotor transmission is mounted on the aft end of the tailboom and has a self-contained lubricant system. The tail rotor is mounted on the output shaft of the transmission and consists of two variable-pitch blades.

**Main Rotor System:**

The helicopter utilizes a five bladed, fully articulated main rotor assembly with unique features. While contemporary helicopters use torsion tension straps in lieu of thrust bearing stacks to contain blade centrifugal loading and allow feathering, the MDHS strap pack arrangement goes three steps further. First, the strap configuration (while secured firmly to the hub) actually allows the centrifugal load exerted by one blade to be countered by the force exerted by the opposite two blades. Thus, very light centrifugal loads are sensed by the hub. Second, the V-legs of the strap pack rotate as driving members to turn the blades. Finally, the straps are configured to allow feathering and flapping of the blades. The main rotor blades are secured to the hub with quick release lever type pins.

**Flight Controls:**

Cyclic, collective, and adjustable pedal controls are provided at the left crew position (right position, military only). Adjustable friction devices, which may be varied to suit the individual pilot, are incorporated in the cyclic, collective and throttle controls. In addition, electrical cyclic trim actuators allow flight loads to be trimmed out. Since stick control forces are low, a hydraulic boost system is unnecessary. An optional dual control system may be easily removed to provide room for passengers or cargo. A more detailed

description of the aircraft is contained in the MD-500D Rotorcraft Flight Manual (ref 1).

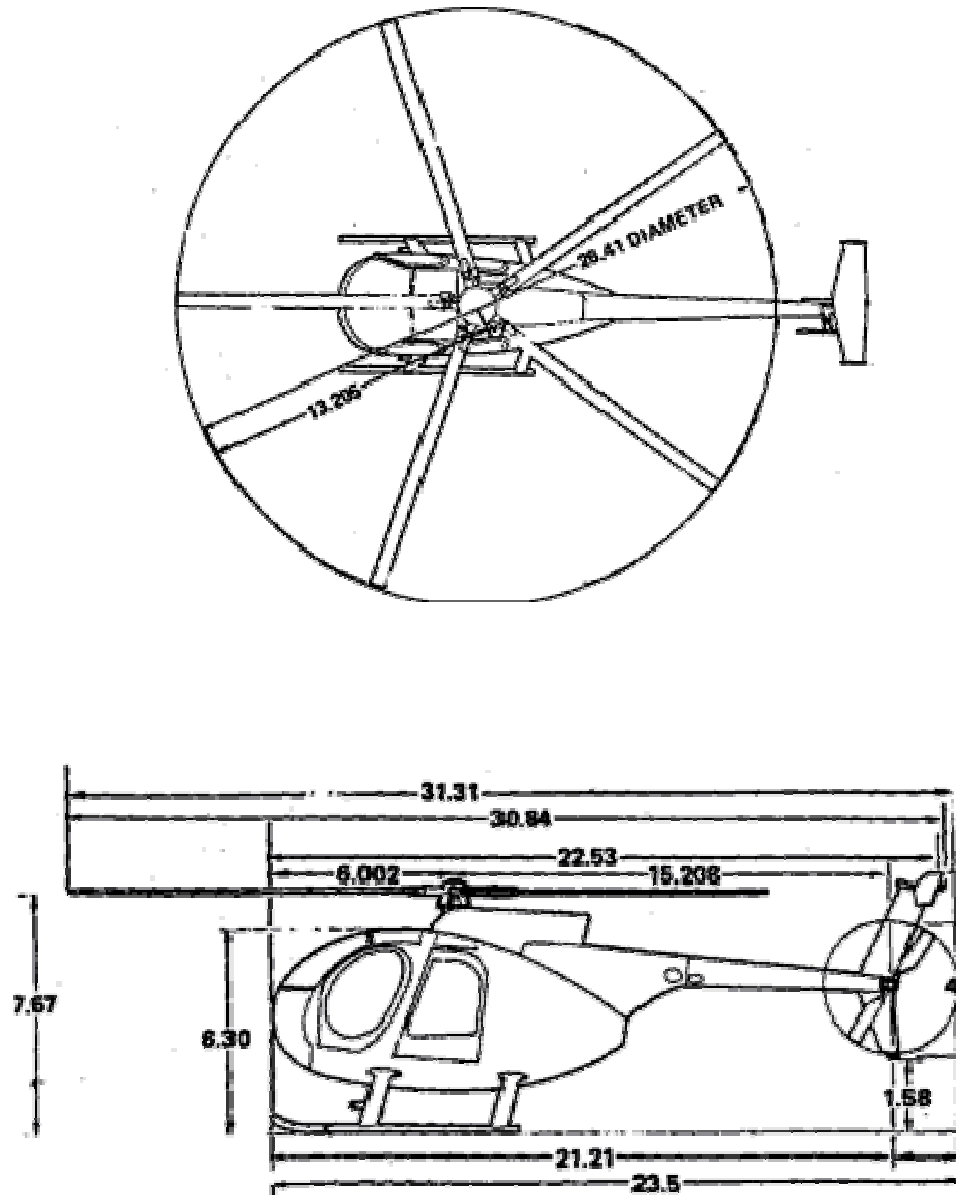


Figure 85. MD-500D Principle Dimensions.



Figure 86. MD-500D (369D) N500VS.

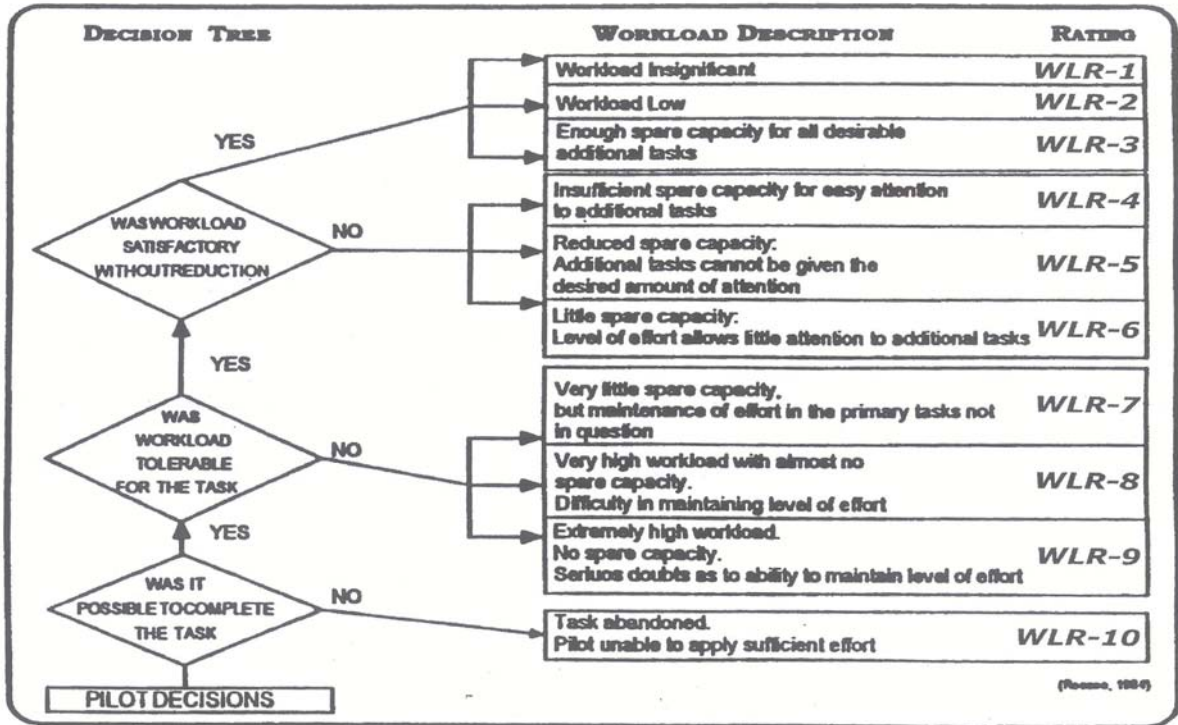


Figure 87. Bedford Workload Rating Scale.

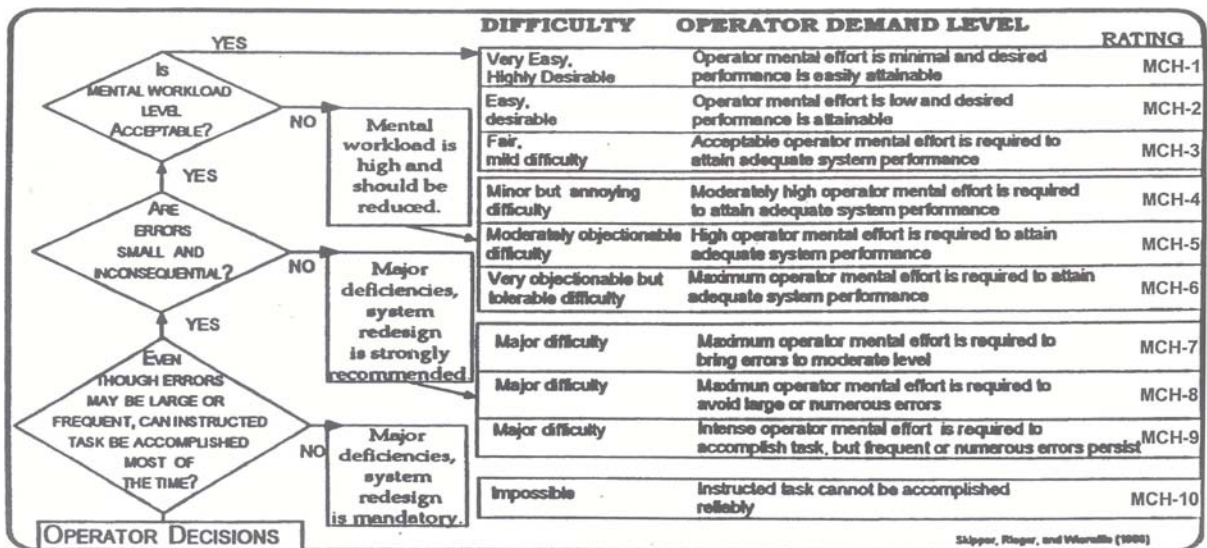


Figure 88. Modified Cooper-Harper Rating Scale.

**Table 20: Test Plan Matrix – Ground Tests.**<sup>(1)(2)(3)</sup>

Event	Test	Sub Test	Altitude (ft-Hp)	Airspeed (KCAS)	Remarks
G-1	Cockpit Evaluation	Field of View	Field Elev.	N/A	<ul style="list-style-type: none"> <li>• Normal entry and egress with compatible helmet and gloves.</li> <li>• Emergency egress simulating a ground emergency.</li> </ul>
G-2		Entry and Egress			



**Table 21: Test Plan Matrix – Performance Tests.**<sup>(1)(2)(3)</sup>

Event	Test	Sub Test	Altitude (ft-Hp) <sup>(4)</sup>	Airspeed (KCAS) <sup>(5)</sup>	Remarks
P-1	Engine Assessment	Engine Assessment Static Droop	0-100 <sup>(6)</sup>	Hover Into wind	<ul style="list-style-type: none"> <li>Free flight, ground referenced takeoff to a hover, using GPS ALT,</li> <li>Wind&lt;10 kts (desired)</li> <li>Note NR droop on takeoff</li> </ul>
P-2		Hover / Level Flight	IGE - 5000 <sup>(6)</sup>	0 -VH	<ul style="list-style-type: none"> <li>Record engine parameters at a wide range of power settings, altitudes, airspeeds.</li> <li>Conduct in conjunction with hover and level flight performance tests.</li> <li>Generate generalized engine performance curves.</li> <li>VH is defined as maximum level flight airspeed.</li> </ul>
P-3		Transient Droop	500-5000 <sup>(6)</sup>	Hover Into wind	<ul style="list-style-type: none"> <li>Min thrust 90% of maximum Q in 8, 6, 4, 3 sec intervals.</li> <li>Knock it off if low rotor conditions occur.</li> </ul>
P-4		Hover Performance	IGE Hover		30 <sup>(7)</sup>

**Table 21: Continued.** <sup>(1)(2)(3)</sup>

Event	Test	Sub Test	Altitude (ft-Hp) (4)	Airspeed (KCAS)(5)	Remarks
P-5	Hover Performance	IGE/OGE Transition	30 – OGE <sup>(7)</sup>		<ul style="list-style-type: none"> <li>• Free flight, ground referenced, using GPS ALT</li> <li>• 3 ft IGE hover up to 50 ft in 10 ft increments, wind&lt;5 kts</li> </ul>
P-6		OGE Hover	OGE <sup>(7)</sup>		<ul style="list-style-type: none"> <li>• Free flight, ground referenced, using GPS ALT, wind&lt;5 kts</li> <li>• Use 95% NR to 104% NR</li> <li>• Use OGE determined from previous test</li> </ul>
P-7	Level Flight Performance	Level Flight	500- 5000 <sup>(6)</sup>	40-VH	<ul style="list-style-type: none"> <li>• Preferred altitude for test will be ~2000 ft MSL. Airspeed buildup will begin at target airspeed of 40 kts, and will then incremented by 10 kts to VH or VNE whichever is lower. NR will be maintained at 103%.</li> </ul>

**Table 22: Test Plan Matrix – Stability and Control Tests.<sup>(1)(2)(3)</sup>**

Event	Test	Sub Test	Altitude (ft-Hp) <sup>(4)</sup>	Airspeed (KCAS) <sup>(5)</sup>	Remarks
S-1	Trimmed Flight Control Positions	Straight and Level	500-5000 <sup>(6)</sup>	40-80	<ul style="list-style-type: none"> <li>Record changes in trim control positions with airspeed in 10 kt increments.</li> <li>Look for apparent longitudinal static stability</li> <li>Note whether you can trim the control forces to zero. Note the speed response to attitude change.</li> </ul>
S-2	Apparent Static Lateral Directional Stability	Steady Heading Sideslip		40 & 80	<ul style="list-style-type: none"> <li>Vary sideslip from trim (collective fixed) without retrimming, record control positions. Limited to 2 ball widths from trim in 1/2 ball increments.</li> </ul>
S-3	Dynamic Longitudinal Stability	Long Term Response <sup>(10)</sup>			<ul style="list-style-type: none"> <li>Trimmed control forces to zero, collective fixed throughout maneuver.</li> <li>Excite artificially if required.</li> <li>Record airspeed and altitude at 5 sec intervals.</li> </ul>
S-4	Dynamic Lateral Directional Stability	Apparent Spiral Stability <sup>(10)</sup>			<ul style="list-style-type: none"> <li>Establish a steady bank angle of 15 and 30 deg. When all rates subside, put the cyclic back to the center trim position and start timing the aircrafts resulting motion. Note the time to half or double amplitude.</li> </ul>

**Table 23: Continued.**<sup>(1)(2)(3)</sup>

Event	Test	Sub Test	Altitude (ft-Hp) <sup>(4)</sup>	Airspeed (KCAS) <sup>(5)</sup>	Remarks
S-5	Dynamic Lateral-Directional Stability	Lateral Directional Oscillation <sup>(10)</sup>	500-5000 <sup>(6)</sup>	40 & 80	<ul style="list-style-type: none"> <li>Conduct a 1 in. ½ Hz pedal doublet to determine characteristics of the dutch roll frequency and damping ratio. Approximate T ½, damping, and <math>\tilde{\omega}</math> estimate</li> <li>Evaluate the ease or difficulty to excite or suppress the LDO and Dutch Roll.</li> <li>Data will be recorded for post flight reduction</li> </ul>
S-6	Control Response	Lateral	500-5000 <sup>(6)</sup>	40, 60, & 80	<ul style="list-style-type: none"> <li>Inputs into a control fixture using up to 2 in. in ¼ in. increments. Knock it off at ± 60 deg or approaching G limitations. Note predictability and steady state rates.</li> <li>Data will be recorded for post flight reduction.</li> </ul>
S-7		Longitudinal			
S-8	Trimmed Flight Control Positions	Critical Azimuth	30 <sup>(7)</sup>	10, 20, & 30 <sup>(8)(9)</sup>	<ul style="list-style-type: none"> <li>Record changes in trim control positions with varying wind azimuth 0 to 315 deg in 45 deg increments maintaining airspeed, heading, and altitude.</li> <li>Note control margins, trimmability, control variations, vibrations, and field of view. Assign HQR's and VAR ratings at each point to determine critical azimuth</li> </ul>

Notes:

1. All tests (except hover tests) will be conducted during daylight with 500 ft ceiling above test altitude, and 3 miles visibility. Terminal conditions must be 300 and 1/2 mile visibility.
2. Configuration will be Bleed Air Systems OFF, crew of one test pilot, and one safety pilot/FTE, NR103% unless otherwise noted.
3. Engineering tests will be conducted IAW FTM's, 106 and 107. Required data collection for each maneuver will be IAW these FTM's as well.
4.  $H_{p_0}$ ; Source: Flight test altimeter set at 29.92 unless otherwise noted.
5.  $V_c$ ; Source: Flight test airspeed indicator unless otherwise noted.
6. Altitude for testing may be adjusted by the test team as required for weather conditions in the local flying area up to 5000 ft hp. Minimum altitude for forward flight engineering tasks is 500 AGL unless otherwise noted.
7. GPS ALT; Source: Flight test GPS.
8. Ground speed: Flight test MFD.
9. Assign HQR, VAR, PIO, and TURB where applicable.
10. Tests not required but may be conducted at the discretion of the project pilot.

## VITA

James J. Wright was born to Barbara and Vincent Wright in October 1962 in New Britain, Connecticut. He graduated from Newington High School, Newington, Connecticut, in 1980. A number of years, passports and pints of Guinness later, he joined the United States Army to attend Warrant Officer Candidate School and the Initial Entry Rotary Wing Aviator Course. He graduated from flight school in April 1989 as distinguished honor graduate, and flew scout helicopters with many of the U.S. Army's Cavalry units for the next eighteen years. He is a veteran of Operation Iraqi Freedom (2003), whose Stetson is rumored to have over 3,000 hours of flight time. Additionally, during this time, he earned his Bachelor of Science Degree from Embry-Riddle Aeronautical University and Commercial/Instrument Pilot certificates for helicopters. He also holds a Private Pilot rating for single engine airplanes. In June of 1995, he married Barbara Richter of Oberzell, Germany. They now have two children, Meghan and Christopher, and a dog named Friday. Jim graduated from the University of Tennessee Space Institute in December 2006 with a Master of Science Degree in Aviation Systems, with follow-on assignment for the U.S. Army C-12, UH-60 and OH-6 Aircraft Qualification Courses enroute to the U.S. Naval Test Pilot School in Patuxent River, Maryland.